CAPROCK CHARACTERISTICS AND UNCERTAINTIES IN GEOLOGICAL CARBON SEQUESTRATION IN THE ILLINOIS BASIN

BY

BRYNNE STORSVED

THESIS

Submitted in partial fulfillment of the requirements
for the degree of Master of Science in Civil Engineering
in the Graduate College of the
University of Illinois at Urbana-Champaign, 2016

Urbana, Illinois

Adviser:

Professor Albert J. Valocchi

ABSTRACT

Geological carbon sequestration in deep saline aquifers has emerged as a promising mitigation strategy for reducing greenhouse gas emissions to the atmosphere. Success of commercial-scale GCS requires containment of injected CO2 and the sealing ability of the overlying caprock has been identified as an important factor related to the long-term storage of CO2. Caprock research is recent and the behavior of caprocks as seals in GCS is not well understood. Geological uncertainty assessment in GCS research is often limited to reservoir properties. This research presents a current review of the dominant physical characteristics of caprocks and their relation to CO2 containment. This work is limited to argillaceous sediments, such as shales and mudrocks, as caprocks in GCS. The ability to retard vertical fluid flow is a complex issue as the CO2 plume will be in contact with the caprock due to buoyancy and involve hydrodynamic, geomechanical, and geochemical processes.

Physical processes which govern leakage through a caprock are often coupled, yet the effective geologic parameters are uncertain. To address caprock geologic parameter uncertainty in GCS modeling, a simplified caprock-reservoir simulation model based on the Eau Claire Formation and the Mt. Simon Formation at the Illinois Basin – Decatur Project (IBDP), a large-scale carbon capture and storage project, is developed. The extended Morris OAT method (Morris, 1991; Campolongo et al., 2007) is used to assess the sensitivity of the pressure response due to brine injection at locations in the caprock and reservoir with respect to four caprock parameters: horizontal permeability, anisotropic permeability ratio, porosity, and rock compressibility. All caprock parameters exhibited nonlinear and non-negligible effects. Horizontal permeability caprock is the dominating factor which aids in the dissipation of pressure in the caprock and reservoir at all times after injection. Caprock compressibility has a positive effect on pressure perturbation in the system at 10 years after injection ends. A higher caprock compressibility allows for greater pressure absorption in the caprock pore space; therefore decreasing the pressure in the underlying reservoir. These results indicate the parameters tested are all deserving of additional research; however, caprock compressibility and permeability are the dominant factors which influence pressure perturbation in the caprock and reservoir.

ACKNOWLEDGEMENTS

This research would not have been possible without the support of many people. I would like to express my gratitude to Dr. Albert Valocchi and Dr. Edward Mehnert for their patience and guidance during my journey through graduate school, and providing me with the opportunity for this research study. I would also like to thank Don Keefer and Laura Keefer for their continual support. I gratefully acknowledge Sallie E. Greenberg Ph.D. and Robert J. Finley Ph.D. for granting me a Graduate Research Assistantship at the Illinois State Geological Survey. The assistantship was funded by the U.S. Department of Energy (DE-FC26-05NT42588). Darian Damiani (National Energy Technology Laboratory) served as US DOE Project Manager.

TABLE OF CONTENTS

CHAPTER 1: INTRODUCTION 1
1.1 Statement of the Problem 1
1.2 Objectives and Scope 2
1.3 Organization of Thesis 3
CHAPTER 2: GEOLOGICAL STORAGE AND THE CAPROCK 4
2.1 Introduction 4
2.2 GCS in Deep Saline Aquifers 5
2.2.1 The Geologic Sink 6
2.2.2 Migration and Trapping Mechanisms of Sequestered CO2 7
2.3 Leakage and Risk Assessment 9
2.4 The Illinois Basin for CO2 Sequestration 10
2.4.1 Regional Geology and Structure 11
2.4.2 Major Stratigraphic Units 12
2.5 Physical Characteristics of Caprocks 17
2.5.1 General Characteristics 18
2.5.2 Hydrodynamics and Capillary Pressure 21
2.6 Summary 26
CHAPTER 3: GEOLOGIC PARAMETER UNCERTAINTY OF A CAPROCK 29
3.1 Introduction 29
3.2 Geological Uncertainty 31
3.2.1 Nature and Source 32
3.2.2 Previous Sensitivity Analyses of Geologic Uncertainty in GCS 34
3.3 Modeling Approach 36
3.3.1 Sensitivity Analysis Methodology 37
3.3.2 Simulation Model Setup 39
3.4 Summary 41

CHAPTER 4: RESULTS AND DISCUSSION 43
4.1 Results 43
4.1.1 Observation Point at the Base of the Caprock 43
4.1.2 Vertical Cross Section 46
4.2 Discussion 47
CHAPTER 5: CONCLUSION AND FUTURE WORK 50
FIGURES 52
REFERENCES 82

CHAPTER 1: INTRODUCTION

1.1 Statement of the Problem

The atmospheric greenhouse effect and its adverse impact on global climate change is a well-understood phenomenon. Methane, ozone, nitrous oxide, water vapor, and carbon dioxide (CO2) naturally contribute to the warming of the Earth's atmosphere by trapping and re-emitting infrared radiation (White et al., 2003). Since the Industrial Revolution, combustion of fossil fuels has led to an unprecedented increase of CO2 concentration in the atmosphere and contributed to the increase in Earth's average temperature (Bachu, 2000). Global anthropogenic greenhouse gas (GHG) emissions in 2010 were estimated to be 31.2 billion metric tons and are projected to increase to 45.5 billion metric tons in the year 2040 (U. S. Energy Information Agency, 2016). Development of technologies to mitigate release of anthropogenic CO2 emissions to the atmosphere has now become an immediate international concern (Pacala and Socolow, 2004).

Currently, it is not possible to effectively replace fossil fuel based energy sources with more sustainable sources without major disturbance to the energy supply. A widely accepted and interim solution for the reduction of GHG emissions is to capture and store CO2 deep underground (Pacala and Socolow, 2004; Bachu et al., 1994). This is known as carbon capture and storage (CCS). Often, these deep sedimentary formations are porous or fractured and are saturated with oil, gas, or brine (Pacala and Socolow, 2004). If the reservoir rock is permeable and has an overlying impermeable confining layer (caprock) that prevents CO2 migration, it may suitable for storing large quantities of CO2. Carbon dioxide injected as a supercritical liquid will rise due to buoyancy and a barrier is needed to prevent leakage into overlying freshwater resources. Injected CO2 can remain in a deep saline reservoir due to several other trapping mechanisms that will be discussed later. Caprock and reservoir integrity as well as an adequate understanding of possible leakage mechanisms through the caprock are technical issues of critical importance to the safe implementation of geological carbon sequestration (GCS) (Song and Zhang, 2013). The Illinois Basin – Decatur Project (IBDP) offers one of the best opportunities to conduct an uncertainty assessment of a caprock system overlying a large scale storage project.

Located in Decatur, Illinois, IBDP is the deep saline reservoir project of the Midwest Geological Sequestration Consortium (MGCS). The Mt. Simon Sandstone has been identified as a safe sink for supercritical CO2 (NETL, 2015), and injection began in November, 2011 and was completed in November, 2014. Although the Mt. Simon Sandstone is believed capable of safely and effectively containing large amounts of CO2, there are a variety of coupled physical and chemical processes which can affect the hydraulic integrity of overlying seals. Research is limited on caprock behavior and leakage in GCS. Sensitivity analysis of geologic uncertainty of a caprock-reservoir system is often limited to reservoir physical parameters. A few authors have studied geologic uncertainty of the caprock in GCS (Mbia et al., 2014; Wainwright et al., 2013; Chang et al., 2013; Hou et al., 2012). This project presents not only the opportunity to carry out an uncertainty analysis of a caprock system, but to gain a better understanding of safety issues associated with caprocks as seals in GCS projects.

1.2 Objectives and Scope

Geological storage of CO2 is a promising technology to reduce GHG emissions into the atmosphere. Such a technology is not without concerns (Nordbotten and Celia, 2011); GCS projects require large spatial scales and long timeframes that distinguish it from other deep subsurface waste disposal methods. Modeling and simulation of GCS systems is integral for risk assessment, yet accompanied by large computational demands and huge geological uncertainties. Little is known about deep saline aquifers compared to our knowledge of oil and gas reservoirs, and even less is known about the sealing properties of caprocks. Consequently, there is a need for uncertainty assessment of the system to gain confidence that GCS is a safe and sound technique. Set in the extensively studied Illinois Basin, the IBDP presents a prime opportunity to address many concerns that GCS raises. The overall goals of this research are to examine the role of a caprock seal in terms of physical characteristics and put into context the implications of geologic uncertainty in caprock formations overlying saline reservoirs considered for CO2 storage. The main research objectives are:

1. Review the current state of knowledge on the physical and lithological characteristics of caprock formations with emphasis on the Eau Claire Formation and identify features that may impact long-term performance of CO2 storage.

2. Investigate sources of geologic uncertainty in caprock-reservoir systems which can impact the sealing capacity and integrity of the caprock.

3. Develop a simplified caprock-reservoir simulation model based on IBDP data for sensitivity analysis of four caprock parameters (horizontal permeability, anisotropic permeability ratio, porosity, and rock compressibility).

4. Evaluate and assess the pressure build up at several locations in the caprock (Eau Claire) from brine injection in an underlying reservoir (Mt Simon) by varying physical parameters of the caprock.

1.3 Organization of Thesis

In Chapter 2, the concept of anthropogenic CO2 sequestration is presented along with an overview of trapping mechanisms. Geologic carbon sequestration efforts in the Illinois Basin are briefly discussed with a review of Cambrian geology and recent research efforts on the Eau Claire Formation. The concept of geological uncertainty associated with CO2 containment is presented in Chapter 3. Previous sensitivity analyses of geological parameters in GCS are also reviewed. An idealized caprock-reservoir simulation model based on the Eau Claire (caprock) and Mt. Simon (reservoir) for an extended Morris Method sensitivity analysis (Morris, 1991; Campolongo et al., 2007) is presented in section 3.3. Chapter 4 reports the simulation and sensitivity analysis results. Overall summary of this research and suggestions for future work are presented in the final chapter.

CHAPTER 2: GEOLOGICAL STORAGE AND THE CAPROCK

2.1 Introduction

Subsurface waste disposal using injection wells began in the early 20th century by the petroleum industry where geologic formations were used for the disposal of oil-field brines (Bergstrom, 1968; Donaldson, 1964). The earliest report of industrial waste injection was published in 1939. Lasting only several days, the Dow Chemical Company had to discontinue its injection as it became apparent the brine had contaminated an overlying freshwater aquifer (Harlow, 1939). Following World War II, federal waste management programs were developed to address and manage high-level radioactive wastes produced during wartime. In 1957, the National Academy of Sciences issued a report (NAS, 1957) stating geologic disposal was technically feasible. With the onset of more stringent regulation of waste disposal into surface water bodies, various industries turned to using deep-well injection. The number of deep industrial-waste injection wells rose to approximately 250 by the 1970s (Warner, 1972). This boom in industrial waste injection wells was largely unregulated and resulted in several well-integrity failures (Lehr, 1986). Motivated by concerns about the safety of injection practices and groundwater supplies, Congress established the Safe Drinking Water Act in 1974 which required the U.S. Environmental Protection Agency (USEPA) to set requirements and standards for underground injection of liquid waste.

In 1992, the United Nations Framework Convention on Climate Change (UNFCCC) stated its goal to reduce greenhouse gas (GHG) emissions and the concept of geological carbon sequestration (GCS) emerged. Through the work of research groups and individuals (Koide et al., 1993; Bachu et al., 1994; Korbol and Kaddour, 1995), GCS began to gain credibility. Deep saline aquifers were identified as optimal candidates for storage of large amounts of GHG (Koide et al., 1993) due to their large volume and expansive distribution across the world. Early research found the overall lack of reliable geologic data limited attempts to identify ideal storage sites that could act as a trap for sequestered CO2, limiting the risk of leakage through an overlying caprock and into freshwater aquifers (Bachu et al., 1994). Among other mitigation options such as fuel switching, nuclear power, and renewable energy, GCS was assessed to be the most viable

strategy with the fewest risks. Two industrial analogs relevant to the GCS are natural gas storage and enhanced oil recovery (EOR). For GCS, the concept materialized in 1996 with the launch of the Sleipner project, the first commercial scale CO2 injection project in a Norwegian offshore saline aquifer (Nordbotten and Celia, 2011). Currently, several demonstration-scale and commercial-scale geological carbon sequestration projects operate worldwide. Notable pioneering projects include the Weyburn Project and the In Salah Project. Located in Saskatchewan, Canada, the Weyburn project is a CO2-enhanced oil recovery project. The In Salah Gas project in Algeria involves storing CO2 in a natural gas reservoir.

This chapter introduces the concept of the geologic sink and GCS in deep saline aquifers. Geologic carbon sequestration efforts in the Illinois Basin are discussed with a review of Cambrian geology. Eau Claire geologic parameter ranges used in the parametric sensitivity analysis presented in Chapter 3 are introduced here. The chapter concludes with a discussion of physical characteristics of caprocks and recent studies focusing on fluid transport in fine-grained sediments.

2.2 GCS in Deep Saline Aquifers

Geological carbon sequestration is the process of capturing then injecting CO2 into the subsurface which otherwise would be released to the atmosphere. GCS is a very complex system. Numerous coupled processes involve geologic (Pearce et al., 1996; Baines and Worden, 2004; Ambrose et al., 2008; Eiken et al., 2011), hydrologic (Bachu et al., 1994; Tsang et al., 2008; Birkholzer and Zhou, 2009; Person et al., 2010), geochemical (Gunter et al., 2004; Soong et al., 2004; Knauss et al., 2005; Xu et al., 2005; Kharaka et al., 2006; Gaus, 2010), and geomechanical (Morris et al., 2011; Rutqvist et al., 2006; Rutqvist et al., 2007; Rutqvist, 2012; Vulin et al., 2012;) factors which impact CO2 storage in a saline aquifer.

To date, GCS techniques are based on experience and knowledge gained from oil and gas production, underground gas storage, and coal-bed methane. This process involves three primary steps: 1) CO2 capture and separation, 2) compression and transportation, and 3) injection into a geological formation at a suitable storage site, which include deep saline aquifers, depleted oil

and gas reservoirs, and unmineable coal beds (U.S. Department of Energy, 2015). This thesis focuses on the storage of GHG in deep saline aquifers.

2.2.1 The Geologic Sink

A suitable geological storage system for CO2 is composed of a porous and permeable reservoir with sufficient injectivity and CO2 storage capacity and a competent overlying caprock with sealing capabilities. The geologic setting should be seismically stable and injection should occur at depths exceeding 800 m so that the CO2 remains in the supercritical state. Under atmospheric pressure and temperature, CO2 exists as a gas. At pressures greater than 7.38 MPa and 31°C (critical point) CO2 reaches supercritical state (Bachu et al., 1994). It is preferred to inject CO2 in its supercritical state due to its increased density, reducing the volume compared to CO2 in a gaseous state (Fig. 2.1). Once injected, phase behavior depends on reservoir temperature and pressure, therefore a suitable storage site needs to be located at depths where once the supercritical CO2 is injected, it retains its supercritical state. Lastly, the region of injection should be sufficiently permeable to allow for high injectivity of CO2.

Caprock seals are the primary long-term barrier against migration of CO2 in GCS. The density of supercritical CO2 is less than the resident brine in the storage aquifer. This difference causes the supercritical CO2 to migrate upward and flow along the top of the saline aquifer; therefore, it is critical for a site to have a low-permeability sealing unit to contain the CO2. The concept of caprock is traditionally used in the hydrocarbon industry, but in this case, a caprock is a regional geologic formation with very high capillary entry pressure, low permeability, and hydraulic sealing capabilities. Stored CO2 will exert geomechanical and geochemical stress on the caprock due to increased pressure and acidification of resident brine. It is critical for the caprock to maintain its hydraulic sealing properties over extensive time scales in a changing environment. There must be enough knowledge and understanding of the physical properties of the caprock to make CO2 storage viable. However, more drilling and sampling of a caprock increases the risk of CO2 leakage through the caprock.

2.2.2 Migration and Trapping Mechanisms of Sequestered CO2

Migration of the CO2 plume through aquifer material involves various rock lithologies, pore fluid dynamics and geochemical alterations. Once injected, geologically sequestered CO2 is subject to a number of trapping mechanisms depending on the nature of the storage formation.

The CO2 plume will spread out laterally as well as rise and migrate toward the caprock under buoyancy (Fig. 2.2). The greater the density difference between the two phases, the greater the buoyancy force will move the less dense CO2 upward. Capillary pressure resists the upward movement of CO2 and in aquifers with slow moving pore fluid, more CO2 may get dissolved into the aquifer brine which results in less CO2 reaching the caprock interface. During and after injection, dissolved, trapped, and mobile CO2 can exist simultaneously in the formation (Fig. 2.3). Trapping mechanisms have been studied extensively (Bachu and Adams, 2003; Bachu et al., 2004; Gunter et al., 2004; Kharaka et al., 2006; Pruess et al., 2003; Soong et al., 2004; Xu et al., 2005; Flett et al., 2004) and five different trapping mechanisms are generally considered:

- Structural and stratigraphic trapping: Some sedimentary basins have closed, bound traps or structures, such as formations occupied by oil, gas or water. Structural traps refer to geologic structures such as domes, faults, extensive fracture networks, and folds that act as permeability barriers. Stratigraphic traps refer to the lithological variations in the storage site. An overlying thick, low-permeable seal, or caprock, acts as the primary barrier to CO2 leakage.

- Mineralization or geochemical trapping: Geochemical reactions between the sequestered CO2 and brine of the aquifer will react to form carbonate minerals. Reaction rates vary from a few days to thousands of years depending on the geochemistry. This mechanism is considered the most permanent of the trapping mechanisms as CO2 is effectively immobilized over very long timescales.

- Hydrodynamic trapping: Once injected CO2 splits into mobile and immobile phases. The CO2 will migrate slowly with the formation brine under hydrodynamic flow of the aquifer, rendering the CO2 immobile for geologically important timescales.

- Solubility trapping or dissolution: Solubility of CO2 in water is a function of temperature, pressure, and water salinity. As supercritical phase CO2 dissolves into the ambient formation waters, creating dense CO2-rich brine, convection currents under the CO2 plume occur.

- Residual Trapping: As the plume migrates, a portion of CO2 can become trapped by capillary forces resulting in a trail of immobile, residual CO2. Over time, residual CO2 can dissolve into the formation brine.

Structural, residual, solubility, and mineral trapping mechanisms are the four main processes which act to contain sequestered CO2 in deep saline aquifers. There has been debate as to whether hydrodynamic and geochemical trapping have the potential of permanently containing CO2 in saline formations lacking a regional seal (Gunter et al., 1993). This issue is beyond the scope of this work and will not be addressed.

Dominance of trapping mechanisms and physical processes in the aquifer and caprock vary significantly over time. The time scale and rate of each process is site specific and depends on the type of formation used for storage, but can be generalized (Fig. 2.4). At early time periods, multiphase flow and transport processes control the behavior of the CO2 plume due to buoyancy and viscous forces (Bachu et al., 1994). At later time periods, dissolved CO2 may react with aquifer minerals, permanently fixing CO2 in newly precipitated carbonate minerals (IPCC, 2005). At all time periods, the caprock seal acts a barrier for the CO2 plume.

The success of large-scale deployment of GCS in deep saline aquifers requires physical containment of the sequestered CO2, therefore a critical element to the containment system is a confining top seal, or caprock. At short and long time scales, the caprock may experience dramatic pressure, temperature, hydraulic, and chemical changes due to the large volumes of injected CO2. It should be able to endure changes in chemical and physical properties due to CO2-brine-caprock mineral interactions in addition to changes in stress field. This process goes on for thousands of years until the CO2 dissolves or is immobilized and converted into solid carbonate minerals. During this period, excessive injection pressure, reservoir pressurization, and dynamic stress patterns can lead to fracture initiation and/or propagation in the caprock. Precipitation and dissolution of carbonate minerals may enhance or decrease fracture

permeability, respectively. These processes can alter the seal capacity and integrity, ultimately impacting the safety and efficiency of the GCS project.

2.3 Leakage and Risk Assessment

The fundamental concept behind GCS is to reduce and remove CO2 from biosphere and atmosphere. Therefore, GCS is similar to natural occurrences of permanent or long-term geological storage of natural gases in several ways, such as geochemical and residual trapping occurring in the injected formation (Pearce et al., 1996; Baines and Worden, 2004; Miocic et al., 2013). This conclusion assumes the caprock is free from faults, fractures, and heterogeneities; however, most regional aquifers are not closed and the overlying confining strata is not perfectly known nor impervious (Neuzil, 1994; Dewhurst et al., 1999). Long-term safe storage of sequestered CO2 is only feasible when the caprock is intact and does not allow significant flow.

Recent progress has been made to assess CO2 leakage from aquifer storage formations through abandoned boreholes (Kopp et al., 2010; Celia et al., 2011, Jung et al., 2013), faults and fractures (Rutqvist et al., 2007; Morris et al., 2011), and to surface or freshwater bodies (Oldenburg and Lewicki, 2006) (Fig. 2.5). The petroleum industry has conducted extensive research investigating causes of caprock failure, self-sealing faults, and the overall properties of caprocks; however caprock in the presence of hydrocarbons exhibit different chemical and wettability properties. Research is limited on caprock behavior and leakage in GCS.

Three primary mechanisms cause leakage through a caprock: capillary breakthrough, flow through fracture networks or faults leaky abandoned boreholes, and diffusive loss. Caprocks can be classified by their failure mechanism: membrane seals and hydraulic seals (Watts, 1987). Membrane seals refer to capillary-sealing efficiency. Hydraulic seals are characterized by very high capillary entry pressures. Caprocks whose primary sealing mechanism is controlled by capillary entry pressure and fail due to capillary leakage are referred to as capillary or membrane seals (Fig. 2.6). Capillary forces exert pressures at the interface between a non-wetting phase (CO_2) and wetting phase (water or brine) in the caprock. The minimum pressure needed to initiate displacement of the wetting phase is referred to as the breakthrough pressure, and the pressure at which a phase enters the caprock is referred to as the entry pressure. As a

generalization, sealing capacity increases with decreasing pore size, decreasing wettability, and increasing interfacial tension. Once the entry capillary pressure has been exceeded, flow and leakage becomes a function of intrinsic permeability (Hildenbrand et al., 2002). Before breakthrough pressure is exceeded, diffusion is the only process in which CO2 can enter a caprock (Krooss et al., 1992; Krooss et al., 2004). Where there is a CO2 concentration gradient, CO2 can migrate by molecular diffusion.

Caprocks exhibiting extremely high or essentially infinite capillary entry pressures are considered hydraulic seals and can fail due to fracturing of the caprock. Where pore pressures in the aquifer or caprock exceed its mechanical strength, hydraulic sealing may fail and result in microcracks or tensile-fracturing (Rutqvist and Tsang, 2002; Rutqvist and Stephansson, 2003; Vilarrasa et al., 2011). Pre-existing faults and fractures can act as preferential flow paths and barriers for migrating CO2. During and after CO2 injection, pore pressures in the storage aquifer can increase. This can change the confining pressure and decrease the effective stress, which can cause propagation of pre-existing faults or fractures in the caprock (Jimeneze and Chalaturnyk, 2001).

2.4 The Illinois Basin for CO2 Sequestration

In 2003, the U.S. Department of Energy (U.S. DOE) initiated the Regional Sequestration Partnership (RCSP) programs to address the technical issues of geological storage of CO2 in various regions of the United States. Each partnership is engaged in assessing risks associated with large-scale and pilot projects with particular emphasis on the feasibility of GCS in saline reservoirs. The MGSC, a partnership that includes three state geological surveys in the Illinois Basin, has partnered with Archer Daniel Midland Company (ADM) and Schlumberger Carbon Services to conduct large-scale deployment of GCS. The large-scale GCS project is called the Illinois Basin – Decatur Project (IBDP) (Fig. 2.7 and Fig. 2.8). An on-site ethanol plant captures and injects CO2 into the lower unit of the Mt. Simon Sandstone, a deep sandstone reservoir extending into Illinois, Minnesota, Wisconsin, Kentucky, and Indiana. The Eau Claire Formation conformably overlies the Mt. Simon Sandstone and acts as the regional caprock and aquitard. The Mt. Simon Sandstone is capable of storing between 26 and 109 billion metric tonnes of CO2 (U.S. Department of Energy, 2015) at an approximate depth of 2,000 m and maximum thickness

of 790 m (Leetaru et al., 2009). The IBDP injected 1,000 metric tons per day into the lower Mt. Simon Sandstone over the three-year injection period. Operational injection began on November 11th, 2011 and was completed on November 26th, 2014.Three wells have been drilled at the IBDP site on ADM property. The injection well, CCS1, is the single injection well drilled to a total depth of 2,205 m. Two monitoring wells, referred to as verification well 1 (VW1) and verification well 2 (VW2), are drilled to 2,216 m and 2,202 m, respectively. Geophysical logs and core obtained from these wells have furthered the lithological understanding of the reservoir and caprock system.

2.4.1 Regional Geology and Structure

The Cambrian-age Mt. Simon Sandstone is the thickest and most wide-spread formation having the potential for CO2 injection in the Illinois basin (Leetaru and McBride, 2009). The Illinois Basin is one of several cratonic basins of North America. It is asymmetrical, spoon-shaped basin which trends northwest-southeast and covers an area of approximately 135,000 square miles in parts of Illinois, Indiana, and Kentucky (Finley, 2005). The thickness of the Mt. Simon Sandstone ranges from less than 150 m in southern Illinois to 790 m in southeastern Illinois at its depocenter (Kolata and Nelson, 2010; Freiburg et al., 2014). The Illinois Basin has the largest number of saline reservoir, natural gas storage fields in the United States and a long history of natural gas storage in Cambrian-age formations (Mehnert et al., 2015). These natural analogs provide valuable information, insights, and a stable scientific foundation in which to analyze GCS in the Illinois Basin (Mehnert et al., 2015).

The Eau Claire Formation is composed of three members. The confining zone consists of the upper two members, the Lombard and Proviso members, and is regarded as the most important regional confining zone in Illinois (Leetaru et al., 2009). The lowermost member of the Eau Claire is the Elmhurst Sandstone. Combined, the Elmhurst and the Mt. Simon Sandstone comprise the injection and storage zones of many natural-gas storage sites in Illinois Basin. The Davis Member of the Franconia Formation, the Maquoketa Formation, and the New Albany Shale form additional seals above the Eau Claire Formation. Additionally, shale interbeds in the Mt. Simon Sandstone act as baffles to vertical flow (Finley, 2005; Finley et al., 2013). For this study, the Eau Claire will be considered the primary seal.

At IBDP, the Mt. Simon Sandstone unconformably overlies a sandstone interval, which has been referred to as the pre-Mt. Simona and the Argenta Formation (Freiburg et al., 2016). Although the Argenta is not formally recognized, it will be referred to as the Argenta Formation in this work. Underlying the Argenta Formation is the Precambrian-age impermeable crystalline basement. The Mt. Simon Sandstone is a member of the Potsdam Supergroup and the lowermost member of the Sauk transgressive sequence in the Illinois Basin. Of the Knox Group, the Eau Claire comformably overlies the Mt. Simon Sandstone (Kolata and Nelson, 1990). The Mt. Simon and Eau Claire Formation extend over a large portion of the Midwestern United States, including the entirety of the Illinois Basin.

There are numerous folds and faults in the Illinois Basin, including several north-trending, asymmetrical anticlines and monoclines (Fig. 2.8). These folds include the DuQuoin monocline, La Salle 'Anticlinorium' (LSA), Louden, and Clay City Anticlines. Although most of the Illinois Basin is considered tectonically stable, several fault systems have been identified. The Wabash Valley Fault System is a major fault system of a series of transgressive reverse faults located in southern Illinois. The New Madrid Seismic Zone (NMSZ), located near the borders of Illinois and Kentucky is a host of seismic activity.

The Illinois Basin is surrounded by prominent arches and domes. The uplifted nature of the Precambrian basement is apparent by the Wisconsin Arch and Kankakee Arches in the north, the Mississippi River Arch to the northwest, the Pascola Arch in the south, and the Cincinnati Arch in the east. The Nashville and Ozark Domes bound the southeast and southwest, respectively.

2.4.2 Major Stratigraphic Units

The following discusses lithological characteristics and hydrogeological significance of Precambrian and Cambrian rocks of the Illinois Basin (Fig. 2.9): the Precambrian basement, Argenta Formation which underlies the Mt. Simon Sandstone, Mt. Simon Sandstone, and confining units of the Eau Claire Formation (Proviso and Lombard).

Precambrian Basement

The Mt. Simon Sandstone lies unconformably on Precambrian basement composed of igneous and metamorphic rock. Displaying some regional variation in rock composition, Precambrian basement rocks are granite and granodiorite in the north, and grano-rhyolite in the south (Leetaru

and McBride, 2009). Using 13 core samples, Sminchak (2011) published average permeability and porosity values as 0.0008 mD and 0.018%, respectively. At IBDP, the uppermost basement is composed of fractured maroon-colored porphyritic rhyolite (Leetaru and Freiburg, 2014). The Precambrian basement rock represents a basal confining, no-flow boundary for proposed injection of CO2 into the Mt. Simon Sandstone.

Precambrian highs have been mapped on the Precambrian basement by Leetaru and McBride (2009) using seismic reflection data and borehole mapping. Precambrian basement strata occur at depths of 4,300 m in southeastern Illinois and can reach highs at 610 m in northern Illinois. Structurally, the Mt. Simon Sandstone is thinnest or nonexistent at Precambrian basement highs and thickest along the flanks of those highs. The contact between the Argenta Formation and the Precambrian basement is sharp; the existence of weathering indicates an unconformity which is consistent with the Precambrian and Cambrian age gap of approximately 1 billion years (Leetaru and Freiburg, 2014).

Argenta Formation

Recent studies have identified a new stratigraphic unit in the Illinois Basin at the IBDP site; the Argenta Formation is the lowermost sedimentary rock at IBDP, unconformably overlying the crystalline basement and underlying the Mt. Simon Sandstone (Freiburg et al., 2016). On the basis of geophysical logs, the formation is correlated into northeastern Illinois. The Argenta Formation is interpreted as dominantly shallow-marine shoreface to fan-delta deposits composed of sandstone conglomerate with rare interbedded mudstone. Characterized by distinctly lower porosity and permeability than the overlying Mt. Simon Sandstone, it acts as a confining unit between the crystalline basement and the lowermost member of the Mt. Simon Sandstone. The top 0.34 m is marked by dark brick-colored well-cemented sandstone with a sharp conformity with the Mt. Simon (see Figure 12A in Freiburg et al., 2014). The bulk of the Argenta consists of pink-grey-tan to dark maroon pebble conglomerates and sandstones. Sandstone lithologies are quartz arenite and wacke with abundant vertical *Skolithos* burrows (see Figures 10B and 10C in Freiburg et al., 2014). The age of the Argenta is uncertain. The Upper Mt. Simon Sandstone is estimated to be Middle Cambrian Age due to the presence of Guzhangian index fossils in the Eau Claire/Bonneterre Formation in Missouri and Iowa. The presence of *Skolithos* trace fossil

burrows indicates that the Argenta must be Cambrian in age, however whether the Argenta is Upper, Middle or Lower Cambrian cannot be determined (Freiburg et al., 2016).

Mt. Simon Sandstone

The Mt. Simon Sandstone is a well-studied formation and has been characterized in recent works (Leetaru and McBride, 2009; Bowen et al., 2011; Leetaru and Freiburg, 2014; Freiburg et al., 2016). Historically, the Mt. Simon Sandstone has been used for natural-gas storage, and detailed analyses for these projects were limited to the upper unit of the Mt. Simon Sandstone (Mehnert et al., 2015). In the past decade, drilling of additional deep wells resulted in better understanding of the Mt. Simon Sandstone.

The Mt. Simon Sandstone outcrops in Minnesota, Wisconsin, and Iowa. Correlative formations may include the Bayfield sandstone in northern Wisconsin and the Lamotte Sandstone in Missouri (Gupta and Bair, 1997). Regionally, the Mt. Simon Sandstone varies in lithology from conglomerate to sandstone to shale. At IBDP, the Mt. Simon can be subdivided into three major lithostratigraphic (Upper, Middle, and Lower) sections based on wireline, core analyses, and vertical seismic profiles (Freiburg et al., 2014; Freiburg et al., 2016). Predominant Mt. Simon Sandstone lithologies are fine- to median-grained quartz or subarkosic arenite with shales, wackes, and sublithic arenites. The Lower Mt. Simon (1,951 to 2,134 m) includes mixed fluvial to eolian deposits predominantly composed of a feldspathic wacke to lithic wacke. The Middle Mt. Simon (1,795 to 1,951 m) includes fluvial to eolian deposits predominantly composed of medium- to coarse-grained cross-bedded subarkosic and quartz arenites with rare mudstones, and fine- to medium-grained planar-laminated and cross-bedded quartz arenites and quartz wackes. The Upper Mt. Simon (1,684 to 1,795 m) is marked by marine deposits composed of medium- to fine-grained bioturbated cross-bedded quartz to subarkosic arenites with thin interbedded black shales and mudrocks. The Upper Mt. Simon transitions upward into the basal marine facies of the Eau Claire. This continental to marine transition is indicative of basin subsidence and marine transgression. The Mt. Simon shows a trend of decreasing porosity with increasing depth (Medina et al., 2011). The Lower section of the Mt. Simon Sandstone contains the highest quality reservoir rocks for GCS and exhibits the highest porosity of all sections; porosity for the Lower Mt. Simon ranges from 16.6% to 27% (Freiburg et al., 2014).

Eau Claire

The Eau Claire is named for an outcrop of thinly bedded, shaly fossiliferous sandstone near Eau Claire, Wisconsin (Walcott, 1914; Willman et al., 1975). The Eau Claire is a laterally extensive and heterolithic formation exhibiting high variation in lithology. It is composed primarily of carbonates and siliciclastic sediments. The Lombard and Proviso members of the Eau Claire form the low permeability confining layer at many of the natural gas storage fields in Illinois. The confining members overly the Elmhurst Member, and the Proviso Member overlies the Lombard Member (Kolata and Nelson, 2010). In the Illinois Basin, the Eau Claire thickness ranges between 60 m in southeastern Wisconsin to 300 m in the southern Illinois Basin (Finley, 2005). The Eau Claire reaches maximum thickness of 838 m near the Illinois Basin depocenter in western Kentucky (Willman et al., 1975). At the ADM injection site, the Eau Claire is 152 m thick (Leetaru and Freiburg, 2014).

Generally, the Eau Claire trends from a siltstone or shale in central Illinois to a sandstone or sandy dolomite in northern Illinois to a fine-grained sandstone in southcentral Wisconsin (Kolata and Nelson, 2010; Aswaserrelert et al., 2008; Finley, 2005). The Proviso member consists primarily of limestone and dolomite interbedded with shale layers. The Lombard member is primarily a sandy and glauconitic dolomite interbedded with shale; sand content increases in the northwest and grades to a shale in the south (Fig. 2.10). Near Missouri, the Bonneterre Formation, a relatively pure dolomite, is correlative to the Lombard member of the Eau Claire. In northern Illinois and south central Wisconsin, the basal of the Eau Claire becomes sandier and is referred to as the Elmhurst sandstone (Visocky et al., 1985). The Elmhurst is widely distributed in the northern half of Illinois with thickness ranging from 3 m to 30 m thick. This unit is a fine- to medium-grained fossiliferous gray, red, or white sandstone interbedded with various amounts of shale layers. Near the Wisconsin border, shale content significantly decreases (Visocky et al., 1985; Willman et al., 1975; Young 1992). The relatively clean Elmhurst sandstone member of the Eau Claire and the Mt. Simon Sandstone are often grouped together in modeling efforts (Visocky et al., 1985; Young, 1992).

The Eau Claire is not well understood nor well researched. Limited coring through the Eau Claire prevents stratigraphic characterization and petrophysical testing. The unit is not typically isolated for packer tests or coring efforts. Historically, the Mt. Simon Sandstone has been the target formation for coring studies at natural gas storage sites. Very few wells at natural gas

storage fields in the Illinois Basin have laboratory core analyses for the Eau Claire. Coring activities at these wells are typically limited to the basal Eau Claire – Mt. Simon contact. Griffith et al. (2011), Neufelder et al. (2012), and Palkovic (2015) have made recent significant advances in characterizing the Eau Claire. Using petrographic analysis of 66 core samples from seven wells across the Illinois Basin (Illinois, Indiana, and Kentucky), five distinct lithofacies were observed in the Eau Claire (Neufelder et al., 2012): sandstone, clean siltstone, muddy siltstone, silty mudstone, and shale. In this study, Eau Claire core porosity ranged from 0.02% to 0.24% and permeability to water values ranged from $1x10^{-5}$ mD ($9.87x10^{-21}$ m^2) to 580 mD ($5.72x10^{-13}$ m^2). Eau Claire porosity and permeability values from VW1 and VW2 at IBDP are plotted with respect to depth in Figures 2.11 and 2.12.

The IBDP provides a comprehensive drill core through the Eau Claire. Verification well #1 provides 31 m of 10-cm core through the lower Eau Claire. Nine meters of whole core was recovered from CCS1 well and 13 m of whole core was recovered from VW2. Palkovic (2015) conducted core and facies analysis of samples from all three wells. At VW1, two lithostratigraphic units of the Eau Claire were identified: a dominantly siliciclastic lower component containing the highest quality seal (9 m) of shale with an average porosity and permeability of 5.8% and $2.0x10^{-5}$ mD or $4.85x10^{-20}$ m^2, and a mixed siliciclastic carbonate environment with a point porosity of 0.01% (Palkovic, 2015). Witherspoon and Neumann (1967) report porosity and permeability of the shale unit of the Eau Claire at the Leaf River Project of Northern Illinois Gas Co, 9.5% and $1.78x10^{-15}$ m^2, respectively. The Midwest RASA model reports a permeability range of $1.5x10^{-16}$ to $2.4x10^{-17}$ m^2 (Mandle and Kontis, 1992).

The Eau Claire has been represented as a simplified confining unit in previous models, and often as a single layer (Feinstein et al., 2010; Feinstein et. al., 2005; Meyer, 2009), and (Gupta and Bair, 1997). In the IBDP basin-scale model, the Eau Claire is represented by three or layers then subdivided into several regional zones defined by varying hydraulic conductivity and porosity. The Regional Aquifer-System Analysis (RASA) Program model of the Cambrian-Ordovician aquifer system in the Midwest United States assigned a single layer in the groundwater model, but recognized the regional lithology differences by assigning zones of vertical hydraulic conductivities. To date, no sensitivity analysis has been performed to test the representation of

the Eau Claire (parameters or model structure) to the above GCS and groundwater simulation models.

2.5 Physical Characteristics of Caprocks

Understanding of the caprock system is a cornerstone to ensuring the long-term storage security of any GCS project. It is important to learn from historical industrial practices of subsurface storage of natural gas and pay attention to the reported potential of gas leakage through caprocks (Krooss et al., 1992; Hildenbrand, 2002). The effectiveness of a seal over geological time periods controls its ability to prevent migration into overlying freshwater aquifers, economic reserves, and eventual migration to the atmosphere.

Lack of complete caprock core limits potential petrophysical investigations to smaller sample sizes. Core material and analysis from reservoir rocks is regularly collected and performed, whereas caprock material is typically available in the form of cuttings. Notable advances in caprock research include Busch et al. (2008), Daniel and Kaldi (2009), Busch and Amann-Hildenbrand (2013), and Wollenweber et al. (2009). Review papers of caprock sealing mechanisms and physical characteristics have been conducted by several authors (Grunau, 1987; Michael et al., 2010; Shukla et al., 2010; Griffith et al., 2011; Song and Zhang, 2013). Landmark research in classifying fine-grained sediments and mudrocks include Grainger (1984), Loucks et al. (2012), and Yang and Aplin (2007).

Any type of lithology can theoretically act as a caprock. Shales, mudrocks, and evaporates are the most common. Evaporites are not present in the Illinois Basin (Kolata and Nelson, 2010). The focus of this work is argillaceous rocks that can provide adequate sealing in GCS. The basic characteristics which have influence on the mechanical properties and performance of mudrocks are grain size, mineralogical composition, and microfabric (Grainger, 1984). An overview of the dominant physical characteristics of caprocks and their relation to CO2 containment in the Illinois Basin are presented. The ability to retard vertical fluid migration is a complex issue as the CO2 will be in direct contact with the seal due to buoyancy and often involves geochemical, geomechanical, and hydrodynamic processes. Due to this complexity, not all factors have been addressed. The scope of this section is limited by the following:

- Fluid transport mechanisms are discussed under saturated conditions. Caprocks in deep saline aquifers are water-saturated, and injection of CO2 is likely to occur at supercritical conditions.

- Argillaceous sediments are the most common caprock lithology. Evaporites are not present in the Illinois Basin. Despite their sealing potential, they are not discussed. Indurated mudrocks are the focus.

- This literature review places emphasis on the physical and hydrodynamic significance of caprocks. Geomechanical aspects of caprocks are limited to a discussion of ductility and bulk compressibility. Discussion of geochemical reactivity with CO2 and caprock mineralogy is incorporated throughout the review.

2.5.1 General Characteristics

Effective caprocks are typically thick, laterally continuous, ductile rocks with high capillary entry pressures (Potter et al., 2005). The assessment of caprocks as reliable seals for GCS can be considered in terms of the caprock's sealing capacity and sealing integrity. This generalization can be helpful as caprock in the presence of CO2 involve several physical processes. Sealing capacity applies to caprock evaluated as capillary or membrane seals where leakage occurs through preexisting interconnected pores. In contrast, sealing integrity applies to caprocks as hydraulic seals where leakage occurs through fractures opened by pressure in the reservoir. This terminology will be used throughout this chapter.

Seal Geometry

Theoretically, a thin layer of homogenous shale is enough to provide an adequate seal. Capillary sealing occurs at the CO2-caprock interface and is independent of the thickness of the overlying caprock (Ingram et al., 1997). Any increase in seal thickness cannot increase the membrane seal capacity as the major rock-related control is the capillary entry pressure (Watts, 1987). However, rarely are thin strata regionally extensive, laterally continuous, and unbroken. Griffith et al. (2011) investigated physical and chemical characteristics of 17 geologic seals considered for GCS in the US, which were generally thick, ranging from 6 m to 352 m. Within their respective site, the seals were generally thick, but not laterally continuous and did not have uniform

lithology. Due to their depositional environment, caprocks can either be in the form of a single, thick, laterally continuous unit, or part of a multi-layered system where permeable layers are interbedded with low permeable layers, or intraformational seals. For hydraulic membranes, thickness exceeding 50 m in areas of low tectonic activity are considered good (Grunau, 1987). Furthermore, thicker seal strata have higher propensity to resist fracturing due to injection pressure and gradual pressure build-up in the reservoir. Conversely, for massive very low permeability seals, mechanical effects become more important where the pore throats in the caprock are so small that chances of capillary breakthrough are very unlikely and the seal may only leak through hydrofracturing, or by forming linked, permeable, dilatant fractures (Ingram et al., 1997).

Lithology

Argillaceous rocks (shales, mudstones, and clays) and evaporites (anhydrites and salts) are typically identified as caprock seals for GCS. These lithologies typically have high entry pressure, laterally continuous, and ductile, and maintain lithology over large areas (Downey, 1984). In addition, Corcoran (2002) estimates argillaceous rocks act as seals for 25 of the largest oil and gas fields across the world. Michael et al. (2010) reviewed the experiences from 17 pilot, demonstration and commercial operations injecting CO2 into saline aquifers. Seal lithology was identified as shale for ten projects and mudstone for three projects. Shale is considered the superior lithology for caprock seals; lithologies other than shale (mudstones, argillaceous limestones, cherts, tight sandstones and conglomerates, and coal beds) are considered subordinate caprocks and are considered partial seals (Grunau, 1987).

Grain composition and depositional environment are major controls on caprocks. Argillaceous rocks require low-energy depositional environments such as a marine shelf or a meandering river and floodplain. Low permeability rocks exhibit unique flow behavior due to depositional and diagenetic issues. Caprock seals typically exhibited lateral facies variation, fractures, and spatial variation in thickness, porosity, and permeability. Attaining qualitative measurement and differentiation of fine-grained argillaceous rocks is difficult (Loucks et al., 2012).

There is lack of agreement on classification systems and terminology for low-permeability rocks differs in the literature (mudstone: Yang and Aplin, 2007; mudrock: Ingram, 1953 and Chang et al., 2013; shale: Keith and Rimstidt, 1985). From a sedimentary geology perspective, shale is

considered a fine-grained and fissile rock. Ingram (1953) coined the term "mudrock" as a rock that contains more than 50% silt and/or clay. Mudrocks can be further classified on the basis of texture and fissility (Folk, 1980).

Grain size of clay fraction	**Non-fissile**	**Fissile**
less than 1/3 clay	Siltstone	Silt-shale
Silt ≈ clay	Mudstone	Mud-shale
more than 2/3 clay	Claystone	Clay-shale

Table 2.1: Classification of indurated mudrocks (adapted from Folk, 1980)

For engineering purposes, mudrocks require more attention than the above classification allows and classification should include the mechanical properties of mudrocks (Grainger, 1984). A durable mudrock can be defined in terms of grain size, composition, texture, and compressive strength perpendicular to the rock fabric, and slake durability: 1) grain size -- fine- to very-fine, where greater than 35% of grains are silt or clay-sized; 2) composition -- at least 65% (total dry weight) silicate minerals, and a minimum of 50% is quartz and clay minerals; 3) texture – greater than 50% of total volume is composed of sedimented, detrital, inorganic grains; 4) compressive strength perpendicular to the fabric (point load testing or cone indenter) is greater than 3.6 MN/m^2, and 5) slake durability greater than 90% (Figures 1 and 2 in Grainger, 1984). Classification of durable mudrocks (Fig. 2.13) is based on fissility, quartz content, and anisotropy (Grainger, 1984). In this case, a "shale" signifies a durable material, where "silty" describes the quartz content. A non-shaley mudrock is referred to as durable mudstone. Mudrocks with quartz content greater than 40% are rarely anisotropic and are referred to as durable siltstones (Grainger, 1984). Slate and argillite have compressive strength greater than 100 MN/ m^2, and are not classified as mudrocks.

The mineral composition of caprock plays a significant role in its ability to perform effectively as a regional seal. It is widely known shales are highly reactive. Mineral dissolution and precipitation has been shown to affect its petrophysical and transport properties; however these

interactions are not clearly defined and require further investigation. Different mineral compositions ranging from quartz, calcite, anorthites, feldspar to muscovite, chlorite, illite, kaolinite and smectite have been reported for mudrocks (Wollenweber et al., 2009). Dominant minerals among the seal formations are quartz, dolomite, and glauconite and illite clay minerals in the shale facies (Griffith et al., 2011). Mudrocks containing pyrite and quartz are considered chemically and mechanically stable; whereas carbonates, feldspars and phosphates are considered relatively mechanically stable and chemically stable (Fig. 2.14). Clays are ductile and deform easily, making them mechanically unstable and can transform into illite with increasing temperature with burial (Loucks et al., 2012). Illite crystallization produces a strengthening of the rock (Grainger, 1984).

Chemical reactivity studies of a shale caprock in the presence of CO2 indicate significant changes in capillary sealing efficiency (Wollenweber et al., 2009; Alemu et al., 2011). The resulting reaction of acidic CO2-rich fluids on the caprock can be either advantageous or disadvantageous for containment. The leaching of minerals within the caprock may increase the shale's permeability leading to potential CO2 movement through the caprock. In contrast, a decrease in permeability could further seal off the caprock and contribute to improved sealing capacity.

2.5.2 Hydrodynamics and Capillary Pressure

The movements of gases and fluids in low permeability media have historically been discussed in terms of hydrocarbon migration. However, principles of hydrocarbon migration are directly applicable to flow properties of sequestered CO2. These theories include the principles of relative permeability, multiphase flow (Ingram et al., 1997; Hildenbrand et al., 2004; Hildenbrand et al., 2013), diffusion (Krooss et al., 1992), flow through naturally fractured shale (Edlmann et al., 2013), flow through tectonically induced fractures (Ingram and Urai, 1999), and leakage risk due to mineral dissolution (Fitts and Peters, 2013). A review and summary of capillary pressures of low permeability rocks is provided by Hildenbrand et al. (2002).

Argillaceous rocks exhibit extremely small particle sizes with very large surface areas, are highly reactive, and exhibit very strong hydromechanical responses. Clay-rich materials exhibit a range of porosity values, but due to low permeability, advective fluid flow is unlikely to be the

dominant transport mechanism. Flow through microfissures is often represented as effective permeability in Darcy's law.

Capillary sealing has been identified as the primary mechanism controlling a caprock's sealing capacity to counterbalance buoyancy forces from the CO2 plume (Song and Zhang, 2013). When CO2 accumulates at the seal boundary, pressure can increase until the capillary breakthrough pressure is exceeded. Breakthrough pressure is defined as the minimum pressure needed to initiate displacement of brine in the caprock. The capillary seal is a function of permeability, pore-throat size, the density difference between brine and CO2, wettability, and interfacial tension (Hildenbrand et al., 2013). Once the CO2 column height exceeds breakthrough pressure, flow of CO2 is controlled by the intrinsic permeability of the caprock. Snap-off pressure is the difference in pressure between CO2 and brine when the pore throat is closed by re-imbibition of the brine in to the pores. Mudstones and shales can hold very large hydrocarbon columns; however, there are wettability and interfacial differences between CO2 and other fluids as indicated by experiments on capillary entry pressure with CO2 on shales. Hildebrand et al. (2004) have carried out extensive research on these properties for argillaceous materials using fluids such as water, N2, and CO2. Highest capillary displacement pressures were found for N2 and lowest capillary displacement pressure were obtained for CO2 tests.

Relative gas permeability theory

In single-phase flow, the ability for a rock to conduct fluid depends on its intrinsic permeability. Intrinsic permeability is estimated using Darcy's law for incompressible porous media. It states flow is proportion to the pressure gradient. A porous rock containing two fluid phases has an effective permeability to each fluid phase dependent on its saturation (Nordbotten and Celia, 2012). In fully saturated conditions, the effective permeability is equal to the intrinsic permeability when a single fluid saturates all pores. Effective permeability of gas in brine saturated media can be calculated using Darcy's law for compressible media:

$$q_{nw} = \frac{kk_{rnw} A \Delta P_{nw}}{\mu_{nw} L}$$

The subscript *nw* represents the nonwetting fluid (CO2 in this case), *q* is the volumetric flow rate, μ is the viscosity, and D*P* is the pressure change along the porous medium in the various

fluid phases. The value kk_{rnw} is the effective permeability of the gas in the brine saturated porous media. This extension of Darcy's law suggests that displacement of the wetting phase will create pore space for the gas phase. However, increasing gas saturation results in decreased gas permeabilities and is believed to occur at the expense of the fluid phase. To account for this effect, the Klinkenberg correction is applied to make the relative gas permeabilities comparable to its intrinsic permeability. Water permeabilities are often estimated to be lower than the Klinkenberg-corrected gas permeabilities. Darcian theory cannot account for the swelling and shrinkage of clays, residual gas trapping, diffuse double layers, and the presence water films on mineral surfaces.

Modeling Permeability for Fine-Grained Sediments

Fluid flow in low-permeability environments is not well understood due to the large variations in transport and mechanical properties (Dewhurst et al., 1999). The ability to perform accurate in situ permeability measurements is limited by instrumentation and the very long time frame required for testing relatively low permeability media. Permeability of argillaceous materials, either soils or rocks, have been extensively researched, but are still subject of debate. However, it is clear that spatial scale, structure, mineralogy, porosity, and geochemistry are parameters that control permeability. The importance of lithology is shown in Figure 2.15 which shows for a given porosity, the siltier sample (lower clay fraction) exhibits higher permeability than the clay-rich sample.

Mudrock permeabilities are anisotropic with higher values parallel to bedding planes. Lithological heterogeneities such as clay laminations and preferential grain alignment are a result of depositional environment and induration, or mechanical compaction. Published permeability data for argillaceous rocks are sparse, and range around six orders of magnitude, with a three orders magnitude range in corresponding porosity (Yang and Aplin, 2010). Due to the low permeabilities in mudrocks, several models have been developed to measure permeability in a laboratory or infer it from geophysical models. Permeability is predicted from empirical permeability-porosity relationships derived from laboratory measures (Yang and Aplin, 2010), or using theoretical models such as Kozeny-Carman (Carman, 1956), models based on pore size distribution (Yang and Aplin, 1998), or dual-permeability models.

Kozeny-Carman model has been used fairly successfully for the prediction of sandstones and soil permeabilities. It models permeability as a function of easily measured petrophysical parameters, porosity, specific surface area, and a particle shape factor. Dewhurst et al. (1999) compared measured porosity-permeability relationships with two mudstones and the permeabilities derived using the Kozeny-Carman equation (Fig. 2.15). The model produced considerable discrepancies between predicted and measured permeability values. Several Hagan-Poiseuille models have been developed based on theoretical pore size distribution and the assumption that porous media is composed of equal diameter parallel tubes. The Kozeny-Carmen and Hagan-Poiseuille models do not consider the wide pore size distribution of mudstones. Both models do not accurately predict permeability of natural clays and routinely overestimate measured values by in excess of two orders of magnitude (Dewhurst et al., 1999).

Lithology is a major control on porosity and permeability relationships. Yang and Aplin (1998) confronted the issue of anisotropy and pore size distribution. Based on Hagan-Poiseuille equations, their model includes parameters for pore size, pore geometry, particle alignment, clay fraction, and dependence on effective stress. Using 261 marine mudrock samples, Yang and Aplin (2010) constructed a log-linear relationship between permeability and porosity, and when clay fraction is used as a quantitative lithological descriptor, the uncertainty in the predicted permeability is greatly decreased. Busch and Amann-Hildenbrand (2013) recently reviewed published petrophysical datasets of low permeability rock samples. The database consists of 233 datasets of mineralogical and petrophysical data including porosity, permeability, specific surface area, capillary breakthrough pressure, and mercury porosimetry estimates. Permeability was predicted using the Yang and Aplin (1998) model from porosity and surface area of samples. The approach produced the accurate predictions for core permeabilities greater than 10^{-20} m^2.

Current permeability models for low permeability rocks are inadequate and can only be used over a culled range of permeabilities and porosities. Furthermore, Neuzil (1994) remarked it is not possible to predict how or where heterogeneity will affect permeability at a larger scale. Therefore, there is permeability scaling issues. For example, if permeability at the well-field scale tends to be higher than core permeability, it may suggest the presence of fractures or faults. Field-scale mudstone permeabilities, both measured and modelled, appear in some cases to be greater than those measured on core plugs in the laboratory (Dewhurst et al., 1999). To test

permeability models effectively, there needs to be more published datasets of argillaceous lithologies.

Geomechanical Characteristics

Stress, strain, pore geometry, ductility, fracture, thickness and material homogeneity play important roles in caprock integrity (Vilarrasa et al., 2011; Shukla et al., 2011; Wang et al., 2010; Grainger, 1984;). These properties are controlled by caprock mineralogy, regional and local stress fields as well as any stress changes induced by injection. Pressure changes during and after injection of CO2 can propagate preexisting faults, fractures, and fissures. Pressurization of the reservoir-caprock system depends on permeability and if the system is open or closed to brine displacement. Seal integrity refers to the propensity of the caprock to either brittle failure or ductile behavior. Also, preexisting faults or fractures can enhance or retard fluid movement in the caprock. Therefore, it is crucial to understand the locations, geometries and permeabilities of such features.

Seal integrity (strength) becomes more important when capillary breakthrough is unlikely in very low permeability shales. A brittle mudrock will increase its permeability by developing dilatant fractures (Fig. 2.16), whereas a ductile shale is able to undergo plastic deformation without increasing its permeability via non-dilatant sealing fractures (Ingram et al., 1997). Microfabric of fissile mudrocks exhibit low cohesion and/or low tensile strength (Grainger, 1984). Mudstones are more likely to fracture by shear forces rather than by extensional forces (Dewhurst et al., 1999) and fractures are more likely to form horizontally along planes of weakness rather than vertically. Strongly anisotropic microfabric produces a general planar fissility and compositional laminations in some mudrocks produce planes of weakness (Grainger, 1984).

Arrangement of particles in sediments is defined by lithology, porosity, porosity distribution, and change due to burial and diagenesis. As muds are buried and exposed over time to higher pressures and temperatures, they decrease in volume and porosity, and become lithified (Loucks et al., 2012). Initial porosity is affected by depositional environment, mineralogy, and other factors. Loucks et al. (2012) classifies mudrocks based on pore type and relation to mineral matrix. Pores found between particles and grains (interparticle pores) and pores located within particles (intraparticle pores). Fabrics composed of soft and ductile grains (clay particles) are susceptible to deformation such as burial and overburden stress, and interparticle pore space can

distort, closing pore space, and decreasing permeability (Loucks et al., 2012). Conversely, rigid grains such as quartz and feldspars are more resistant to compaction. In older mudrocks, intraparticle pores are typically absent, presumably destroyed to mechanical compaction or have been filled with cement. Clay-rich sediments are more compressible than silt-rich samples (Dewhurst et al., 1998) and that small pores are inherently stronger than large pores and require a higher effective stress to cause pore collapse.

Pressure propagation through a caprock due to injected CO2 has been evaluated in a few studies (Benisch and Bauer, 2013; Chang et al., 2013; Birkolzer and Zhou 2009). Neglecting rock compressibility will lead to an overestimation of the pressure build-up of injected CO2 and underestimate storage capacity (Benisch and Bauer, 2013). Caprock compressibility values used in CO2 reservoir simulation studies is often $4.5x10^{-9}$ Pa^{-1} (Birkholzer et al., 2009; Zhou et al., 2008). Compressibility for the Eau Claire caprock in the large-scale GCS model of the Illinois Basin is $7.42x10^{-10}$ Pa^{-1} (Mehnert et al., 2014). The relationship between compressibility and applied pressure of 16 argillaceous sediments is reported in Rieke and Chilingarian (1974). Bulk compressibility of the oil shale unit in the Green River Formation and a pure illite clay saturated in distilled water were found estimated at various net-confining (hydrostatic) pressures. At 10, 20, and 25 MPa, the experimental bulk compressibility estimates for the illite clay sample were $1.3x10^{-8}$, $5.8x10^{-9}$, and $2.18x10^{-9}$ Pa^{-1}, respectively (Cebell and Chilingarian, 1972). At the same three overburden pressures, the experimental bulk compressibility estimates for the shale sample were all approximately $3.63x10^{-11}$ Pa^{-1} (Rieke and Chilingarian, 1974).

2.6 Summary

The success of a commercial scale deployment of GCS requires containment of the injected CO2. Therefore, it is important to understand the caprock-reservoir system so as to minimize leakage risk. The foregoing discussion has presented an intriguing picture of the ability of argillaceous sediments to act as caprock for carbon storage. Core data from target reservoirs are collected regularly for petrophysical laboratory experimentation, yet caprock core samples are rarely collected. There exists a distinct lack of geological understanding of the processes caprocks play in GCS projects; however the role of caprocks in GCS productions is critical. The

uncertainties in transport properties of mudrocks in the presence of CO2 are a critical issue that needs to be addressed (Yang and Aplin, 2007; Dewhurst et al., 1999).

Geochemical, geomechanical and hydrological processes are expected to interact over time. Geochemical and geomechanical processes are often coupled, and can result in permeability alterations. This can affect storage capacity and seal effectiveness. Permeability can be reduced by mineral precipitation in pore spaces of the caprock or in fractures. Alternatively, mineral dissolution or fracture initiation/reactivation can cause permeability enhancement. Lithology is a major control on fluid transport in mudrocks. Several efforts have been made to model permeability and porosity relationships in fine-grained sediments; however these models are applicable for homogeneous mudrock core and cutting samples (Yang and Aplin, 2010).

At this point, it is difficult to provide strict criteria for valuation of an effective caprock seal for GCS in deep saline aquifers. Complex physical and geomechanical processes which affect the ability of a caprock to provide sufficient barrier to migrating CO2 are difficult to model, and require additional research. A few general guidelines can be suggested:

- Shale lithologies are superior to other fine-grained argillaceous sediments.
- Ductile lithologies are preferred to brittle materials.
- Caprock must have high strength under tension and compression to be able to accommodate the change in stress fields during injection of CO2 and after injection.
- Thick strata are preferred due to the increased chances the unit is laterally extensive and intact.
- Caprock should be greater than 50 m thick and located in areas of low tectonic activity.
- Lithologies containing pyrite, quartz, and illite minerals are optimal for chemical and geomechanical stability.

The Eau Claire is not a conventional caprock seal. Lateral and regional lithology is hypothesized; however, the thick shale facies at IBDP indicates it can act as an effective seal. The recent coring activities at IBDP have increased our knowledge of the Eau Claire as a caprock for the Mt. Simon Sandstone. The thick shale layer found in the Eau Claire core at VW1 may provide

sufficient sealing to prevent upward migration of CO2. The upper lithostratigraphic unit of the Eau Claire exhibits the highest porosity and permeability and Palkovic (2015) suggests it does not meet the criteria for an effective caprock. However, the interbedded mudstones in the Eau Claire Formation may serve as impermeable baffles.

CHAPTER 3: GEOLOGIC PARAMETER UNCERTAINTY OF A CAPROCK

3.1 Introduction

Accurate and meaningful risk evaluation of GCS is of utmost importance for the public, government, and decision-makers. Subsurface storage of CO2 involves many complex physical and chemical processes. Computational models used to simulate GCS are an abstraction of these processes, and necessarily include estimations and assumptions which introduce errors and imperfections into the model. This leads to a degree of variability that influences the performance of the model to correctly match the physics of the subsurface system. Any prediction of the long-term fate of injected CO2 is subject to various sources of uncertainty, namely geological and mathematical model uncertainty.

Geology is often represented in models as a conceptual geologic structure populated by effective parameter values; conceptual geological model and parameter identification are central issues of modeling subsurface processes (Yeh, 1986; Konikow and Bredehoeft, 1992; Anderson and Voessner, 2002; Beven, 2002; Neuman and Wierenga, 2002; Højberg and Refsgaard, 2005; Gorokhovski, 2012; Refsgaard et al., 2012). Geological uncertainty can be regarded in terms of parametric uncertainty, conceptual/geologic model uncertainty, and local-scale heterogeneities of the model parameters. If uncertainties in input variables of a model are reduced, the uncertainty of the predictive output would also reduce and the confidence in the model performance would increase. However, due to the intrinsic uncertainty of subsurface systems, many questions are raised related to its uncertainty quantification. Often, improving knowledge of these input variables may not be an efficient course in effectively reducing model output uncertainty; the influence of a change in an input variable on the output must also be investigated. This is known as a sensitivity analysis (SA): the study of how uncertainty in model output can be apportioned to different sources of uncertainty in the model input (Saltelli et al., 2008). Quantifying geologic uncertainty is often performed by SA.

Sensitivity analysis can prioritize which parameters or factors are most deserving of additional research, delineate which factors interact, and identify which parameters can be fixed therefore simplifying the model. Generally, these techniques can be categorized as either local (derivative-based) or global (variance-based), and are characterized by different properties, computational cost, and application. Thorough reviews of sensitivity analyses methods are available (Cacuci et al., 2005, Saltelli et al., 2000, Frey and Patil, 2002). Most SA found in literature are local, based on derivatives; the derivative $\partial Y_j / \partial X_i$ of output Y_j versus an input X_i can be thought of as a mathematical definition of the sensitivity of Y_j versus X_i (Saltelli et al., 2008). This concept is at the heart of the simplest class of sensitivity experiments: the classical One Factor at a Time (OAT) screening technique defined by varying one factor at a time and measures the variation in the output (Campolongo et al., 2007). While computationally efficient, a limiting factor of derivative methods is that the choice of point can heavily influence the outcome of the SA, particularly when there is uncertainty in the input and the model response depends nonlinearly on the input. In other words, the results from a classical OAT experiment are only meaningful if the model's input-output relation can be adequately represented by a first-order polynomial in the model's parameters (Cacuci et al., 2005). Global (variance-based) SA methods tackle this limitation by considering the full ranges of uncertainty of the inputs. Variance-based methods have the capacity to capture the full influence of the full range of variation of each input factor and interaction effects among input factors (Saltelli et al., 2008). In contrast to the classical OAT screening methods, global methods require a high number of model evaluations. The Elementary Effects (EE) method by Morris (1991), also referred to as global or extended OAT (Cacuci et al., 2005), has proven to be a good compromise between accuracy and efficiency for sensitivity analyses of large models (Campolongo et al., 2007).

The objective of this study is to explore which input variables characterizing caprock properties are deserving of additional focus and research in order to improve the confidence in GCS predictions. The sensitivity analysis method employed here is the Elementary Effects method by Morris (1991) enhanced by Campolongo et al. (2007). The model presented here is a hypothetical layered reservoir-caprock system modeled after the Mt. Simon Sandstone and the Eau Claire Formation in the Illinois Basin. These sensitivity analysis methods are employed to study how uncertainty in pressure propagation due to fluid (brine) injection in the reservoir can

be apportioned to four caprock parameters (horizontal permeability, anisotropic permeability ratio, porosity, and rock compressibility).

The current chapter begins with a discussion of geological uncertainty and a review of SA studies of geological uncertainty to predictive output in GCS. Regarding parametric SA of geologic structure and properties in GCS, the majority of studies are primarily concerned with the reservoir rock and less attention is given to the caprock. Caprocks (mudrocks, shales) and reservoir rocks are modeled differently, and their respective parametric sensitivity analyses also differ. Sensitivity methodology and simulation model set up are discussed in section 3.3. Results of the sensitivity analyses are presented in the following chapter.

3.2 Geological Uncertainty

Subsurface systems are inaccessible to direct observation, complex and only partially defined; therefore, their description, qualitative or quantitative, will continue to be incomplete. Uncertainty assessment is necessary in the development and use of models. Understanding how geology fits into the larger picture of total model uncertainty is important as it aids in identifying the correct or incorrect uncertainty assessment method.

Uncertainty is more than simply a lack of knowledge; it is any departure from an unachievable ideal. In this research, the definition of uncertainty is adopted from Refsgaard et al. (2007); uncertainty is considered a *degree of confidence* a scientist has about the probabilities and/or possibilities of outcomes of a model. There is not a common typology for geologically-related uncertainty in computational modelling, and it is not the aim of this section to suggest a common language. For in depth discussion on typologies and definitions of uncertainty, see Refsgaard et al. (2007). The aim of this discussion is to provide a conceptual basis for the systematic treatment of geological uncertainty in the context of large-scale models of natural systems.

Varying degrees or states of knowledge create an uncertainty spectrum ranging from complete and total ignorance to the perfectly known (Walker et al., 2003). A specific uncertainty or state of knowledge falls between determinism and indeterminacy. These two extremes provide a framework with which to further interpret uncertainty. Those discussing uncertainty in scholarly fora agree that uncertainty has several dimensions (Walker et al., 2003; Refsgaard et al., 2007) in

the case of models of natural systems, uncertainty has two dimensions: nature and source. Nature characterizes whether the uncertainty is due to imperfect knowledge or inherent variability/randomness. Source describes where the uncertainty manifests within the entire model.

Geological uncertainty in GCS is the uncertainty in properties of the caprock-reservoir system that come from limited knowledge of the properties and conditions due to inherent geologic heterogeneity, sparse and uncertain measurements, and unknown geologic structures. Mathematical model uncertainty are the uncertainties in the mathematical models that represent the complex physics of the GCS system such as simplifying assumptions, mathematical approximations, empirical relationships, and numerical dispersion in the solution procedures (Nordbotten and Celia, 2012).

Parametric uncertainty arises from the inherent randomness of the physical phenomenon that the parameter is representing and/or the lack of knowledge about the parameter. Parametric uncertainty can be found in the 1) physical parameters which represent intrinsic characteristics of the geologic system, such as permeability, porosity, rock compressibility, and reservoir temperature, and 2) constitutive relationship parameters within the constitutive equations that are idealized parameter correlations, such as porosity-permeability relationships, capillary pressure-saturation relationships, and relative permeability-saturation relationships. A conceptual geologic model is the geological model consisting of structural elements derived from stratigraphic reasoning and a method to handle geologic heterogeneity (Refsgaard et al. 2012). A conceptual geologic model is a simplification of an unknown system; therefore many alternative geologic models are equally reasonable. Local-scale heterogeneities account for the uncertainty due to variations of the physical or intrinsic relationship parameters within each structural element. Many measures of performance and risk assessment often include uncertainty in one or more of these categories.

3.2.1 Nature and Source

The *nature* of uncertainty can be categorized into two distinct groups (Walker et al., 2003; Cacuci et al., 2005; Refsgaard et al., 2007): epistemic uncertainty and aleatory uncertainty. Epistemic uncertainty is the uncertainty due to imperfect knowledge and is reducible by

additional studies. Aleatory uncertainty is uncertainty due to its inherent random nature which varies in space and time and cannot be reduced by additional studies.

This distinction in the nature of uncertainty is well recognized in the literature regarding uncertainty although terminology may differ. Epistemic uncertainty is also referred to as subjective uncertainty; aleatory uncertainty is often referred to as objective, stochastic, statistical, or variable uncertainty. Only recently has this distinction been used in the field of subsurface hydrology (Srinivasan et al., 2007; Montanari, et al., 2009; Ross, et al., 2009). Epistemic uncertainty is due to limited data and knowledge. It is the scientific uncertainty in the process of the model which may be resolved by further research and improved understanding of the system. Epistemic uncertainty is apparent in parameter uncertainty resulting from an inability to assess exactly the parametric values from test or calibration data due to limited number of observations. Alternatively, aleatory uncertainty is due to the natural randomness in a process and is often described in statistical terms. Additional studies may not provide an improvement in the model output. An example of aleatory uncertainty is measurement uncertainty associated with all input data. Measurements can never precisely be the "true" value of what is measured.

Distinguishing the nature of uncertainty is not a simple task. When all possible outcomes and probabilities of a process or event are known, uncertainty is considered to be bounded (aleatory). Conversely, when all possible outcomes and probabilities are unknown and cannot be assumed, uncertainty is considered unbounded (epistemic). In the case of input parameter uncertainty, if the parameter can sometimes have one value and sometimes have another value, then the nature of its uncertainty is random. If the parameter always has one single correct value, but that value is unknown, then the nature of the uncertainty is epistemic.

Sources of uncertainty are locations where uncertainty occurs in a model. Disregarding errors in the applied numerical code, sources of uncertainty in groundwater simulations are related to 1) data as model input, 2) parameter estimation, and 3) model structure. The model structure is the mathematical formulation of a hypothesis or conceptualization about the behavior and the relationships between various components of the subsurface. The model structure requires a set of parameters in order to be used for simulation. Hydrogeological data is used for both building the simulation model and as conditioning data for calibrating model parameters. Various methodologies have been developed to quantify uncertainty originating from data and parameter

estimation, such as Monte Carlo analyses or regression-based methods. For recent reviews and environmental and groundwater applications of these methods, see Refsgaard et al., 2012; Nilsson et al., 2007; Hojberg and Refsgaard; 2005.

Uncertainties due to model structure are more complex and numerous than the previously discussed factors, and are not exclusive to 1) choice of processes in the model (e.g. solute-transport, geochemical, geomechanical, etc.), 2) governing equations and mathematical formulations of these processes, 3) initial conditions (e.g. pressure, temperature, salinity, saturation etc.), 4) boundary conditions (e.g. Dirichlet, Neumann, Cauchy, etc.), and 5) hydrogeological interpretation and representation. Historically, model structural error is assessed through validation tests where field test data is compared to simulated output. This approach is limited by access and availability of test data. To get around this limitation, assessing multiple model simulations is one way to test the model structure.

Geological uncertainty is both epistemic and aleatory. Historically, subsurface models are constructed using a single geological model structure with the best geological representation of lithology, stratigraphy, and simplifications of heterogeneity (Anderson and Voessner, 2002). The geologic model is populated with effective parameter values estimated through calibration procedures which are expected to reproduce average properties within a given geological structure. These effective parameter values capture large-scale variation within the geologic structure, but local-scale parameter heterogeneity within a geological element is often lost during modeling (Refsgaard et al., 2012). This is a deterministic approach, where the geologic structure and input parameters are imperfectly known, yet deterministic quantities. This traditional approach to building a geological conceptual model has errors associated with the definition of the geological structure, spatiotemporal variations in parameters not fully resolved by the model, and scaling behavior of the parameters (Nilsson et al., 2007).

3.2.2 Previous Sensitivity Analyses of Geologic Uncertainty in GCS

Due to the complexity of GCS process and many sources of geologic uncertainty in GCS, sensitivity analysis can be used to identify important physical parameters and reduce the number of parameters to be perturbed. To date, SA of geological uncertainty in a GCS context has been conducted in a limited number of studies. Sifuentes et al. (2009), Zhao et al. (2010), Han et al.

(2011) studied the contribution of various parameters to the residual trapping and solubility trapping mechanisms in a homogenous saline aquifer. Sensitivity of CO2 injection costs to petrophysical parameters of a homogeneous (Cheng et al., 2013) and heterogeneous (Heath et al., 2012) saline aquifer were investigated. Various parameters of a hydro-mechanical model were used as input for sensitivity analyses of a layered aquifer system (Bao et al., 2013) to injection pressure and leakage. Sensitivity of CO2 saturation distribution, plume arrival time, site injectivity and storage capacity to the heterogeneity in porosity and permeability fields of the storage formation were investigated (Lengler et al., 2010, Deng et al., 2012). Ashraf et al. (2013) modeled CO2 injection in several geologic conceptual model realizations of a shallow-marine aquifer using arbitrary polynomial chaos expansion. Optimal heterogeneity resolution of a heterogeneous deep saline aquifer conceptual model was investigated using multiscale permeability upscaling combined with a sensitivity analysis of boundary conditions (Li et al., 2011).

To date, sensitivity analyses which consider geological uncertainty of the caprock, either directly or indirectly, have been conducted in a limited number of studies (Mbia et al., 2014; Wainwright et al., 2013; Chang et al., 2013; Hou et al., 2012). Using dimensional analysis, Chang et al., (2013) show pressure evolution in a layered reservoir-caprock system is controlled by ratios of permeability and specific storage of the aquifer and the caprock. Their results suggest dissipation into ambient mudrocks can significantly reduce lateral spread of the pressure plume, whereas nonlinearities of two-phase flow or phase change near the injection well do not affect radial pressure propagation.

Wainwright et al., (2013) demonstrated the use of three sensitivity analysis methods on an idealized caprock-reservoir system with an injection well and a leaky well. Seven parameters were perturbed: well conductivity, permeability and storativity for reservoir, aquifer, and caprock. The change in pressure at the leaky well is the performance measure used for the sensitivity analyses. Sensitivity measures are estimated using the local sensitivity method, EE Morris method, and Sobol'/Saltelli sensitivity method (Sobol', 2001; Saltelli et al., 2008). Reservoir storage is influential at early times, whereas aquifer and reservoir permeability are primary effects thereafter. Leaky-well hydraulic conductivity is the least influential factor. For

the Sobol' indices, all parameters displayed interaction effects. Aquifer permeability shows nonlinear effects.

Bao et al., (2013) performed a sensitivity analysis for geomechanical response to CO2 injection through caprocks using the Subsurface Transport Over Multiple Phases (STOMP) simulator. Quasi-Monte Carlo sampling was used to sample hydrogeological input parameters of reservoir and caprock including porosity, permeability, van Genuchten *n*, entry pressure, Young's modulus, and Poisson ratio. Injection rate was also considered. The sensitivity of the responses (ground surface deformation and pressure at the injection point) to the input parameters, generalized cross variance (GCV) and analysis of variance (ANOVA) methods were used. Reservoir permeability, injection pressure, and reservoir porosity were ranked the top three factors for both deformation and pressure. The next three important factors were caprock permeability, caprock *n* , and caprock porosity.

Hou et al., (2012) investigated factors affecting sealing capabilities and CO2 leakage through caprocks using the STOMP simulator and quasi-Monte Carlo sampling method. Five parameters were sampled for the sensitivity analysis: caprock thickness, caprock porosity, caprock permeability, reservoir porosity, and reservoir permeability. A generalized linear model (GLM) was used for ranking parameters. In terms of CO2 leakage, the most important factors are ranked: caprock thickness, caprock permeability, reservoir permeability, caprock porosity and reservoir porosity.

3.3 Modeling Approach

Reservoir properties have typically been the focus of geologic uncertainty analyses in GCS, and caprock uncertainty quantification has been neglected. No modeling methodology used for characterizing caprock is perfect. Physical processes which govern leakage through caprock are often coupled, yet input parameters which model these processes are inherently uncertain. Pressure build-up is a major factor on the capacity and injectivity of the storage reservoir, and caprock lithology can impact the volume of stored CO2. To date, there have been few sensitivity analysis studies that investigate the effect of geologic caprock parameters to the pressure

response of injected brine in the reservoir-caprock system. Additionally, no studies have been conducted using geologic parameter ranges of the Eau Claire.

The model presented in this research considers an idealized layered reservoir-caprock system modeled after the Mt. Simon and Eau Claire in the Illinois Basin. The Morris method (Morris, 1991) enhanced by Campolongo et al. (2007) is employed to study how uncertainty in pressure propagation due to brine injection in the reservoir can be apportioned to four caprock parameters (horizontal permeability, anisotropic permeability ratio, rock compressibility, and porosity). Numerical simulations are performed with TOUGH2-ECO2n code (Pruess et al., 1999; Pruess, 2005) – a numerical simulator for multiphase flow. Output from numerical simulations is analyzed via the R statistical software and the Global Sensitivity Analysis of Model Outputs ("sensitivity") package (Pugol et al., 2016).

3.3.1 Sensitivity Analysis Methodology

The Elementary Effects Morris method can be considered an extension of the local OAT experiments. The method is based on calculating for each input a number of incremental ratios, Elementary Effects (EE), from which basic statistics are computed to derive sensitivity information (Campologno et al., 2007). An elementary effect is defined as follows. Consider a model f with k independent factor inputs X_i, $i = 1, \ldots, k$ and with scalar output y. Each model input is assumed to vary in a k-dimensional unit cube across p selected levels. The region of experimentation Ω is therefore a k-dimensional p-level grid. For a given $\mathbf{X}$, the elementary effect of the ith input factor is defined as:

$$EE_i = \frac{\left[Y\ \ X_1,\ldots,X_{i-1},X_1+\Delta,\ldots,X_k\ \ -Y\ \ X_1,\ldots,X_k\ \right]}{\Delta}$$

where p is the number of levels, Δ is a value in $\{1/(p-1), \ldots, 1-1/(p-1)\}$, and $\boldsymbol{X} = (X_1, X_2, \ldots, X_k)$ is any selected value in Ω such that transformed point $(\boldsymbol{X} = \boldsymbol{e_i}\Delta)$ is still in Ω for each index $i = 1,\ldots,k$, and $\boldsymbol{e_i}$ is a vector of zeros, but with a unit as its ith component. The so-called distribution of elementary effects associated with the ith factor is obtained by randomly sampling different $\mathbf{X}$ from Ω, and is denoted by F_i, i.e. $EE_i \sim F_i$. The distribution F_i is finite and the number of elements of each F_i is $p^{k-1}[p-\Delta(p-1)]$ (Campolongo et al., 2007).

For each input factor, three sensitivity measures are calculated: (a) the mean, μ, of F_i, (b) the standard deviation, σ, of F_i, and (c) the mean, μ^*, of the absolute values of the elementary effects. To estimate μ and σ for *k* factors, we create an ensemble of elementary effects for each factor by sampling *r* elementary effects via a trajectory or path of *k* + 1 points. The total number of simulations needed is $r(k+1)$. Trajectories *r* are generated by starting at a randomly selected base parameter set in Ω and increasing one or more of its factors by Δ in a way that the end point remains inside Ω (Saltelli et al., 2008) (Figure 3.1) The base parameter set is not included in **X.** The number of trajectories and value of grid jump is selected in a way as to maximize the "spread" of and optimizing the Euclidean distance among the sample points (Campolongo et al., 2007). This sampling strategy is an improvement from the original Morris sampling method, where one factor at a time would move in a random order.

Once r elementary effects are available $\left(EE_i^j, i = 1, \dots, k, j = 1, \dots, r\right)$, the statistical measures $\mu_i,\ \mu_i^*\ and\ \sigma_i^2$ of F_i can be computed for each input factor *i* (Saltelli et al., 2008). The standard deviation, σ_i , is the square root of the variance, σ_i^2.

$$\mu_i = \frac{1}{r}\sum_{j=1}^{r} EE_i^j$$

$$\mu_i^* = \frac{1}{r}\sum_{j=1}^{r} | EE_i^j |$$

$$\sigma_i^2 = \frac{1}{r-1}\sum_{j=1}^{r} \left(EE_i^j - \mu \right)^2$$

The mean μ is a measure of the overall influence of the factor on the output. It represents the average effect of the factor over the entire parameter space; therefore it can be considered a global sensitivity measure (Saltelli et al., 2007). The standard deviation σ is an estimate of the ensemble of the input factor's effects, whether nonlinear and/or due to interactions with other input factors (Saltelli et al., 2008). The absolute mean μ^* was proposed by Campolongo et al. (2007) to handle a distribution F_i that is non-monotonic, i.e. contains positive and negative elements that cancel each other out resulting in a very low mean μ and a high standard deviation σ. This method is easy to implement, however it provides a qualitative (not quantitative) indication of the interactions of a parameter with the rest of the model. It cannot provide specific

sensitivity information about the interactions between individual parameters tested (Cacuci et al., 2005).

3.3.2 Simulation Model Setup

The two-dimensional grid was built using mView – a powerful pre- and post-processor for TOUGH2 (Avis et al., 2012). The mesh of the model consists of 52 layers, 60 columns, and 3,120 elements. Mesh discretization increases logarithmically from the injection well to the 100 km boundary. The geological model is 40 m thick consisting of a 20 m thick caprock representing the Eau Claire and an underlying 20 m thick reservoir representing the Mt. Simon (Fig. 3.2). The caprock consists of 26 layers. Layers 1-16 are 1 m thick, layers 17-22 are 0.5 m thick, and layers 23-26 are 0.25 m thick. The underlying reservoir consists of 26 layers. Directly below the caprock, layers 27-30 are 0.25 m thick. Layers 31-36 are 0.5 m thick, and the bottom 16 layers are 1 m thick. To make the sensitivity analysis manageable, the simulation model assumes an axisymmetric geometry, homogeneous and fracture-free rock properties, and a single injection well.

The vertical injection well is located at the lowermost 10 m of the reservoir. Brine is injected at a rate of 0.5 Mt per year for 10 years and the injection fluid is the same salinity as the ambient rock fluid. Single phase flow simulation models are acceptable to assess the pressure buildup away from the injection well and a hypothetical CO2 plume (Nicot, 2011; Nordbotten and Celia, 2012). This simplification renders assessing the pressure response due to CO2 injection computationally tractable. The pressure response and fluid fluxes at the boundary are similar in multiphase and single phase flow models (Nicot, 2011). The simulation was evaluated monthly during the first year of injection, yearly during the remaining injection period, and for 40 years following injection. The simulated domain has closed boundaries; however the volume of the far field elements located at the 100 km boundary were adjusted to have an indefinite volume so that the lateral boundaries do not affect the results. The domain is considered isothermal 49.2°C and under hydrostatic conditions at the top of the caprock (196 bars). Geomechanical and chemical reactivity effects are not considered. Relevant geological and TOUGH2-ECO2n simulation input parameters for the Mt. Simon reservoir and Eau Claire caprock are found in Table 3.1 and 3.2.

In the SA, four caprock parameters are perturbed: horizontal permeability K_h, anisotropic permeability ratio K_v/K_h, porosity ϕ, and rock compressibility β_r. Caprock parameter ranges are informed by various studies across the Illinois Basin and the literature review on mudrocks and shales found in Chapter 3. Table 3.1 shows the parameter ranges. Rock compressibility and permeability anisotropy estimates are not available for the Eau Claire at this time. Rock compressibility ranges are taken from Rieke and Chilingarian (1974). A uniform distribution is assumed within the given range for each parameter. Time-dependent pressure build up (ΔP) at several locations in the caprock and reservoir are of interest (Fig. 3.1). An observation point is located at the base of the caprock 10 m from the injection well. A vertical cross section cutting through the caprock and the top 10 m of the reservoir was constructed to investigate the spatial variation in elementary effects.

A schematic showing the sensitivity analysis methodology is shown in Figure 3.3. The TOUGH2 simulation and sensitivity analysis work flow is detailed below.

Part 1: Pre-processing: The input parameters were generated using the *morris* function in the Global Sensitivity Analysis of Model Outputs ("sensitivity") package. A TOUGH2 input file template and grid file was generated using mView. Generic python scripting was used to write TOUGH2 input files from the sample parameter set and the TOUGH2 input file template, Each TOUGH2 input file was saved in a separate directory.

Part 2: Simulations: Basic python scripting was used to run the TOUGH2 simulations. Initial pressure conditions were created by running each simulation without injection for 6 months. The injection simulations were executed and output files were saved in their respective directories.

Part 3: Post-processing: In this step, mView was used to calculate the change in pressure at the observation point and at the vertical cross section from each simulation. The time-series pressure data is then written out to text files and ingested into R. The elementary effects and their variances were then calculated at 3 time steps: immediately after injection ends, 10 years after the injection period, and 40 years after the injection period.

Caprock Parameter	Range	Source
β_r , rock compressibility (Pa^{-1})	$4.84x10^{-11} – 1x10^{-8}$	Rieke and Chilingarian (1974)
ϕ, porosity (%)	5.8 – 24%	Palkovic (2015); Neufelder et al. (2012)
K_h , horizontal permeability (m^2)	$1x10^{-19} – 1.78x10^{-15}$	Witherspoon and Neumann (1967)
K_v/K_h permeability anisotropic ratio	1 – 100	Loucks et al. (2012); Grainger (1984)

Table 3.1: Geologic parameters varied for sensitivity analyses

Properties		Caprock	Reservoir
Horizontal permeability, Kr	m^2	varies	$4.94x10^{-14}$
Vertical permeability, Kz	m^2	varies	$4.94x10^{-15}$
Rock compressibility, β_r	Pa^{-1}	varies	$3.71x10^{-10}$
Porosity	%	varies	16
Temperature	C	49.2	49.2
Salt Mass Fraction		0.2	0.2

Table 3.2. Relevant input parameters for TOUGH2-ECO2n and parameter ranges for the sensitivity analysis.

3.4 Summary

The modeling approach taken in this study requires a realistic characterization of parameter uncertainty; therefore the properties of the Eau Claire in the Illinois Basin at IBDP are used to

characterize parameter ranges in during a hypothetical brine injection scenario. The sensitivity analysis presented here distinguishes between parameters with the same significance in the model structure. All of the previous sensitivity analyses are parametric. The geology is assumed homogenous within simulation model layers and the geologic structure was not analyzed. The modeling approach in this research draws from these studies and focuses on only the caprock properties in relation to pressure perturbation due to brine injection in an underlying reservoir.

The objective of this sensitivity analysis is to identify which caprock parameters most significantly impact the uncertainty in the pressure build up in the model. Parametric uncertainty cannot be related in a direct way to the uncertainty in the pressure perturbation because each parameter has varying degrees of uncertainty. Differences in uncertainty arise due to spatial and temporal variability in the output. To analyze the spatial and temporal variability in ΔP with respect to caprock parameters, the sensitivity measures at an observation point located at the base of the caprock, and a vertical cross section at three time steps: when injection ends, 10 years after the injection period, and 40 years after the injection period.

The modeling approach taken in this study requires a realistic characterization of parameter uncertainty; therefore the properties of the Eau Claire in the Illinois Basin at IBDP are used to characterize parameter ranges in during a hypothetical brine injection scenario. The sensitivity analysis presented here distinguishes between parameters with the same significance in the model structure. While the results of the simulation and sensitivity analysis are specific to the synthetic problem presented in this research, the methodology is applicable to other GCS sites and the Illinois Basin - Decatur Project.

CHAPTER 4: RESULTS AND DISCUSSION

4.1 Results

The Morris elementary effects method can determine which input factors are a) negligible, b) linear and additive, or c) nonlinear or involved in interactions with other factors (Saltelli et al., 2008). For a given factor, low μ^* and low σ indicate little effect, high σ indicates a high nonlinear or non-additive effect, and high μ^* indicates a high linear effect (Campolongo et al., 2007). If a factor has a high σ relative to its μ^*, it implies the value of the elementary effects are strongly affected by the choice of the sample point by which it is computed. Alternatively, a very low σ indicates very similar values among the elementary effects for a given factor (Saltelli et al., 2008).

Elementary effects were computed using 250 simulations. For this study, an eight level-grid (p=8) with a grid jump of 4 (Δ=4) and 50 trajectories (r=50) are chosen for the four-dimensional input space (k=4). Each parameter range was scaled to unit [0, 1] for sampling and elementary effect calculations. The parameter set was transformed back into their respective ranges for input in TOUGH2 simulation (Table 3.1). Figure 4.1 displays the parameter set. The mean μ, absolute mean μ^*, and standard deviation σ for the ensemble of elementary effects were computed at an observation point at the top of the caprock (Fig. 3.2). The elementary effects for horizontal permeability K_h, anisotropic permeability ratio K_v/K_h, porosity ϕ, and rock compressibility β_r are denoted as E1, E2, E3, and E4, respectively. Figure 4.2 shows the time evolution of the pressure perturbation at the observation point for 250 Monte Carlo simulations.

4.1.1 Observation Point at the Base of the Caprock

Sensitivity measures for the observation point located at the base of the caprock and 10 m from the injection well are reported in Table 4.1. Ranked elementary effects and their sensitivity measures μ, μ^*, and σ at each time period are represented in bar charts in Figures 4.3 through 4.5. Graphical representation in the (μ^*, σ) plane allows for another interpretation of the results and ranking of input factors (Figures 4.6 through 4.8).

At the time injection ends (Fig. 4.3 and Fig. 4.6), the input factors can be ranked in order of importance: E1, E4, E3, and E2. E1 (K_h) exhibits the highest absolute mean and standard deviation in relation to other factors. E4 (β_r) exhibits a slightly lower absolute mean, and a much lower standard deviation. Compared to the other factors, E3 (porosity ϕ) and E2 (K_v/K_h) exhibit lower absolute means but the values are not near zero, therefore these factors are considered less important than E1 and E2, but are not negligible. Rock compressibility (E4) at the time injection ends appears to be of secondary importance compared to E1, and has a linear effect on the change in pressure at the observation point. The high absolute mean and standard deviation of E1 (K_h) indicates the factor is important and exhibits nonlinearity in relation to pressure perturbation or the factor is interacting with other model parameters. It is expected that horizontal permeability is a dominant factor and the anisotropic permeability ratio is a less influential parameter effecting pressure response at the base of the caprock. Higher horizontal permeability leads to higher lateral brine mobility which leads to greater lateral dissipation of pressure. The negative means of E1, E4, and E3 indicate the rate of pressure change is negative. This can be interpreted as the pressure is dissipating at this location of the caprock. The anisotropic permeability ratio has a positive mean (effect) on the rate of pressure change. Qualitatively, the anisotropic permeability ratio is aiding in the pressure buildup and inhibiting pressure dissipation.

Ten years post injection (Fig. 4.4 and Fig 4.7), the input factors at the observation point at the base of the caprock can be ranked in order of importance: E1, E2, E4, and E3. Standard deviation values exceed absolute mean estimates for all factors. The stark difference between E1 (K_h) and the remaining factors indicate E2, E4, and E3 indicate K_h. is highly important. Nonlinear effects in horizontal permeability 10 years after injection are similar to the nonlinear effects immediately after injection ends. Compressibility and porosity have negative mean (effects) at the time injection ends and positive means (effects) in the post injection period. A highly compressible caprock can absorb the pressure in the pore network during the injection period and slowly recover post injection. The anisotropic permeability ratio continues to inhibit pressure dissipation.

Forty years after injection ends (Fig. 4.5 and 4.8), input factors at the observation point can be ranked in order of importance: E1, E4, E2, and E3. Nonlinear or interaction effects for all input

factors here are similar to the nonlinear/interaction effects at 10 years post-injection (Fig. 4.4). E1 (K_h) remains the most important factor. Rock compressibility became a more important factor at 40 years after injection ends when compared to the absolute mean estimate at 10 years after injection ends. During the observation period following injection, the caprock will begin to equilibrate back to hydrostatic pressure as the pressure dissipates away from the injection well. Between 10 years and 40 years post-injection, the horizontal permeability remains a negative effect on the change in pressure; however the mean and absolute mean elementary effect for porosity, permeability anisotropic ratio, and compressibility increase with time. A high porosity combined with a high pore compressibility value means that more brine can be stored per unit of caprock and a slower dissipation of pressure.

Time	**Elementary Effect**	**μ**	**μ***	**σ**
End of injection	K_h (E1)	-1.53513	1.53513	1.64852
	K_vK_h (E2)	0.59197	0.59197	0.39708
	ϕ (E3)	-0.78579	0.78579	0.38494
	β_r (E4)	-1.39036	1.39036	0.78081
10 years post-injection period	K_h (E1)	-1.36852	1.41872	2.44672
	K_vK_h (E2)	0.20513	0.32527	0.83783
	ϕ (E3)	0.07566	0.16661	0.43000
	β_r (E4)	0.07933	0.26835	0.64226
40 years post-injection period	K_h (E1)	-1.24059	1.32873	2.45186
	K_vK_h (E2)	0.33838	0.42333	0.95822
	ϕ (E3)	0.23451	0.31301	0.85336
	β_r (E4)	0.28865	0.68200	1.41640

Table 4.1: Sensitivity measures for the elementary effects at the observation point for three observation times.

4.1.2 Vertical Cross Section

To qualitatively investigate the spatial distribution of the importance of input factors, sensitivity measures for a vertical cross section located at 10 m from the injection well which cuts though 20 m of caprock and 10 m of reservoir was constructed for three time periods: immediately after injection ends, 10 years after the injection period, and 40 years after the injection period (Figures 4.9 through 4.11). For each time period, the change in pressure with respect to depth was extracted from TOUGH2 simulation output and ingested into the sensitivity model. The change in pressure at the lower 10 m of the reservoir was negligible, therefore not included in elementary effect calculation. In Figures 4.6 through 4.8, solid lines represent the absolute mean, and dashed lines represent the standard deviation.

Figure 4.9 shows the sensitivity measures plotted with respect to depth immediately after injection ends. Input factors at the top of the caprock are ranked in order of importance: E4, E2, E3, and E1. Respective absolute mean estimates are similar to their standard deviation values for all factors. This indicates all the factors experience nonlinear or interaction effects. Rock compressibility is the only factor that has a standard deviation that is less than its absolute mean. As depth increases, both sensitivity measures for rock compressibility (E4), anisotropic permeability ratio (E2) and porosity (E3) all decrease. These three factors exhibit standard deviation estimates lower than their respective absolute means. This indicates the factors act linear with respect to the change in pressure, but are relatively less important at the base of the caprock. Horizontal permeability becomes the dominant factor near the caprock-reservoir contact. However, its standard deviation exceeds its absolute mean. This high absolute mean and high standard deviation suggest the factor is important and possibly interacting with other input factors. The sensitivity of caprock input parameters with respect to the change in pressure in the reservoir was calculated for 10 m below the caprock. The sensitivity measures stay consistent below -20 m. The input factors listed in order of importance: E1, E4, E3, and E2. Horizontal permeability in the caprock is the most significant factor that affects the change in pressure in the reservoir; however the standard deviation of this parameter suggests nonlinear behavior. Caprock compressibility is the second most important parameter and coupled with its low standard deviation suggests a high linear effect. Brine injection causes an increase in the reservoir formation pressure and will cause displacement of ambient brine in the formation as well as

leakage into the caprock. When a caprock has a higher horizontal permeability, pressure in the reservoir is less. A highly compressible and permeale caprock allows for greater lateral pressure dissipation in the caprock-reservoir system.

Figure 4.10 shows the cross section at 10 years after injection has ended. At this point, pressure is dissipating into the caprock. From the top to the base of the caprock, all factors are characterized by highly nonlinear or interaction effects. Between -10 m and -20 m, E2, E3, and E4 drop in importance and E1 (K_h) remains highly significant and non-negligible. Below the caprock, the sensitivity measures remain consistent with increasing depth in the reservoir. Caprock input parameters can be ranked in order of importance: E4, E2, E1, and E3. Standard deviation for all factors is less than their respective absolute means. This suggests all factors exhibit linear effects to the pressure perturbation, however caprock horizontal permeability (E1) and porosity (E3) are less important than anisotropic permeability ratio (E2). Caprock compressibility is the most significant input parameter and exhibits a highly linear effect with respect to the change in pressure in the reservoir.

Figure 4.11 shows the cross section at 40 years following the end of injection. Pressure changes due to brine injection in the reservoir have further dissipated in to the caprock. At the top of the caprock, standard deviations for all factors exceed the factors' respective absolute means. In the 10 m section above the caprock, input factors can be ranked in order of importance: E4, E1, E2, and E4. Porosity (E3) and anisotropic permeability ratio (E2) are negligible factors for all depths in the cross section at 40 years after injection ends. Caprock compressibility remains the dominant factor which affects the pressure change in the reservoir. The influence of caprock horizontal permeability to the pressure change in the reservoir is negligible. Caprock compressibility exhibits high standard deviation in the reservoir which suggests a high nonlinear effect or interaction with other factors.

4.2 Discussion

Geological CO2 storage studies typically focus on the target storage reservoir because low-permeability mudrocks prevent upward migration of CO2 due to high capillary entry pressure. However, regional aquifers are not closed hydrogeologic systems and overlying caprocks are not

perfectly imperious (Dewhurst e al., 1999). The greatest changes in pressure in the caprock due to injection of brine in the reservoir will occur at the base of the caprock at the reservoir contact. Pressure will increase in the reservoir and caprock during injection and dissipate after injection ends. Figure 4.1 shows the pressure response for all simulations at an observation point located at the base of the caprock. Caprock horizontal permeability, vertical permeability, porosity and compressibility will affect how this pressure dissipates into the overlying caprock. Flow through a caprock seal depends mainly on its permeability. The flow occurs first in the largest interconnected pores. Unlike other sedimentary rocks, mudrocks and shales have very low permeability that often prevents vertical escape of pore fluid. With higher caprock permeability, there is a less pressurization in the reservoir and caprock. Pressure propagation is faster when permeability increases and pore compressibility decreases. Higher caprock compressibility allows for greater pressure absorption in its pore network therefore decreasing the pressure in the reservoir.

Immediately after injection ends, horizontal permeability (E1) is the dominant factor affecting pressure changes at the base of the caprock (Fig. 4.3 and Fig 4.6). The standard deviation for the ensemble of elementary effects for horizontal permeability consistently exceeds its absolute mean at 10 years and 40 years after the injection period. Throughout this observation period, estimates for standard deviation of horizontal permeability (E1) increase. After 10 years of observation, horizontal permeability continues to be the most influential factor (Fig. 4.4 and Fig. 4.7). Anisotropic permeability ratio (E2), porosity (E3), and rock compressibility (E4) are less influential factors and exhibit nonlinear or interaction effects. After 40 years of observation, rock compressibility (E4) becomes a more influential input parameter.

Pressure changes in the reservoir are sensitive to caprock parameters. As pressure in the reservoir dissipates following injection, caprock horizontal permeability (E1) and rock compressibility (E4) are influential factors that affect the pressure perturbation below the caprock (Fig. 4.7 and Fig. 4.8). Caprock porosity (E3) and anisotropic permeability ratio (E2) are less influential factors that affect the pressure changes in the reservoir. Simulations with high caprock compressibility exhibit the lowest pressure response in the caprock; however the caprock remains pressurized at longer time scales when compared to simulations with high caprock

compressibility. This result is in agreement with Mbia et al. (2014); overestimating caprock compressibility can underestimate overpressure within the injection reservoir.

Due to the scarcity of data for the Eau Claire, uniform prior distributions were assigned to the horizontal permeability, anisotropic permeability ratio, porosity, and rock compressibility parameters. The high standard deviations of the input factors and negative mean value for E1 (K_h) at the observation point indicate the factor is highly sensitive to the choice of point in Ω. Additional characterization of the physical properties of the Eau Claire caprock is needed to gain better understanding of the sensitivity of these parameters with respect to the pressure response.

CHAPTER 5: CONCLUSION AND FUTURE WORK

Low permeability rocks (mudrocks and shales) are present at every natural gas accumulation or subsurface carbon storage site; however our knowledge of caprock-reservoir systems is distinctly lop-sided. Research interest in the characterization of caprock seals for GCS is recent. Historically, target reservoirs are heavily researched whereas their respective caprock has been viewed as an obstacle to drilling. A major limitation to caprock research appears to be a widespread lack of data. Lithology and mineralogy of the caprock is usually known, however properties of fluid flow, thickness, continuity and extent are usually estimated. Caprocks, viewed as an impermeable capillary seal, are often excluded from CO2 storage studies, or represented as a single layer in simulation models and assigned a very low permeability value. The Eau Claire is not a conventional caprock. The Eau Claire trends from a fine-grained sandstone in southcentral Wisconsin to a sandstone or sandy dolomite in northern Illinois to a siltstone or shale in central Illinois (Kolata and Nelson, 2010; Finley, 2005). Limited coring through the Eau Claire limits further stratigraphic characterization and petrophysical testing. However, recent coring activities at the Illinois Basin – Decatur Project have enhanced our understanding of the Eau Claire Formation as a caprock for GCS. The thick shale facies indentified at VW1 may act as an effective seal (Palkovic, 2015).

The influence of caprock permeability, porosity and compressibility, and the consequences of pressure buildup due to brine injection have been studied for a simplified caprock-reservoir system based on the Eau Claire and Mt. Simon in the Illinois Basin. The results from the sensitivity analysis showing the influence of compressibility and permeability on the pressure propagation and dissipation in the caprock suggest that additional research needs to be done on these caprock properties to improve the accuracy of GCS model prediction. Underestimating caprock compressibility can lead to overestimation of the pressure buildup within the caprock and storage formation. Horizontal permeability exhibits a negative mean effect that indicates it aids in the dissipation of pressure in the caprock and reservoir. This is expected as flow through porous media depends on its intrinsic permeability. The anisotropic permeability ratio has a

positive mean effect on the rate of pressure change in the caprock which indicates it inhibits pressure dissipation and aids in pressure buildup after injection and the years during observation.

Limited available caprock data coupled with a general lack of understanding of the physics of caprock behavior generates uncertainty in the output of GCS simulation models. The primary drawback to parametric SA is that the objects of investigation are the physical parameters that represent the intrinsic characteristics of the caprock and the constitutive relationship parameters within the constitutive equations (capillary pressure relationships, relative permeability equations, etc.) that are simplifications of the real world – not the geologic structure of the caprock. One way to reduce geological uncertainty further is to investigate the uncertainty related to the caprock conceptual geologic model. If a single geological structure is used, sensitivity analysis is limited to the effective parameters and constitutive relationships. This presents the dilemma of uniqueness of the subsurface and the non-uniqueness of the corresponding predictive simulation model. One way to investigate this epistemic uncertainty in is by testing equally probable alternative geologic models that represent the caprock lithology.

FIGURES

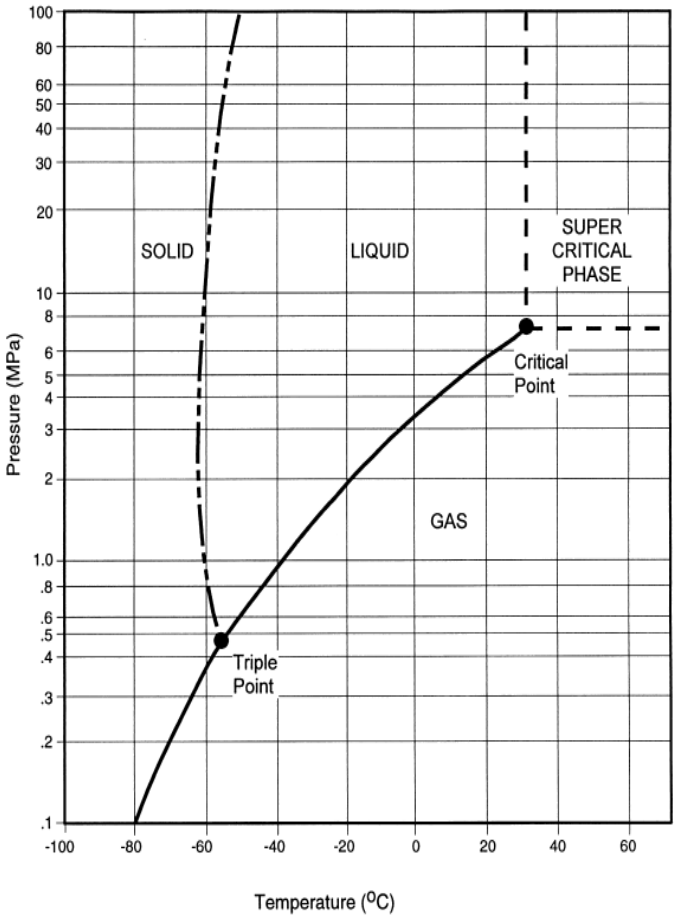

Figure 2.1: Carbon dioxide phase diagram (Bachu, 2000).

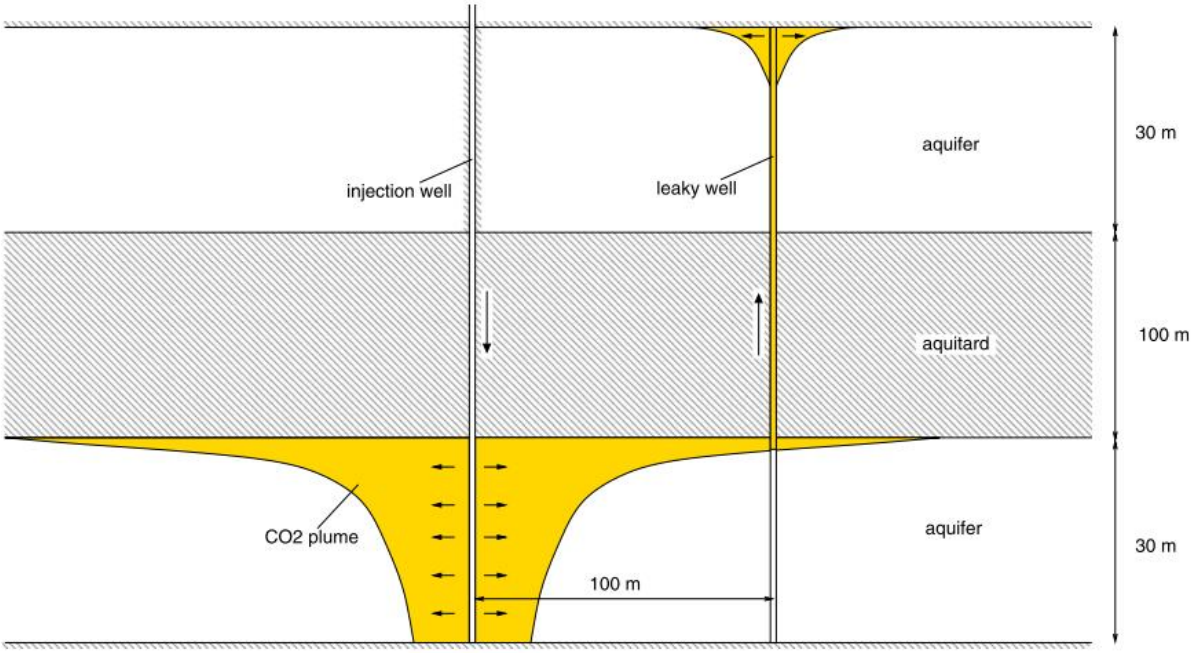

Figure 2.2: Schematic of CO2 plume spreading beneath a caprock (Class et al., 2009).

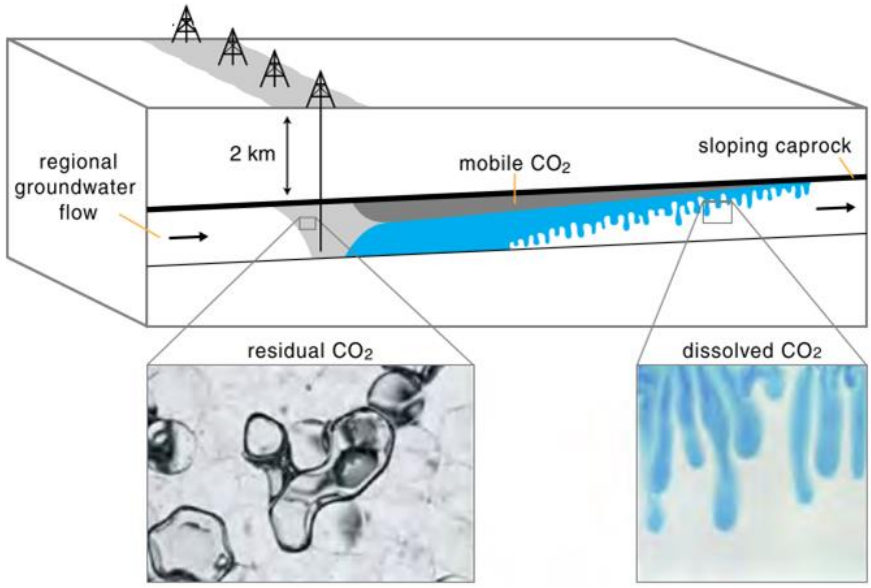

Figure 2.3: Residual and solubility trapping are the key trapping mehcanisms that contribute to CO2 storage capacity (adapted from Szulczewski et al., 2012).

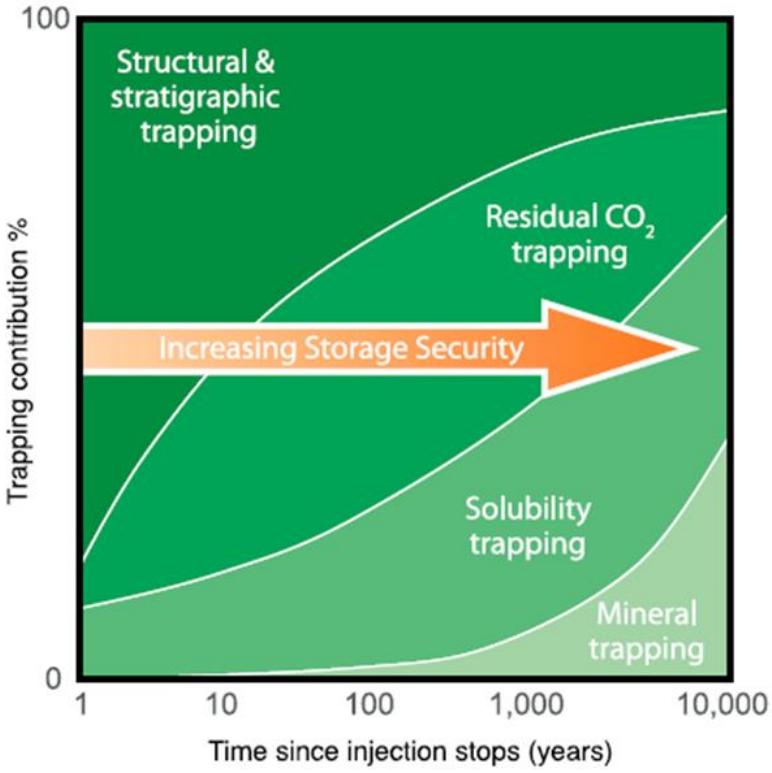

Figure 2.4: Storage security of sequestered CO2 depends on physical and geochemical trapping. Over time, the physical process of residual CO2 trapping and geochemical processes of solubility trapping and mineral trapping increase (IPCC, 2005).

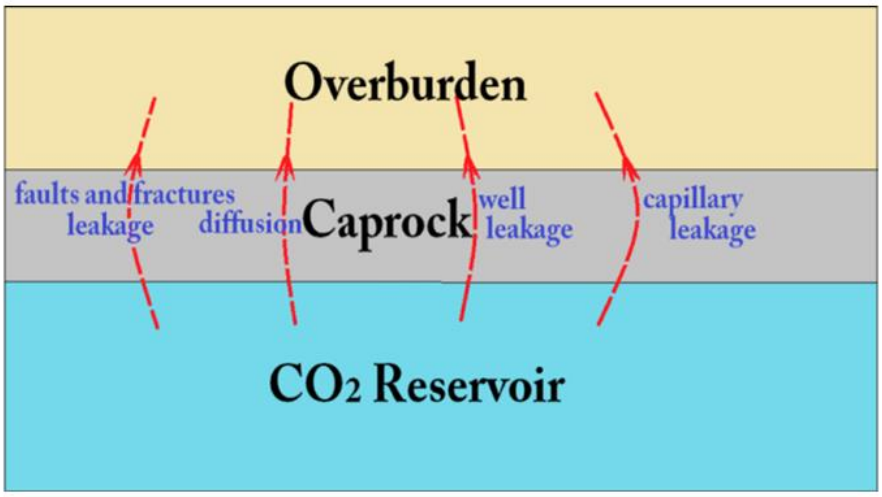

Figure 2.5: Leakage mechanisms involving the caprock (Song and Zhang, 2013). Leakage of CO2 into overlying caprock can occur through a leaky well or abandoned borehole, diffusion of CO2, flow through faults or fractures in the caprock, or through capillary leakage.

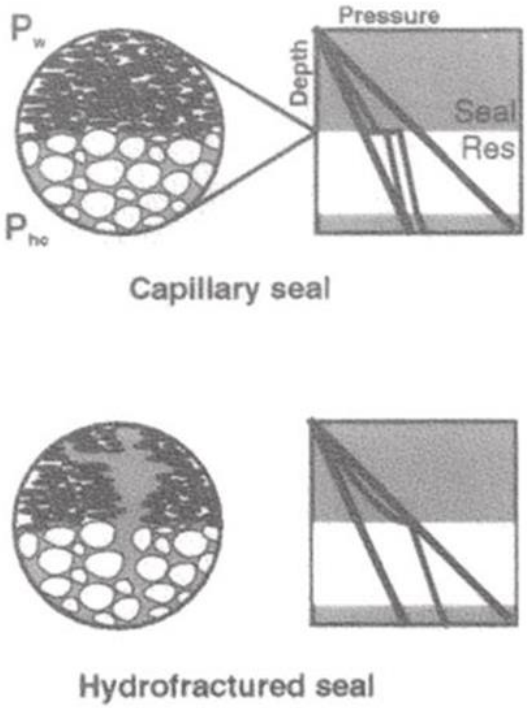

Figure 2.6: Membrane or capillary seals (top) fail due to capillary leakage. Hydraulic seals (bottom) have higher capillary entry pressure and fail due to hydraulic fracturing (Ingram et al., 1997).

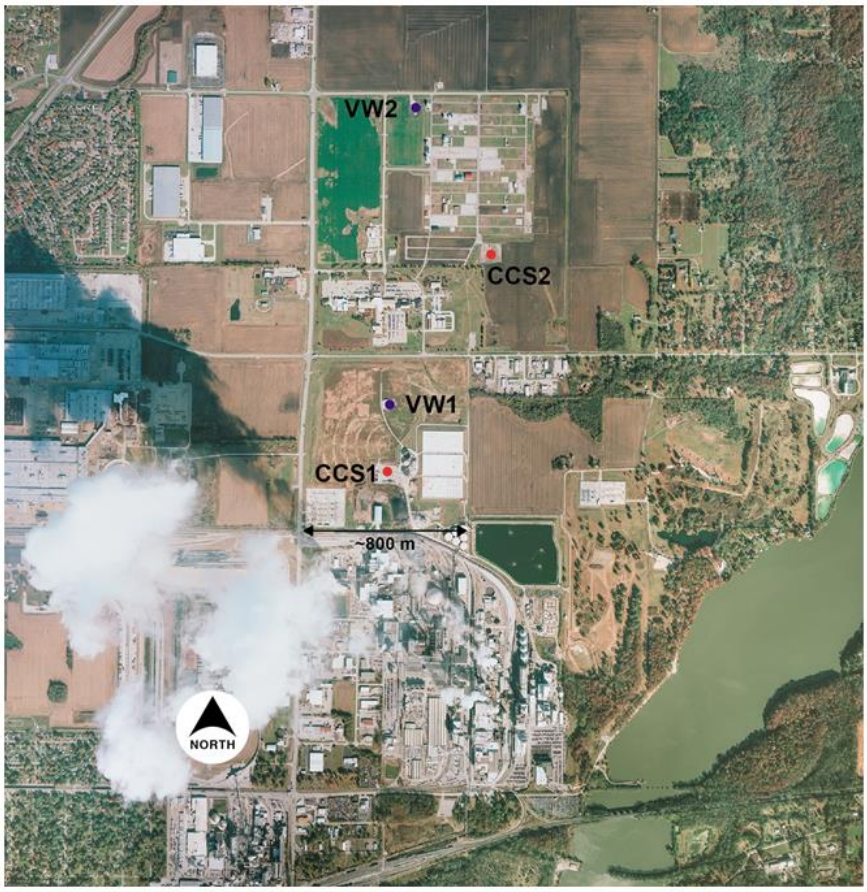

Figure 2.7: Aerial view of Illinois Basin – Decatur Project showing injection wells (CCS1 and CCS2) and verification wells (VW1 and VW2) (Leetaru and Freiburg, 2014).

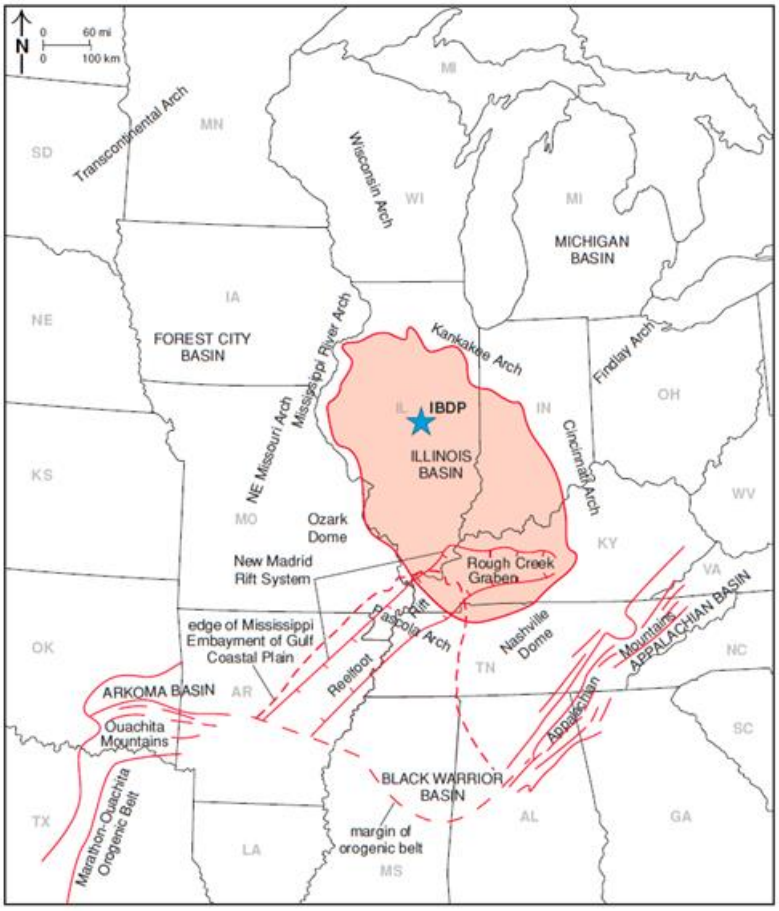

Figure 2.8: Regional map of the Midwestern United States showing the Illinois Basin – Decatur Project within the Illinois Basin and relevant structural features (Finley, 2014).

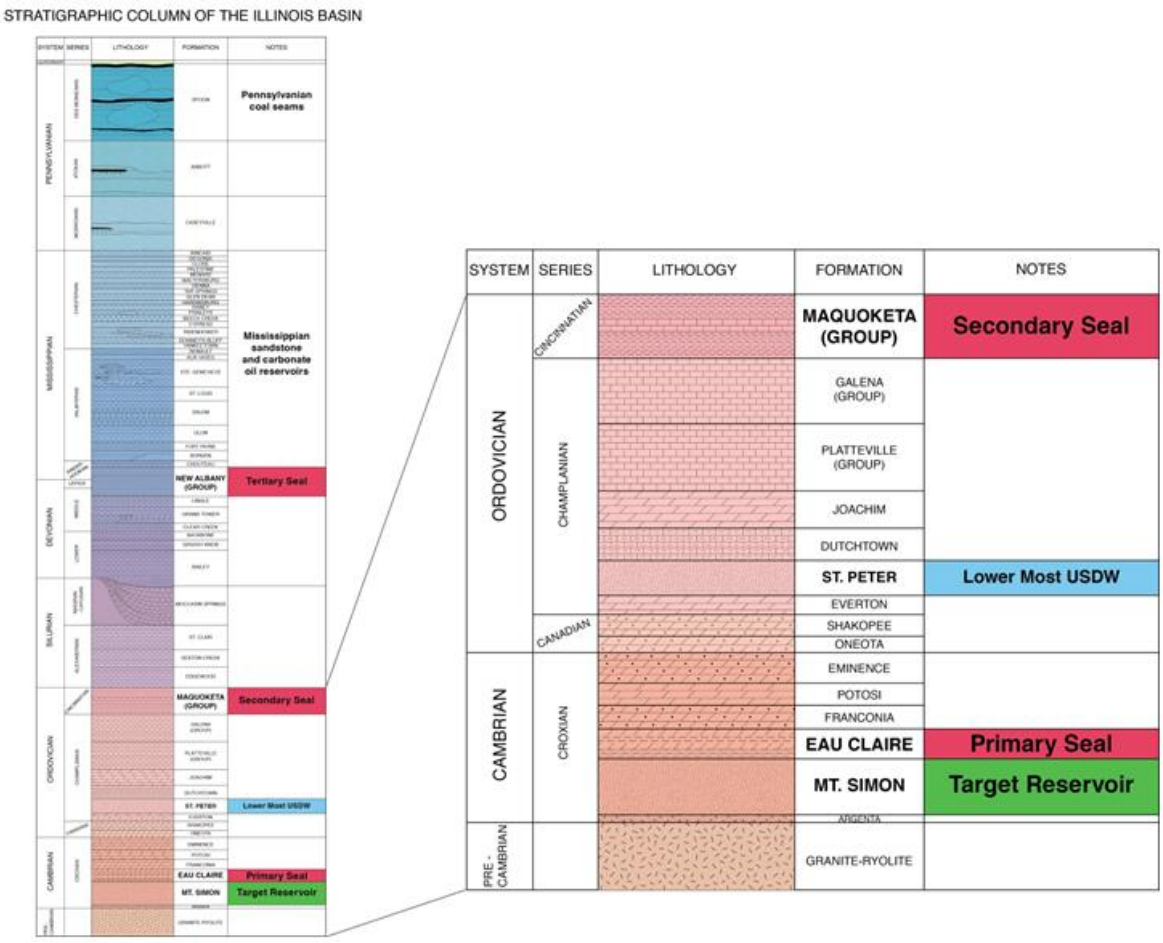

Figure 2.9: Stratigraphic column of the Illinois Basin with emphasis on the Precambrian and Cambrian lithology (personal communication with Sallie Greenberg Ph.D., 2016). Low permeability formations can act as primary and secondary seals to GCS are noted.

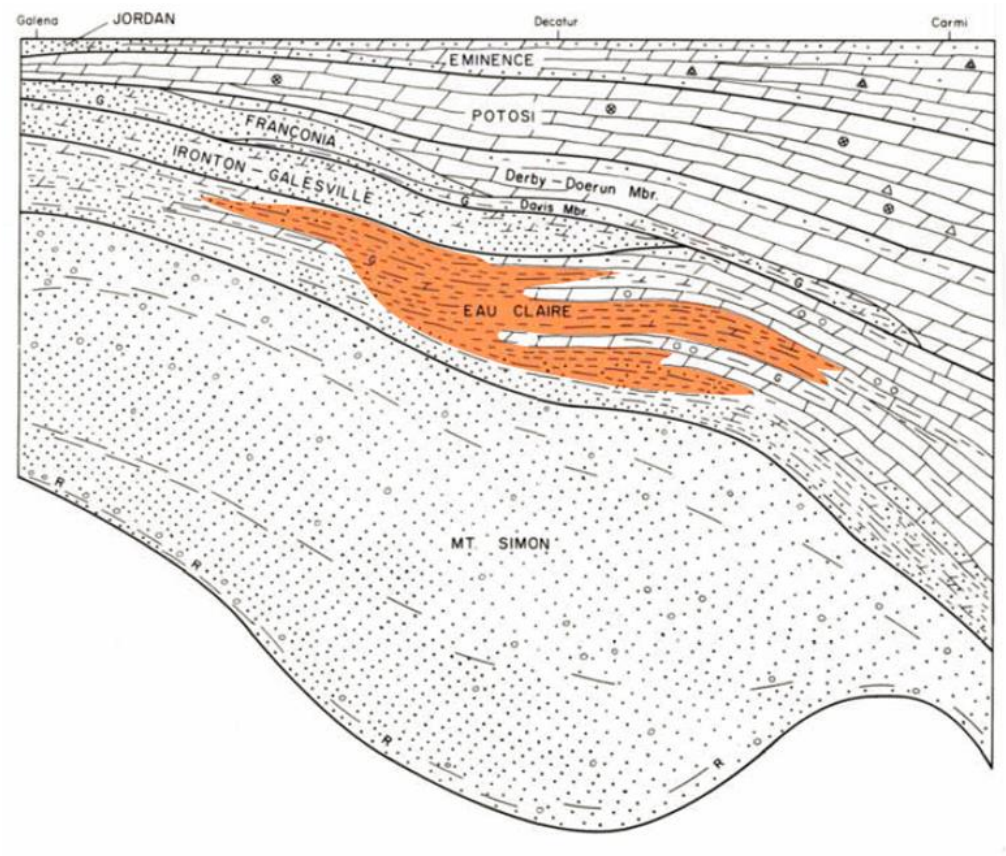

Figure 2.10: Diagrammatic cross section of Cambrian lithology from northwestern Illinois to southeastern Illinois. Orange area indicates where the Eau Claire is primarily shale near IBDP (from Finley, 2005 *modified after Willman et al., 1975).*

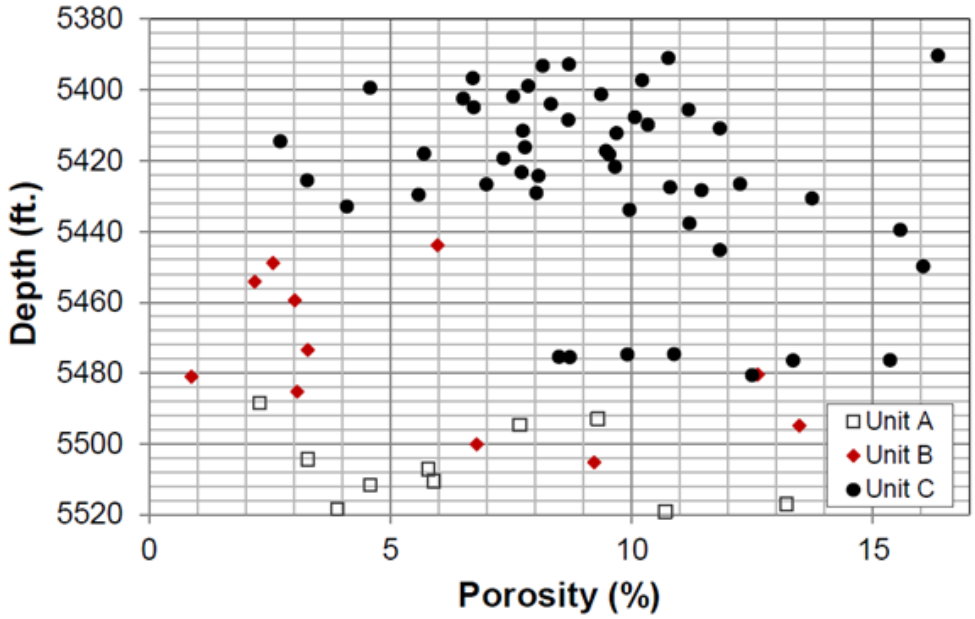

Figure 2.11: Depth (ft) vs porosity (%) for the Eau Claire at VW1, VW2 and CCS1 wells at IBDP (Palkovic, 2015).

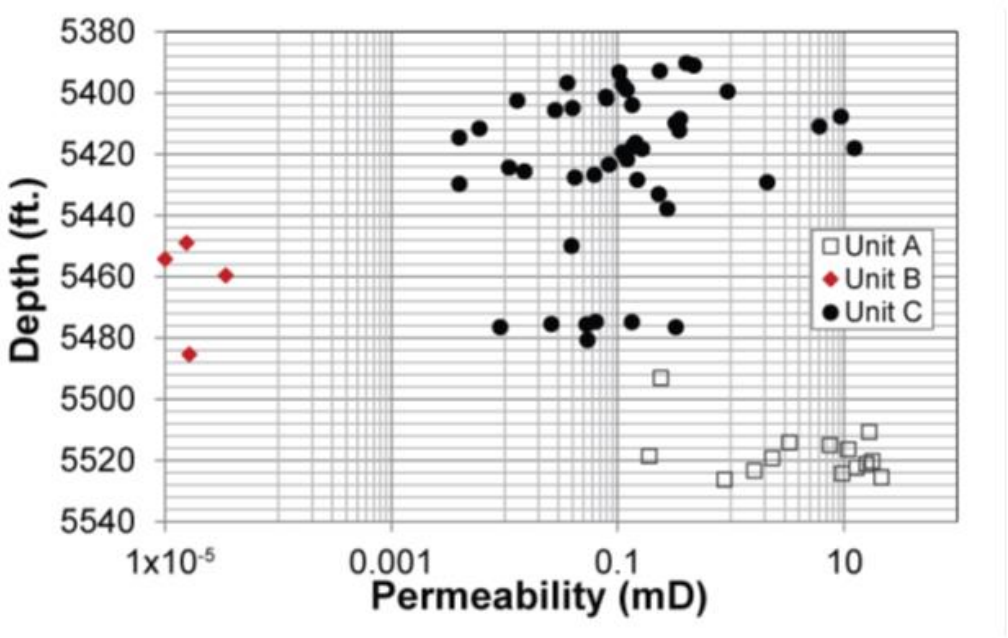

Figure 2.12: Depth (ft) vs air permeability (mD) for the Eau Claire at VW1, VW2, and CCS1 wells at IBDP (Palkovic, 2015).

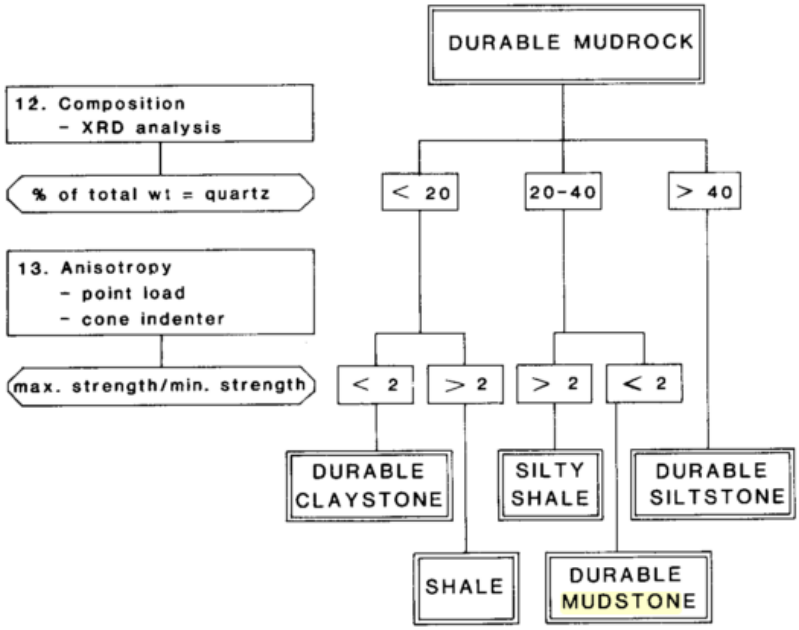

Figure 2.13: Classification of durable mudrocks (adapted from Grainger, 1984).

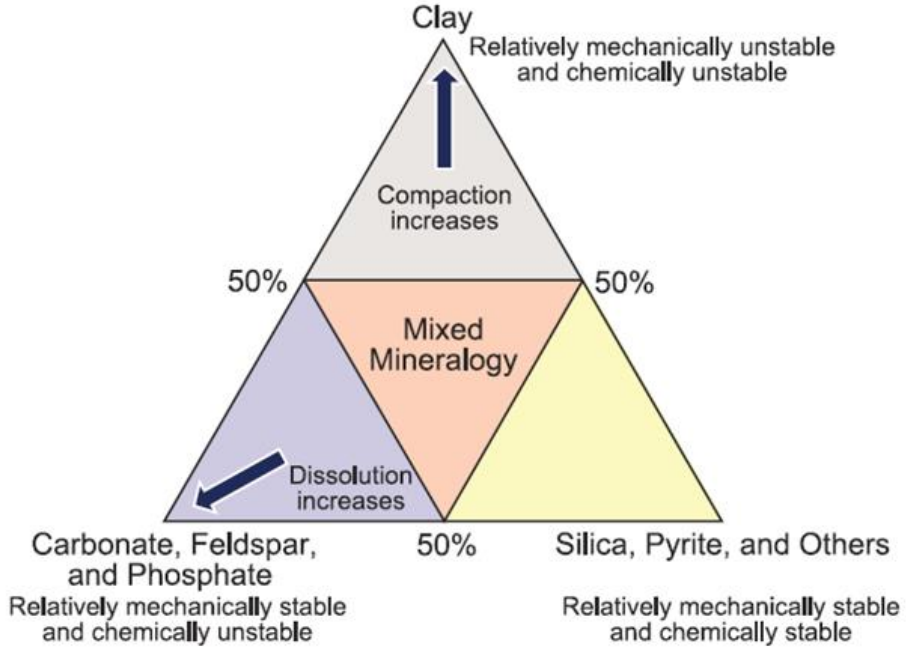

Figure 2.14: Compositional diagram for mudrocks showing stability relationships (Loucks et al., 2012).

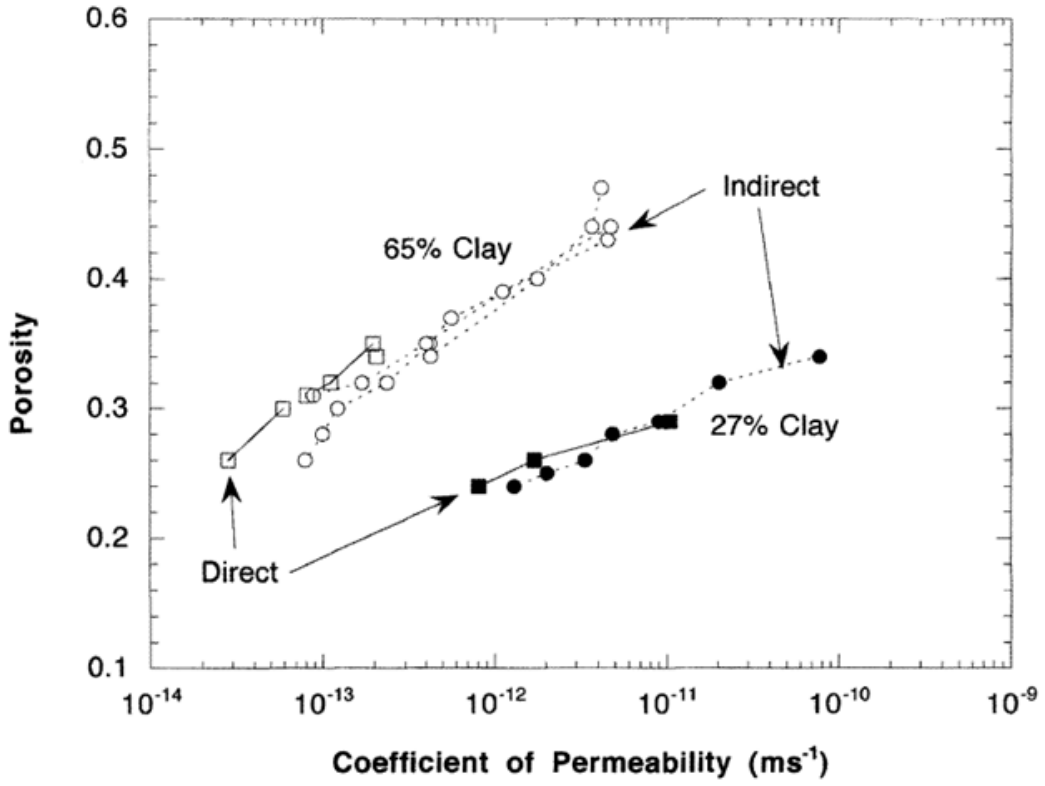

Figure 2.15: Experimentally derived porosity-permeability relationship for two clays (Dewhurst et al., 1999).

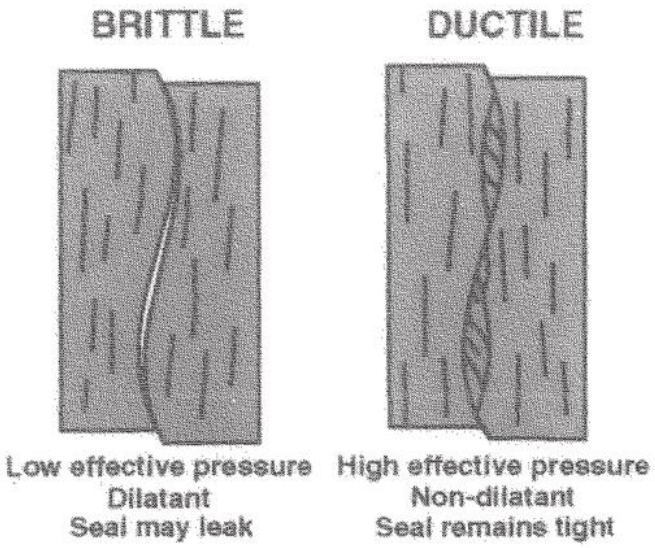

Figure 2.16: Microscale processes leading to dilatant or non-dilatant fractures (Ingram et al., 1997).

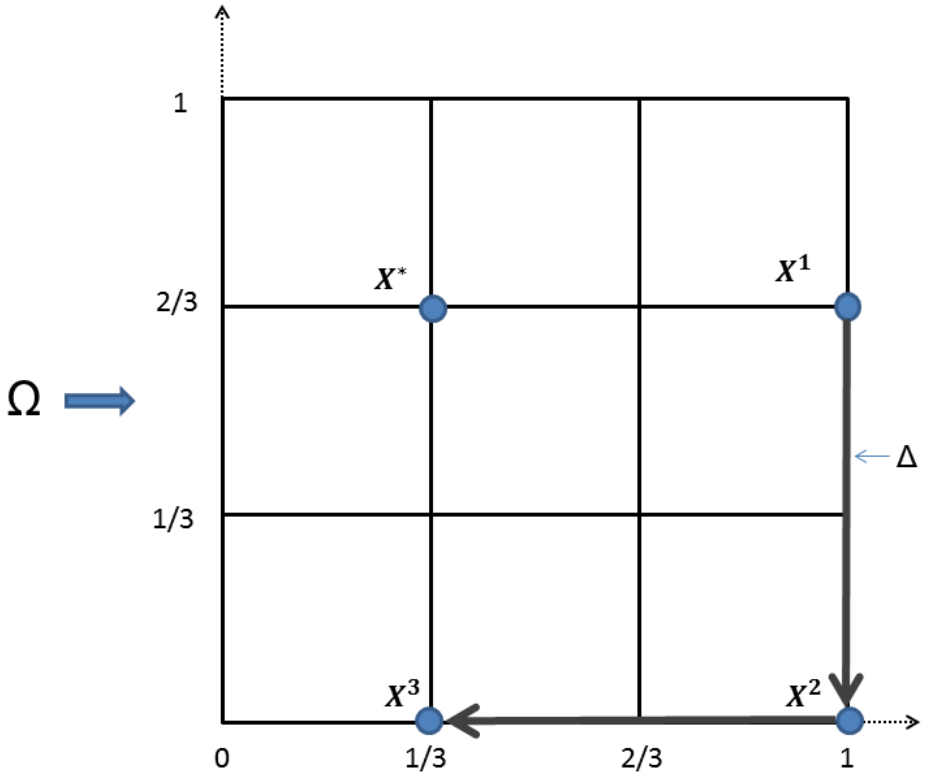

Figure 3.1: Example of a trajectory *r* in input space Ω when *k*=2 and Δ=2/3 and *p*=4. One of the factors in the randomly selected base X* is increased by Δ (X^1) to begin the trajectory.

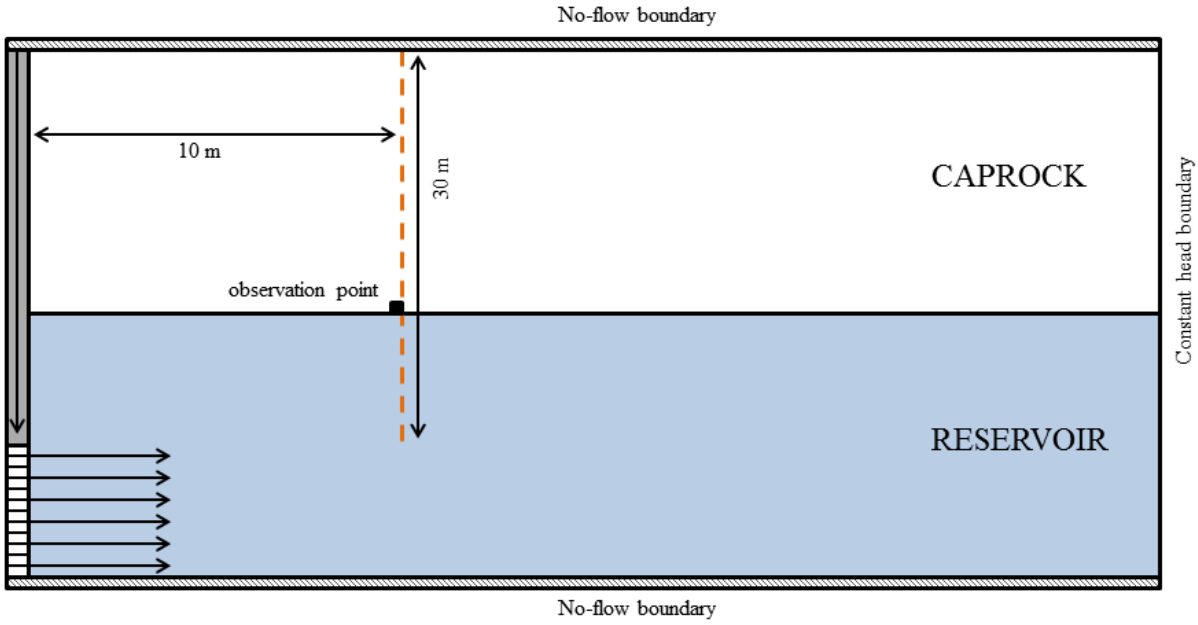

Figure 3.2. Schematic of TOUGH2 simulation model and locations of interest for the sensitivity anlaysis. The observation point is located 10 m from the injection well and at the base of the caprock. The 30 m vertical cross section passes through the caprock and the top 10 m of the reservoir.

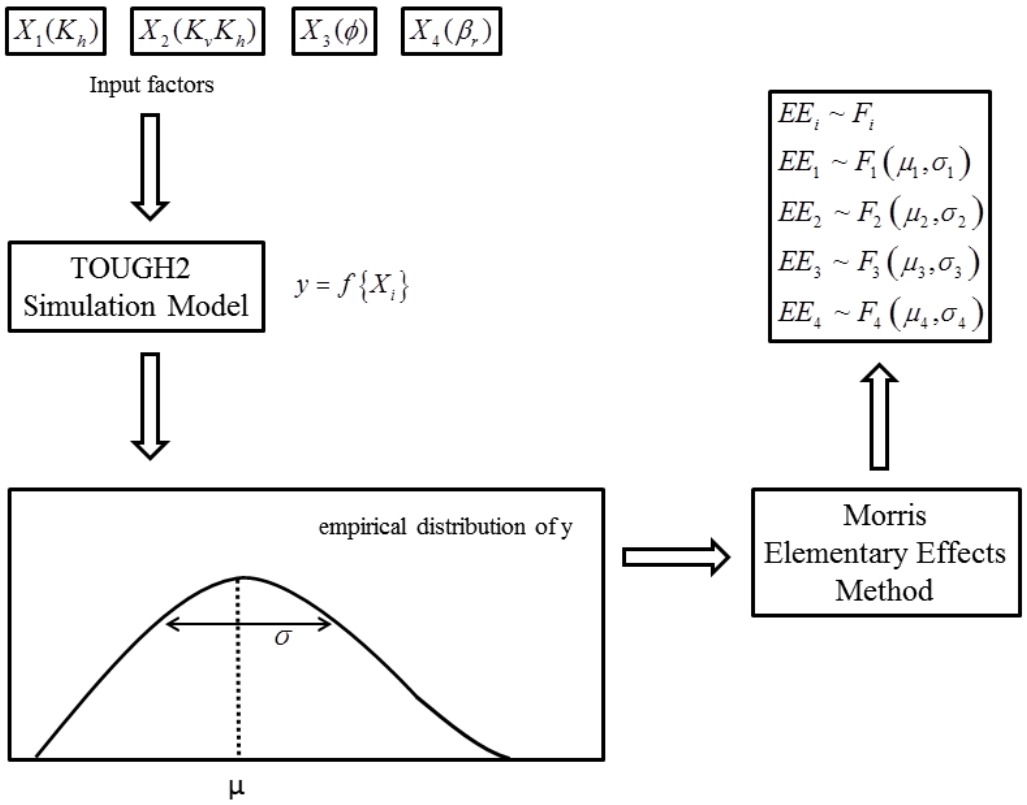

Figure 3.3: Schematic of TOUGH2 simulation output *y* (ΔP) used in the Morris method sensitivity analysis.

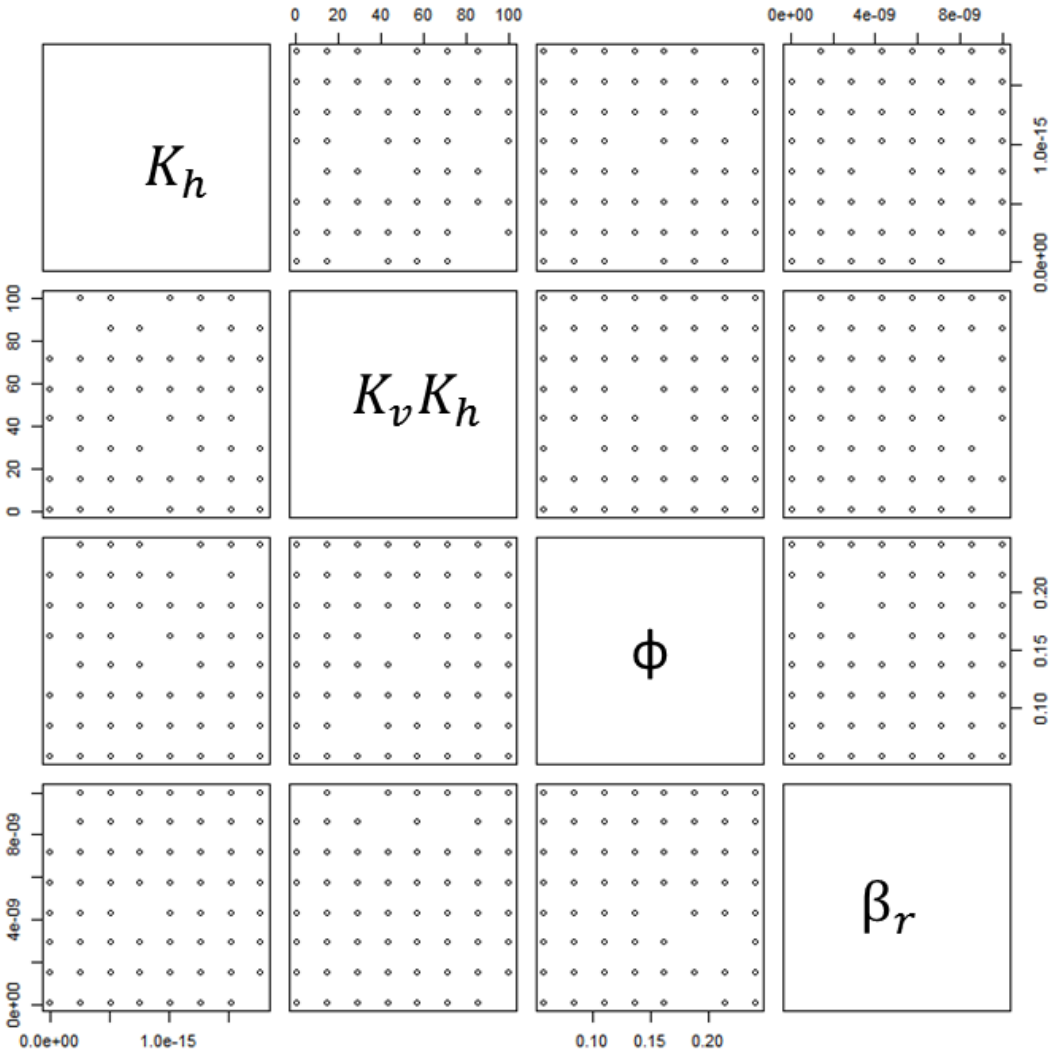

Figure 4.1: The caprock parameter sample set (Kh – horizontal permeability, KvKh – anisotropic permeability ratio, ϕ - porosity, and βr – rock compressibility) generated for Morris sensitivity analysis as input for the TOUGH2 simulations. Each circle corresponds to a single set of the four caprock parameters that will be used in simulation. Total number of simulations is 250.

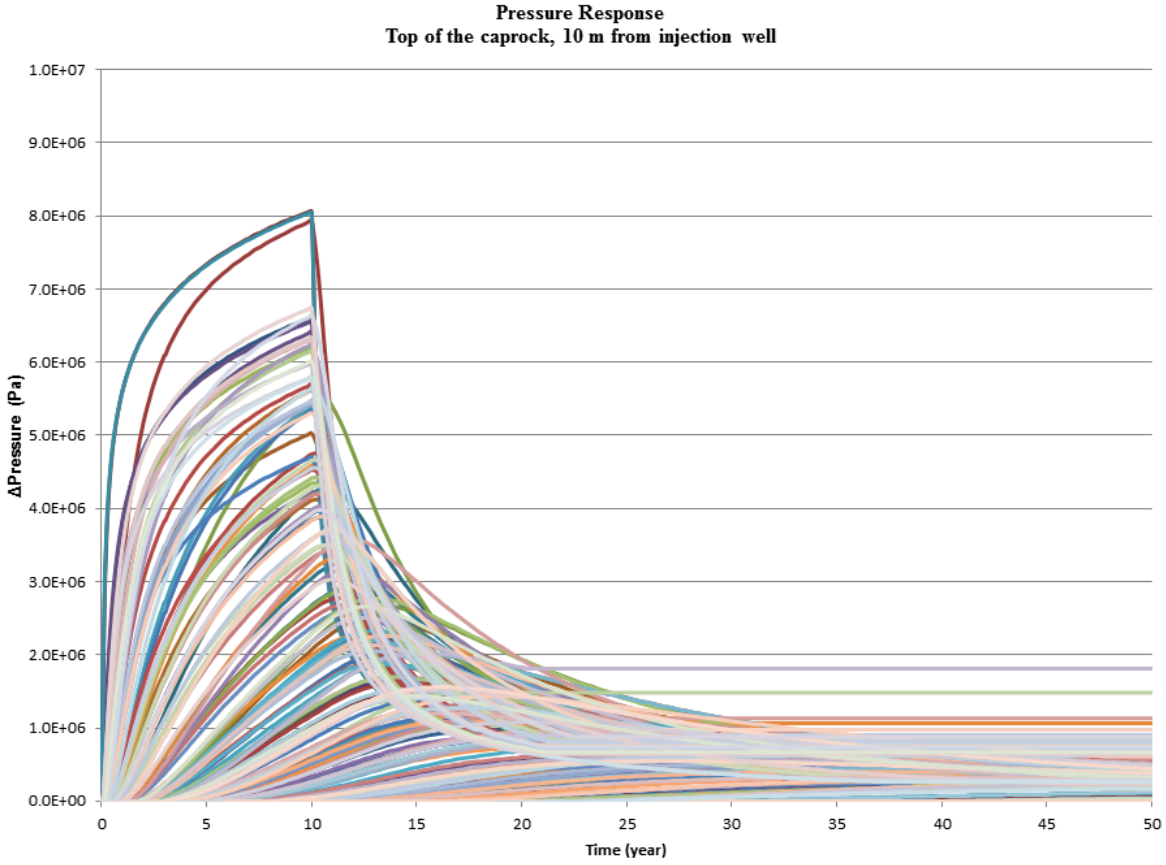

Figure 4.2: The simulated pressure change at the observation point located at the top of the caprock 10m from the injection well for 250 simulations.

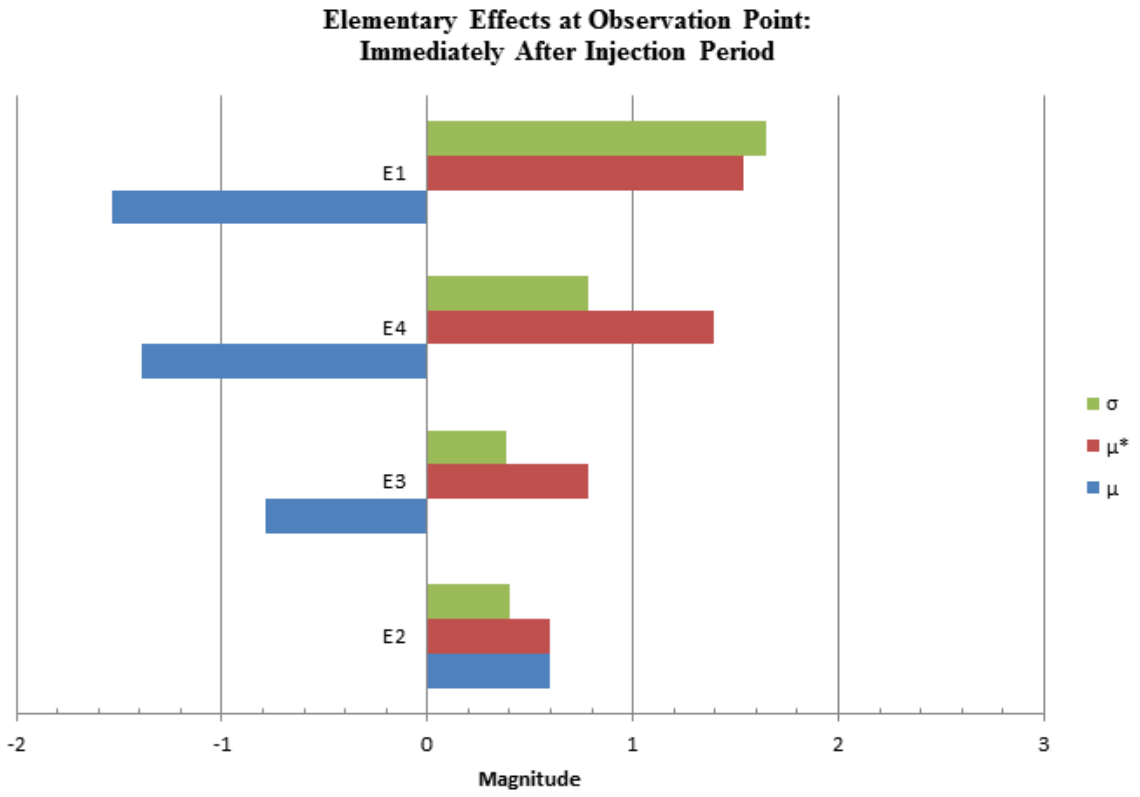

Figure 4.3: The mean μ, absolute mean, μ* and standard deviation σ of the elementary effects at observation point at immediately after injection ends. E1 = horizontal permeability, E2 = anisotropic permeability ratio, E3 = porosity, and E4 = rock compressibility.

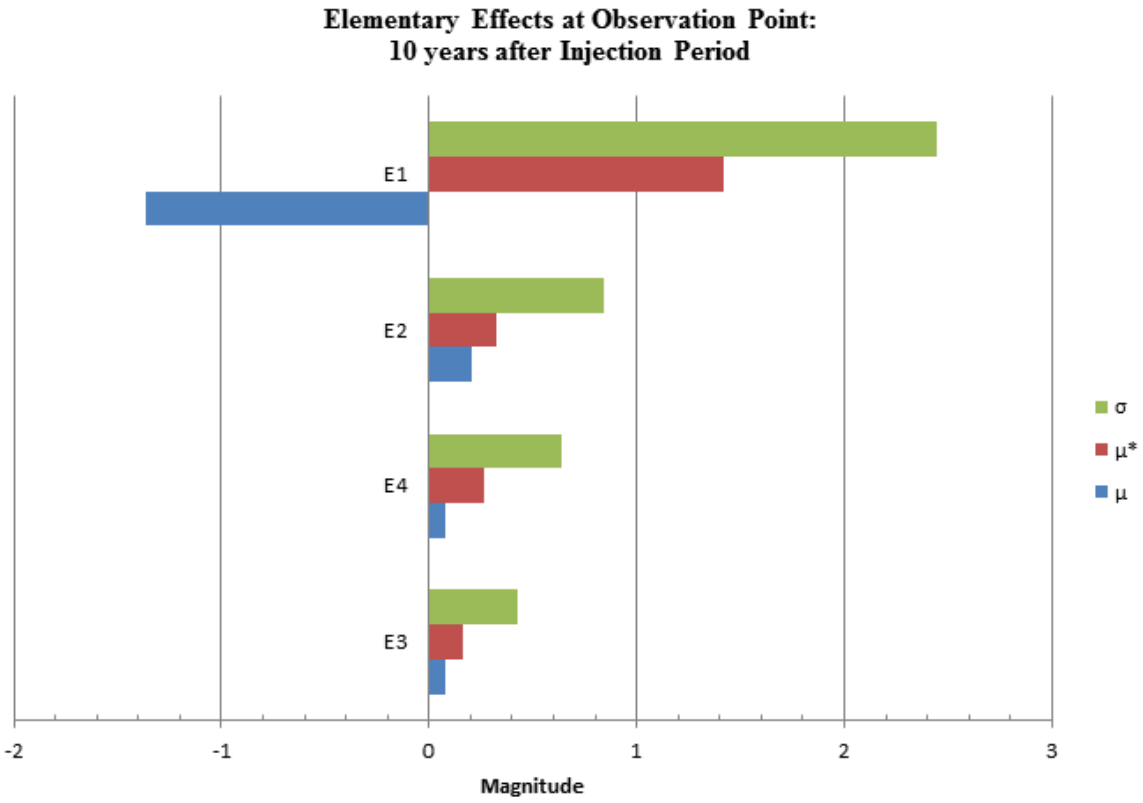

Figure 4.4: The mean μ, absolute mean, μ* and standard deviation σ of the elementary effects at observation point at 10 years post injection. E1 = horizontal permeability, E2 = anisotropic permeability ratio, E3 = porosity, and E4 = rock compressibility.

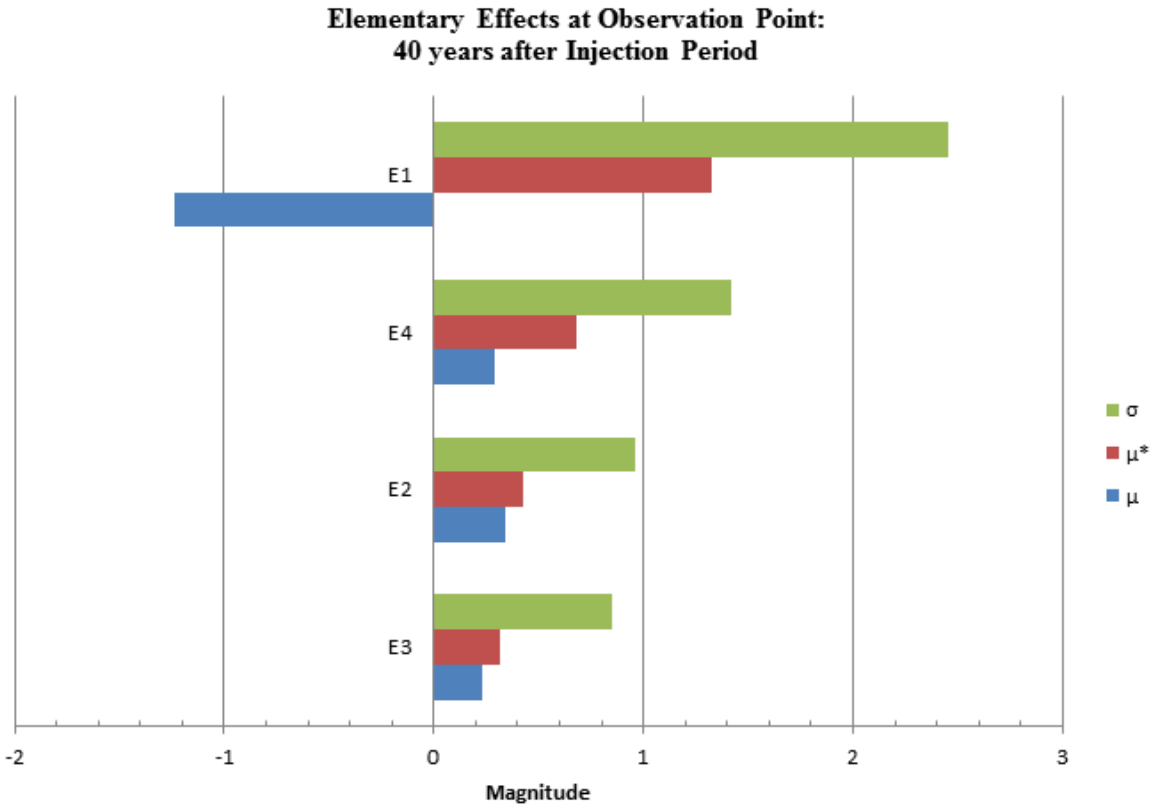

Figure 4.5: The mean μ, absolute mean, μ* and standard deviation σ of the elementary effects at observation point at 40 years post injection. E1 = horizontal permeability, E2 = anisotropic permeability ratio, E3 = porosity, and E4 = rock compressibility.

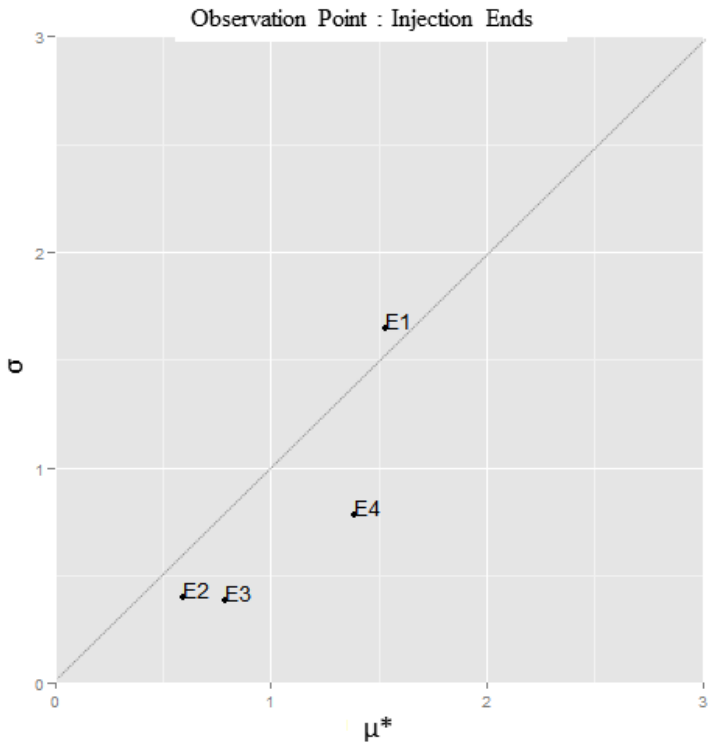

Figure 4.6: The absolute mean μ* vs standard deviation σ of the elementary effects at observation point immediately after injection ends. E1 = horizontal permeability, E2 = anisotropic permeability ratio, E3 = porosity, and E4 = rock compressibility.

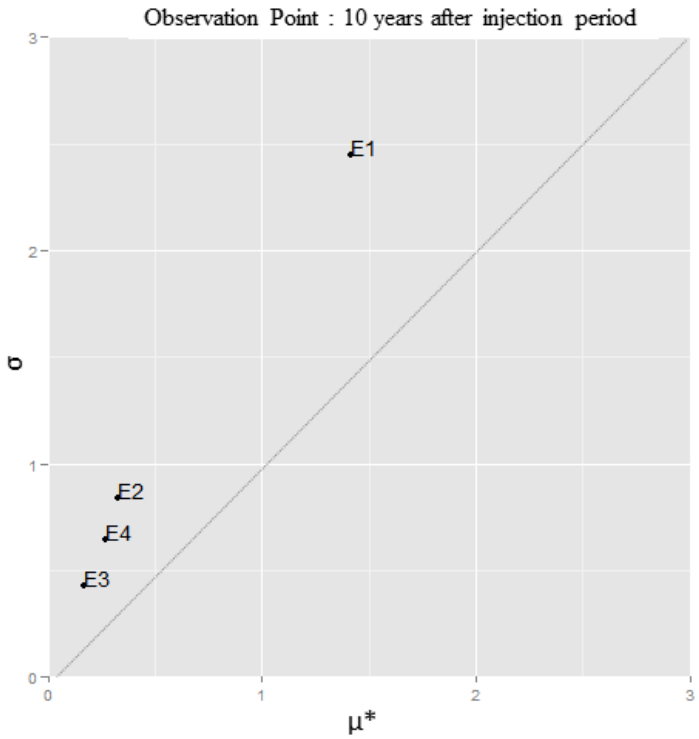

Figure 4.7: The absolute mean μ* vs standard deviation σ of the elementary effects at observation point at 10 years post injection. E1 = horizontal permeability, E2 = anisotropic permeability ratio, E3 = porosity, and E4 = rock compressibility.

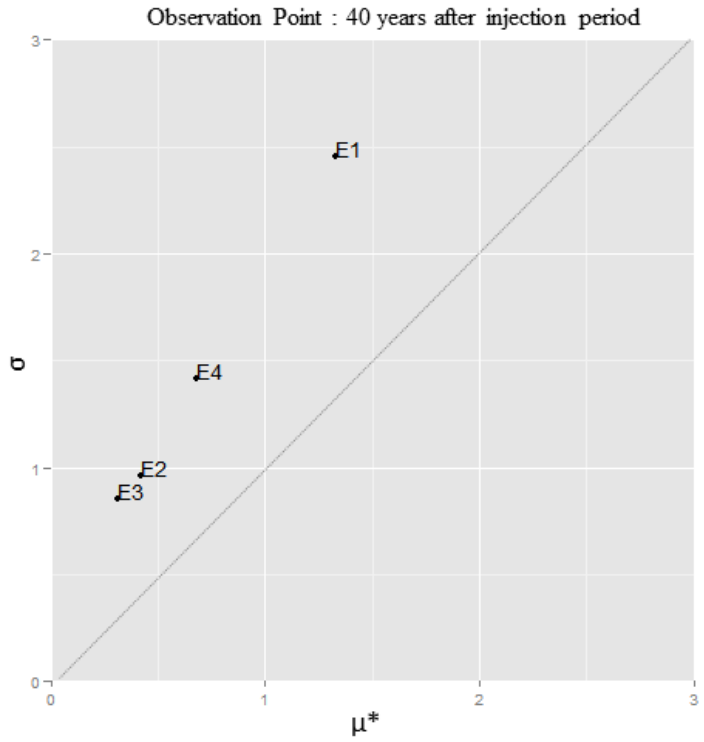

Figure 4.8: The absolute mean μ* vs standard deviation σ of the elementary effects at observation point at 40 years post injection. E1 = horizontal permeability, E2 = anisotropic permeability ratio, E3 = porosity, and E4 = rock compressibility.

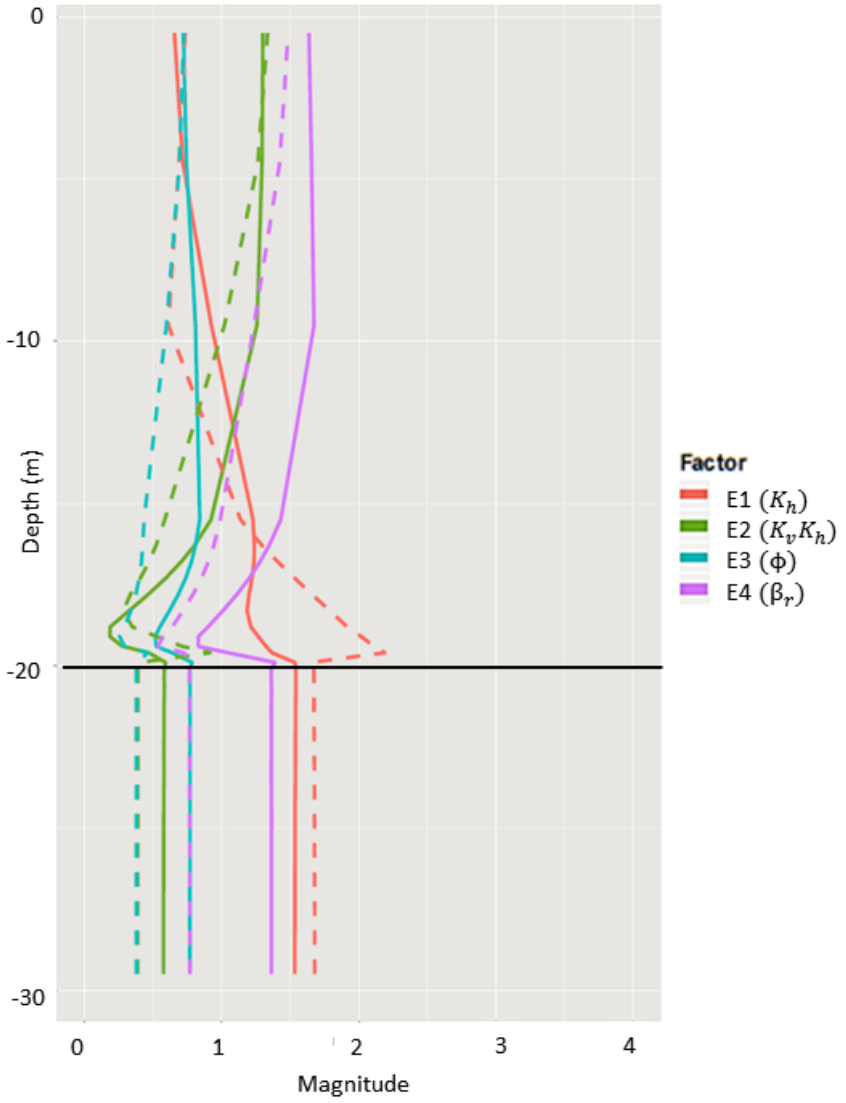

Figure 4.9: Elementary effects at vertical cross section, 10 m from injection well when injection ends. The bottom 10 m of the reservoir was not included in the sensitivity analysis. Solid lines are μ* and dashed lines represent σ. Black line indicates the caprock-reservoir boundary.

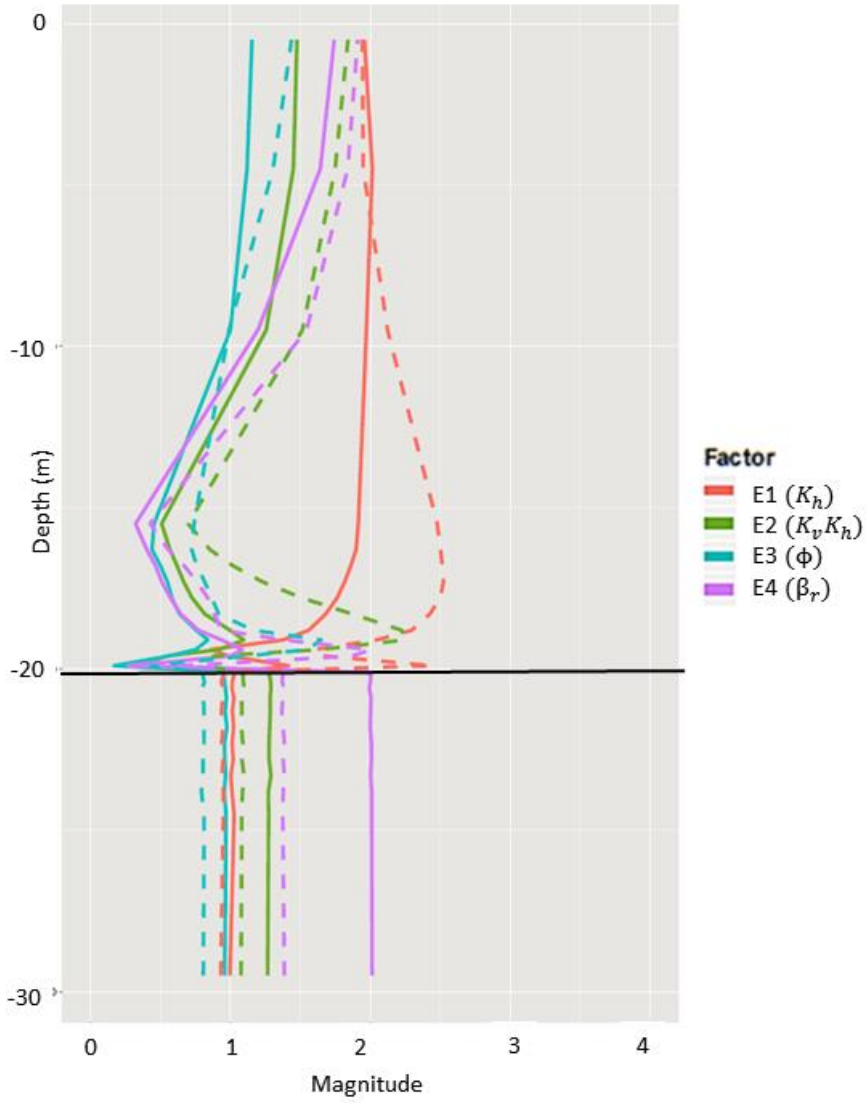

Figure 4.10: Elementary effects at vertical cross section, 10 m from injection well 10 years after injection ends. The bottom 10 m of the reservoir was not included in the sensitivity analysis. Solid lines are μ* and dashed lines represent σ. Black line indicates the caprock-reservoir boundary.

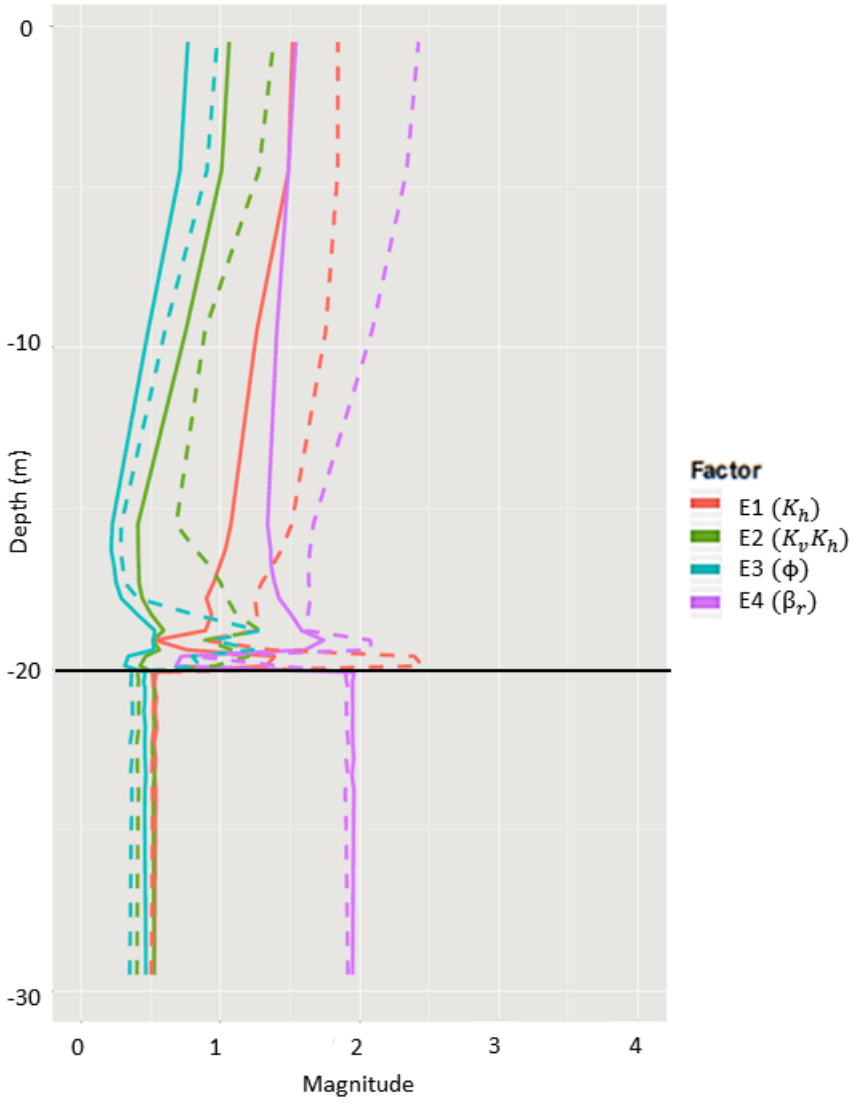

Figure 4.11: Elementary effects at vertical cross section, 10 m from injection well 40 years after injection ends. The bottom 10 m of the reservoir was not included in the sensitivity analysis. Solid lines are μ* and dashed lines represent σ. Black line indicates the caprock-reservoir boundary.

REFERENCES

Alemu, B. L., Aagaard, P., Munz, I. A., & Skurtveit, E. (2011). Caprock interaction with CO2: A laboratory study of reactivity of shale with supercritical CO2 and brine. *Applied Geochemistry*, *26*(12), 1975–1989.

Amann-Hildenbrand, A., Bertier, P., Busch, A., & Krooss, B. M. (2013). Experimental investigation of the sealing capacity of generic clay-rich caprocks. *International Journal of Greenhouse Gas Control*, *19*, 620-641.

Ambrose, W. a., Lakshminarasimhan, S., Holtz, M. H., Núñez-López, V., Hovorka, S. D., & Duncan, I. (2008). Geologic factors controlling CO2 storage capacity and permanence: case studies based on experience with heterogeneity in oil and gas reservoirs applied to CO2 storage. *Environmental Geology*, *54*(8), 1619–1633.

Anderson, M. P., & Woessner, W. W. (2002). Applied groundwater modeling: Simulation to flow and advective transport. *Journal of Contaminant Hydrology*, *10*(4), 339–340.

Ashraf, M., Oladyshkin, S., & Nowak, W. (2013). Geological storage of CO2: Application, feasibility and efficiency of global sensitivity analysis and risk assessment using the arbitrary polynomial chaos. *International Journal of Greenhouse Gas Control*, *19*, 704–719.

Aswasereelert, W., Simo, J. A. T., & Lepain, D. L. (2008). Deposition of the Cambrian Eau Claire Formation , Wisconsin : Hydrostratigraphic Implications of Fine-Grained Cratonic Sandstones. *Geoscience Wisconsin*, *19*(Part 1), 22.

Bachu, S., & Adams, J. J. (2003). Sequestration of CO2 in geological media in response to climate change: Capacity of deep saline aquifers to sequester CO2 in solution. *Energy Conversion and Management*, *44*(20), 3151–3175.

Bachu, S., Gunter, W. D., & Perkins, E. H. (1994). Aquifer disposal of CO2: Hydrodynamic and mineral trapping. *Energy Conversion and Management*, *35*(4), 269–279.

Baines, S. J., & Worden, R. H. (2004). The long-term fate of CO2 in the subsurface: natural analogues for CO2 storage. *Geological Society, London, Special Publications*, *233*(1), 59–85.

Bao, J., Xu, Z., Lin, G., & Fang, Y. (2013). Evaluating the impact of aquifer layer properties on geomechanical response during CO2 geological sequestration. *Computers & Geosciences*, *54*, 28–37.

Bergstrom, R. E. (1968). *Feasibility of Subsurface Disposal of Industrial Wastes in Illinois*, Illinois State Geological Survey Circular: 426.

Beven, K. (2002). Towards a coherent philosophy for modelling the environment. *Proceedings of the Royal Society of London Series A-Mathematical Physical and Engineering Science*, *458*, 1–20.

Birkholzer, J. T., & Zhou, Q. (2009). Basin-scale hydrogeologic impacts of CO2 storage: Capacity and regulatory implications. *International Journal of Greenhouse Gas Control*, *3*(6), 745–756.

Bowen, B. B., Ochoa, R. I., Wilkens, N. D., Brophy, J., Lovell, T. R., Fischietto, N., … Rupp, J. a. (2011). Depositional and diagenetic variability within the Cambrian Mount Simon Sandstone: Implications for carbon dioxide sequestration. *Environmental Geosciences*, *18*(2), 69–89.

Busch, A., Alles, S., Gensterblum, Y., Prinz, D., Dewhurst, D. N., Raven, M. D., … Krooss, B. M. (2008). Carbon dioxide storage potential of shales. *International Journal of Greenhouse Gas Control*, *2*(3), 297–308.

Busch, A., & Amann-Hildenbrand, A. (2013). Predicting capillarity of mudrocks. *Marine and Petroleum Geology*, *45*, 208–223.

Cacuci, D. G., Ionescu-bujor, M., & Navon, I. M. (2005). A COMPARATIVE REVIEW OF SENSITIVITY AND LARGE-SCALE SYSTEMS. *SENSITIVITY UNCERTAINTY Applications to Large-Scale Systems, Volume II* (pp. 1-35).

Campolongo, F., Cariboni, J., & Saltelli, A. (2007). An effective screening design for sensitivity analysis of large models. *Environmental Modelling & Software*, *22*(10), 1509–1518.

Cebell, W. A., & Chilingarian, G. V. (1972). Some Data on Compressibility and Density Anomalies in Halloysite, Hectorite, and Illite Clays. *AAPG Bulletin*, *56*(4), 796–802.

Celia, M. A., Nordbotten, J. M., Court, B., Dobossy, M., & Bachu, S. (2011). Field-scale application of a semi-analytical model for estimation of CO2 and brine leakage along old wells. *International Journal of Greenhouse Gas Control*, *5*(2), 257–269.

Chang, K. W., Hesse, M. a., & Nicot, J.-P. (2013). Reduction of lateral pressure propagation due to dissipation into ambient mudrocks during geological carbon dioxide storage. *Water Resources Research*, *49*(5), 2573–2588.

Cheng, C.-L., Gragg, M. J., Perfect, E., White, M. D., Lemiszki, P. J., & McKay, L. D. (2013). Sensitivity of injection costs to input petrophysical parameters in numerical geologic carbon sequestration models. *International Journal of Greenhouse Gas Control*, *18*, 277–284.

Daniel, R. F., & Kaldi, J. G. (2008). Evaluating seal capacity of caprocks and intraformational barriers for the geosequestration of CO2. *Pesa Eabs Iii*, 475-484.

Deng, H., Stauffer, P. H., Dai, Z., Jiao, Z., & Surdam, R. C. (2012). Simulation of industrial-scale CO2 storage: Multi-scale heterogeneity and its impacts on storage capacity, injectivity and leakage. *International Journal of Greenhouse Gas Control*, *10*, 397–418.

Dewhurst, D. N., Yang, Y., & Aplin, A. C. (1999). Permeability and fluid flow in natural mudstones. *Geological Society, London, Special Publications*, *158*(1), 23–43.

Dewhurst, D. N., Aplin, A. C., Sarda, J.-P., & Yang, Y. (1998). Compaction-driven evolution of porosity and permeability in natural mudstones: An experimental study. *J. Geophys. Res.*, *103*(B1), 651–661.

Donaldson, E. C. (1964). *Subsurface disposal of industrial wastes in the United States*. US Bureau Mines Inf Circ, 8212.

Downey, M. W. (1984). EVALUATING SEALS FOR HYDROCARBON ACCUMULATIONS. *American Association of Petroleum Geologists Bulletin*, *68*(11), 1752–1763.

Edlmann, K., Haszeldine, S., & McDermott, C. I. (2013). Experimental investigation into the sealing capability of naturally fractured shale caprocks to supercritical carbon dioxide flow. *Environmental Earth Sciences*, *70*(7), 3393–3409.

Eiken, O., Ringrose, P., Hermanrud, C., Nazarian, B., Torp, T. a., & Høier, L. (2011). Lessons learned from 14 years of CCS operations: Sleipner, In Salah and Snøhvit. *Energy Procedia*, *4*, 5541–5548.

Feinstein, D.T., T.T. Eaton, D.J. Hart, J.T. Krohelski and K.R. Bradbury. (2005). *Regional aquifer model for southeastern Wisconsin; Report 1: Data collection, conceptual model development, numerical model construction, and model calibration.* Wisconsin Geological and Natural History Survey administrative report prepared for Southeastern Wisconsin Regional Planning Commission.

Feinstein. (2010). *Regional Groundwater-Flow Model of the Lake Michigan Basin in Support of Great Lakes Basin Water Availability and Use Studies*. *Regional Groundwater-Flow Model, Lake Michigan Basin, in Support of Great Lakes Water Availability and Use Studies*.

Finley, R. (2005). *An assessment of geological carbon sequestration options in the Illinois Basin*. Illinois State Geological Survey Final Report, US DOE Contract DE-FC26-03NT41994, Champaign, Illinois.

Finley, R. J., Frailey, S. M., Leetaru, H. E., Senel, O., Couëslan, M. L., & Scott, M. (2013). Early Operational Experience at a One-million Tonne CCS Demonstration Project, Decatur, Illinois, USA. *Energy Procedia*, *37*, 6149–6155.

Fitts, J. P., & Peters, C. a. (2013). Caprock Fracture Dissolution and CO2 Leakage. *Reviews in Mineralogy and Geochemistry*, *77*(1), 459–479.

Flett, M., Gurton, R., & Taggart, I. (2004). The Function of Gas-Water Relative Permeability Hysteresis in the Sequestration of Carbon Dioxide in Saline Formations. *SPE Asia Pacific Oil and Gas Conference and Exhibition*.

Folk, R. L. (1968). Petrology of the sedimentary rocks. *Geomorphology*, 190.

Freiburg, J. T., Ritzi, R. W., & Kehoe, K. S. (2016). Depositional and diagenetic controls on anomalously high porosity within a deeply buried CO2 storage reservoir—The Cambrian Mt. Simon Sandstone, Illinois Basin, USA. *International Journal of Greenhouse Gas Control*, *55*, 42–54.

Freiburg, J.T., Morse, D.G., Leetaru, H.E., Hoss, R.P., and Yan, Q. (2014). *A depositional and diagenetic characterization of the Mt. Simon Sandstone at the Illinois Basin - Decatur Project (IBDP) carbon capture and storage (CCS) site: Decatur, Illinois, USA*, Illinois State Geological Survey, Circular 583.

Gaus, I. (2010). Role and impact of CO2-rock interactions during CO2 storage in sedimentary rocks. *International Journal of Greenhouse Gas Control*.

Gorokhovski, V. (2012). *Effective Parameters of Hydrogeological Models*.

Grainger, P. (1984). The classification of mudrocks for engineering purposes. *Quarterly Journal of Engineering Geology*, *17*, 381–387.

Griffith, C. a., Dzombak, D. a., & Lowry, G. V. (2011). Physical and chemical characteristics of potential seal strata in regions considered for demonstrating geological saline CO2 sequestration. *Environmental Earth Sciences*, *64*(4), 925–948.

Grunau, H. R. (1987). A worldwide look at the cap rock problem. *Journal of Petroleum Geology*, *10*(3), 245–266.

Gunter, W. D., Bachu, S., & Benson, S. (2004). The role of hydrogeological and geochemical trapping in sedimentary basins for secure geological storage of carbon dioxide. *Geological Society, London, Special Publications*.

Gunter, W. D., Perkins, E. H., & McCann, T. J. (1993). Aquifer disposal of CO2-rich gases: Reaction design for added capacity. *Energy Conversion and Management*, *34*(9–11), 941–948.

Gupta, N., & Bair, E. S. (1997). Variable-density flow in the midcontinent basins and arches region of the United States. *Water Resources Research*, *33*(8), 1785.

Han, W. S., Kim, K.-Y., Esser, R. P., Park, E., & McPherson, B. J. (2011). Sensitivity Study of Simulation Parameters Controlling CO2 Trapping Mechanisms in Saline Formations. *Transport in Porous Media*, *90*(3), 807–829.

Harlow, I. F. (1939). Waste Problems of a Chemical Company. *Industrial and Engineering Chemistry*, *31*(11), 1346–1349.

Heath, J. E., Dewers, T. a., McPherson, B. J. O. L., Nemer, M. B., & Kotula, P. G. (2012). Pore-lining phases and capillary breakthrough pressure of mudstone caprocks: Sealing efficiency of geologic CO2 storage sites. *International Journal of Greenhouse Gas Control*, *11*, 204–220.

Hildenbrand, A., Schlömer, S., & Krooss, B. (2002). Gas breakthrough experiments on fine-grained sedimentary rocks. *Geofluids*, 3–23.

Hildenbrand, a, Schlömer, S., Krooss, B. M., & Littke, R. (2004). Gas breakthrough experiments on pelitics rocks: comparitive study with N2, CO2 and CH4. *Geofluids*, *4*, 61-80.

Højberg, a L., & Refsgaard, J. C. (2005). Model uncertainty--parameter uncertainty versus conceptual models. *Water Science and Technology : A Journal of the International Association on Water Pollution Research*, *52*(6), 177–86.

Hou, Z., Rockhold, M. L., & Murray, C. J. (2012). Evaluating the impact of caprock and reservoir properties on potential risk of CO2 leakage after injection. *Environmental Earth Sciences*, *66*(8), 2403–2415.

Ingram, G. M., & Urai, J. L. (1999). Top-seal leakage through faults and fractures: the role of mudrock properties. *Geological Society, London, Special Publications*, *158*(1), 125–135.

Ingram, G. M., Urai, J. L., & Naylor, M. A. (1997). Sealing processes and top seal assessment. *Norwegian Petroleum Society Special Publications*, *7*(C), 165-174.

Ingram, R. L. (1953). Fissility of mudrocks. *Bulletin of the Geological Society of America*, *64*(8), 869–878.

IPCC. (2005). *IPCC special report on carbon dioxide capture and storage*. *IPCC Special Report on Carbon Dioxide Capture and Storage* (Vol. 2).

Jimenez, J.A. and Chalaturnyk, R.J. (2001). Geomechanical Behaviour of Stiff Clays and Mudstones as Caprocks for Geological Sequestration of CO2. In: 2001 an Earth Odyssey: 54th Canadian Geotechnical Conference. Ed. CGS. Calgary, AB 7.

Jung, Y., Zhou, Q., & Birkholzer, J. T. (2013). Early detection of brine and CO2 leakage through abandoned wells using pressure and surface-deformation monitoring data: Concept and demonstration. *Advances in Water Resources, 62, 555-569.*

Keith, L. A., & Rimstidt, J. D. (1985). A numerical compaction model of overpressuring in shales. *Journal of the International Association for Mathematical Geology*, *17*(2), 115–135.

Kharaka, Y. K., Cole, D. R., Thordsen, J. J., Kakouros, E., & Nance, H. S. (2006). Gas-water-rock interactions in sedimentary basins: CO2 sequestration in the Frio Formation, Texas, USA. *Journal of Geochemical Exploration*, *89*(1–3 SPEC. ISS.), 183–186.

Knauss, K. G., Johnson, J. W., & Steefel, C. I. (2005). Evaluation of the impact of CO2, co-contaminant gas, aqueous fluid and reservoir rock interactions on the geologic sequestration of CO2. *Chemical Geology*, *217*(3–4), 339–350.

Kolata, D.R., and Nelson, W.J. (2010). Geology of Illinois. University of Illinois, Champaign.

Koide H, Tazaki Y, Noguchi Y, Iiijima, M., Ito, K., Shindo, Y. (1993). Underground storage of carbon dioxide in depleted natural gas reservoirs and in useless aquifers. *Engineering Geology*, *34*(3-4): 175-179.

Konikow, L. F., & Bredehoeft, J. D. (1992). Ground-water models cannot be validated. *Advances in Water Resources*, *15*(1), 75–83.

Kopp, A., Binning, P. J., Johannsen, K., Helmig, R., & Class, H. (2010). A contribution to risk analysis for leakage through abandoned wells in geological CO2 storage. *Advances in Water Resources*, *33*(8), 867–879.

Korbøl, R., & Kaddour, A. (1995). Sleipner vest CO2 disposal - injection of removed CO2 into the Utsira formation. *Energy Conversion and Management*, *36*(6–9), 509–512.

Krooss, B. M., Leythaeuser, D., & Schaefer, R. G. (1992). The quantification of diffusive hydrocarbon losses through cap rocks of natural gas reservoirs - a reevaluation. *American Association of Petroleum Geologists Bulletin*.

Leetaru, H. E., & Freiburg, J. T. (2014). Litho-facies and reservoir characterization of the Mt Simon Sandstone at the Illinois Basin-Decatur Project. *Greenhouse Gases: Science and Technology*. Blackwell Publishing Ltd.

Leetaru, H. E., & McBride, J. H. (2009). Reservoir uncertainty, Precambrian topography, and carbon sequestration in the Mt. Simon Sandstone, Illinois Basin. *Environmental Geosciences*, *16*(4), 235–243

Leetaru, H.E., S. Frailey, D. Morse, R.J. Finley, J.A. Rupp, J.A. Drahozval, & J.H. McBride. (2009). Carbon sequestration in the Mt. Simon Sandstone saline reservoir, in M. Grobe, J.C. Pashin, and R.L. Dodge, eds., *Carbon dioxide sequestration in geological media—State of the science: AAPG Studies in Geology, 59*, 261-277.

Lehr, J.H. (1986). Underground Injection: A Positive Advocate. *Ground Water Monitoring Review, 6(*3), 4-6.

Lengler, U., De Lucia, M., & Kühn, M. (2010). The impact of heterogeneity on the distribution of CO2: Numerical simulation of CO2 storage at Ketzin. *International Journal of Greenhouse Gas Control*, *4*(6), 1016–1025.

Li, S., Zhang, Y., & Zhang, X. (2011). A study of conceptual model uncertainty in large-scale CO 2 storage simulation. *Water Resources Research*, *47*(5), 1–23.

Loucks, R. G., Reed, R. M., Ruppel, S. C., & Hammes, U. (2012). Spectrum of pore types and networks in mudrocks and a descriptive classification for matrix-related mudrock pores. *AAPG Bulletin*, *96*(6), 1071–1098.

Mandle, R.J., & Kontis, A.L. (1992). *Simulation of regional ground-water flow in the Cambrian-Ordovician aquifer system in the northern Midwest, United States*. Professional Paper 1405-C, U.S. Geological Survey, USA.

Mbia, E. N., Frykman, P., Nielsen, C. M., Fabricius, I. L., Pickup, G. E., & Bernstone, C. (2014). Caprock compressibility and permeability and the consequences for pressure development in CO2 storage sites. *International Journal of Greenhouse Gas Control*, *22*, 139–153.

Medina, C. R., J. Rupp, and D. A. Barnes (2011) Effects of reduction in porosity and permeability with depth on storage capacity and injectivity in deep saline aquifers: A case study from the Mount Simon Sandstone aquifer. *International Journal of Greenhouse Gas Control (5)*,146–156.

Mehnert, E., Damico, J., Frailey, S., Leetaru, H., Okwen, R., Storsved, B., & Valocchi, A. (2014). Basin-scale modeling for CO2 sequestration in the basal sandstone reservoir of the Illinois Basin-improving the geologic model. *Energy Procedia*, *63*, 2949–2960.

Mehnert, E., N. Adams, Z. Askari-Khorasgani, S.M. Benson, P.M. Berger, S.K. Butler, M. D'Alessio, J.T. Freiburg, K.C. Hackley, W.R. Kelly, N.C. Krothe, J. Krothe, Y.-F. F. Lin, S.V. Panno, C. Ray, R.J. Rice, W.R. Roy, B.A. Storsved, C.W. Strandli, and L.E. Yoksoulian. (2015). *Protecting Drinking Water by Reducing Uncertainties Associated with Geologic Carbon Sequestration in Deep Saline Aquifers, Illinois State Geological Survey Final Contract Report*, 241.

Meyer, S. C., Roadcap, G. S., Lin, Y.-feng, & Walker, D. D. (2009). Kane County Water Resources Investigations : Simulation of Groundwater Flow in Kane County and Northeastern Illinois -- Contract Report 2009-07.

Michael, K., Golab, a., Shulakova, V., Ennis-King, J., Allinson, G., Sharma, S., & Aiken, T. (2010). Geological storage of CO2 in saline aquifers—A review of the experience from existing storage operations. *International Journal of Greenhouse Gas Control*, *4*(4), 659–667.

Miocic, J. M., Gilfillan, S. M. V., McDermott, C., & Haszeldine, R. S. (2013). Mechanisms for CO2 Leakage Prevention – A Global Dataset of Natural Analogues. *Energy Procedia*, *40*, 320–328.

Montanari, A., Shoemaker, C. a., van de Giesen, N. (2009). Introduction to special section on Uncertainty Assessment in Surface and Subsurface Hydrology: An overview of issues and challenges. *Water Resources Research*, *45*(12).

Morris, J. P., Detwiler, R. L., Friedmann, S. J., Vorobiev, O. Y., & Hao, Y. (2011). The large-scale geomechanical and hydrogeological effects of multiple CO2 injection sites on formation stability. *International Journal of Greenhouse Gas Control*, *5*(1), 69–74.

Morris, M. D., & May, N. (1991). Factorial Sampling Plans for Preliminary Computational Experiments. *Technometrics*, *33*(2), 161–174.

NETL. (2015). Carbon Storage Atlas – Fifth Edition.

Neufelder, R. J., Bowen, B. B., Lahann, R. W., & Rupp, J. a. (2012). Lithologic, mineralogical, and petrophysical characteristics of the Eau Claire Formation: Complexities of a carbon storage system seal. *Environmental Geosciences*, *19*(3), 81–104.

Neuman, S. P., & Wierenga, P. J. (2003). *A Comprehensive Strategy of Hydrogeologic Modeling and Uncertainty Analysis for Nuclear Facilities and Sites.* NUREG/CR-6805.

Neuzil, C. E. (1994). How permeable are clays and shales? *Water Resources Research*, *30*(2), 145–150.

Nordbotten, J. M., & Celia, M. a. (2012). *Geological Storage of CO2: Modeling Approaches for Large-Scale Simulatio*n, 225–226.

Oldenburg, C. M., & Lewicki, J. L. (2006). On leakage and seepage of CO2 from geologic storage sites into surface water. *Environmental Geology*, *50*(5), 691–705.

P.C. Carman. (1957). Flow of Gases Through Porous Media. *Combustion and Flame*, *1*(1), 187.

Pacala, S., & Socolow, R. (2004). Stabilization wedges: solving the climate problem for the next 50 years with current technologies. *Science (New York, N.Y.)*, *305*(5686), 968–972.

Palkovic, M. J. (2015). DEPOSITIONAL CHARACTERIZATION OF THE EAU CLAIRE FORMATION AT THE ILLINOIS BASIN – DECATUR PROJECT: FACIES, MINERALOGY AND GEOCHEMISTRY. (Master's Thesis). University of Illinois at Urbana-Champaign, Urbana, IL.

Pearce, J. M., Halloway, S., Wacker, H., Nelis, M. K., Rochelle, C., & Bateman, K. (1996). Natural Occurrences as Analogues for the Geological Disposal of Carbon Dioxide. *Energy Conservation Managment*, *37*(95), 1123–1128.

Person, M., Banerjee, A., Rupp, J., Medina, C., Lichtner, P., Gable, C., … Bense, V. (2010). Assessment of basin-scale hydrologic impacts of CO2 sequestration, Illinois Basin. *International Journal of Greenhouse Gas Control*, *4*(5), 840–854.

Potter, P. E., Maynard, J. B., & Depetris, P. J. (2005). *Mud and mudstones: Introduction and overview*. *Mud and Mudstones: Introduction and Overview*.

Pruess, K. (2005). *ECO2N: A TOUGH2 Fluid Property Module for Mixtures of Water, NaCl, and CO2*. Lawrence Berkeley National Laboratory Report LBNL-57952, Berkeley.

Pruess, K., Oldenburg, C., Moridis, G. (1999). *TOUGH2 User's guide, Version 2.0.* Lawrence Berkeley National Laboratory Report LBNL-43134, Berkeley.

Pujol, G. (2009). Simplex-based screening designs for estimating metamodels. *Reliability Engineering and System Safety*, *94*(7), 1156–1160.

Refsgaard, J. C., Christensen, S., Sonnenborg, T. O., Seifert, D., Højberg, A. L., & Troldborg, L. (2012). Review of strategies for handling geological uncertainty in groundwater flow and transport modeling. *Advances in Water Resources*, *36*, 36–50.

Refsgaard, J. C., van der Sluijs, J. P., Højberg, A. L., & Vanrolleghem, P. a. (2007). Uncertainty in the environmental modelling process – A framework and guidance. *Environmental Modelling & Software*, *22*(11), 1543–1556.

Rieke, H. H., & Chilingarian, G. V. (1974). Compaction of argillaceous sediments. *Developments in Sedimentology*.

Ross, J. L., Ozbek, M. M., & Pinder, G. F. (2009). Aleatoric and epistemic uncertainty in groundwater flow and transport simulation. *Water Resources Research*, *45*(12).

Rutqvist, J., Birkholzer, J., Cappa, F., & Tsang, C. F. (2007). Estimating maximum sustainable injection pressure during geological sequestration of CO2 using coupled fluid flow and geomechanical fault-slip analysis. *Energy Conversion and Management*, *48*(6), 1798–1807.

Rutqvist, J. (2012). The Geomechanics of CO2 Storage in Deep Sedimentary Formations. *Geotechnical and Geological Engineering*, *30*(3), 525–551.

Rutqvist, J., Birkholzer, J. T., & Tsang, C.-F. (2006). Modeling of geomechanical proceses during injection in a multilayered reservoir-caprock system and implications on site characterization. *Proceedings, CO2SC Symposium*.

Rutqvist, J., & Stephansson, O. (2003). The role of hydromechanical coupling in fractured rock engineering. *Hydrogeology Journal*, *11*(1), 7–40.

Rutqvist, J., & Tsang, C.-F. (2002). A study of caprock hydromechanical changes associated with CO2-injection into a brine formation. *Environmental Geology*, *42*(2–3), 296–305.

Saltelli, A., Chan, K., & Scott, E. M. (2000). *Sensitivity Analysis*. *Wiley series in probability and statistics*.

Saltelli, A., Ratto, M., Andres, T., Campolongo, F., Cariboni, J., Gatelli, D., … Tarantola, S. (2008). *Global sensitivity analysis: the primer*. *Operations Research*.

Shukla, R., Ranjith, P. G., Asce, M., Choi, S. K., & Haque, A. (2011). Study of Caprock Integrity in Geosequestration of Carbon Dioxide. *International Journal of Geomechanics*, (August), 294–301.

Shukla, R., Ranjith, P., Haque, A., & Choi, X. (2010). A review of studies on CO2 sequestration and caprock integrity. *Fuel*, *89*(10), 2651–2664.

Sifuentes, W., Blunt, M. J., & Giddins, M. A. (2009). Modeling CO2 Storage in Aquifers : Assessing the Key Contributors to Uncertainty. *SPE Offshore Europe Oil & Gas Conference & Exhibition*, (July), SPE123582.

Sminchak J. (2011). *Conceptual Model Summary Report Simulation Framework for Regional Geologic CO2 Storage Along Arches Province of Midwestern United States, Topical Report.* Battelle Memorial Institute, Columbus, Ohio.

Song, J., & Zhang, D. (2013). Comprehensive review of caprock-sealing mechanisms for geologic carbon sequestration. *Environmental Science & Technology*, *47*(1), 9–22.

Soong, Y., Goodman, A. L., McCarthy-Jones, J. R., & Baltrus, J. P. (2004). Experimental and simulation studies on mineral trapping of CO2 with brine. *Energy Conversion and Management*, *45*(11–12), 1845–1859.

Srinivasan, G., Tartakovsky, D. M., Robinson, B. a., & Aceves, A. B. (2007). Quantification of uncertainty in geochemical reactions. *Water Resources Research*, *43*(12).

Szulczewski, M. L., MacMinn, C. W., Herzog, H. J., & Juanes, R. (2012). Lifetime of carbon capture and storage as a climate-change mitigation technology. *Proceedings of the National Academy of Sciences of the United States of America*, *109*(14), 5185–9.

Tsang, C.-F., Birkholzer, J. T., & Rutqvist, J. (2008). A comparative review of hydrologic issues involved in geologic storage of CO2 and injection disposal of liquid waste. *Environmental Geology*, *54*(8), 1723–1737.

U.S. Energy Information Agency. (2013). *International Energy Outlook 2013*.

Vilarrasa, V., Olivella, S., & Carrera, J. (2011). Geomechanical stability of the caprock during CO2 sequestration in deep saline aquifers. *Energy Procedia*, *4*, 5306–5313.

Visocky, A. P., Sherrill, M. G., & Cartwright, K. (1985). *GEOLOGY , HYDROLOGY , AND WATER QUALITY OF THE CAMBRIAN AND ORDOVlClAN SYSTEMS*. Champaign, IL.

Vulin, D., Kurevija, T., & Kolenkovic, I. (2012). The effect of mechanical rock properties on CO2 storage capacity. *Energy*, *45*(1), 512–518.

Wainwright, H. M., Finsterle, S., Jung, Y., Zhou, Q., & Birkholzer, J. T. (2013). Making sense of global sensitivity analyses. *Computers & Geosciences*.

Wainwright, H., Finsterle, S., Zhou, Q., & Birkholzer, J. T. (2012). *Modeling the Performance of Large-Scale CO2 Storage Systems: A Comparison of Different Sensitivity Analysis Methods*. Berkeley, California.

Walcott, C. D., 1914, *Cambrian geology and paleontology: Smithsonian Miscellaneous Collections*, *57*, 345–412.

Walker, W. E., Harremoes, P., Rotmans, J., Van Der Sluijs, J. P., Van Asselt, M. B. A., Janssen, P., & Krayer Von Krauss, M. P. (2003). Defining Uncertainty: A Conceptual Basis for Uncertainty Management in Model-Based Decision Support. *Integrated Assessment*, *4*(1), 5–17.

Wang, H.-X., Wang, G., Chen, Z.-X. (John), & Wong, R. C. K. (2010). Deformational characteristics of rock in low permeable reservoir and their effect on permeability. *Journal of Petroleum Science and Engineering*, *75*(1–2), 240–243.

Warner, D.L. (1972). Survey of Industrial Waste Injection Wells, final report, U.S. Geological Survey Contract No. 14-08-0001-12280, University of Missouri, Rolla, Missouri.

Watts, N. L. (1987). Theoretical aspects of cap-rock and fault seals for single- and two-phase hydrocarbon columns. *Marine and Petroleum Geology*, *4*(4), 274–307.

White, C. M., Strazisar, B. R., Granite, E. J., Hoffman, J. S., & Pennline, H. W. (2003). Separation and Capture of CO2 from Large Stationary Sources and Sequestration in Geological Formations—Coalbeds and Deep Saline Aquifers. *Journal of the Air & Waste Management Association*, *53*(6), 645–715.

Willman, H. B., E. Atherton, T. C. Buschbach, C. Collinson, J. C. Frye, M. E. Hopkins, J. A. Lineback, and J. A. Simon. (1975). *Handbook of Illinois stratigraphy*. Illinois State Geological Survey Bulletin, *95*.

Witherspoon, P. & Neuman, S.. (1967). Evaluating a lightly permeable caprock in aquifer gas storage. *AIME, 240*, 949.

Wollenweber, J., Alles, S., Kronimus, A., Busch, A., Stanjek, H., & Krooss, B. M. (2009). Caprock and overburden processes in geological CO2 storage: An experimental study on sealing efficiency and mineral alterations. *Energy Procedia*, *1*(1), 3469–3476.

Xu, T., Apps, J. A., & Pruess, K. (2005). Mineral sequestration of carbon dioxide in a sandstone-shale system. *Chemical Geology*.

Yang, Y., & Aplin, A. C. (2007). Permeability and petrophysical properties of 30 natural mudstones. *Journal of Geophysical Research*, *112*(B3), B03206.

Yang, Y., & Aplin, A. C. (1998). Influence of lithology and compaction on the pore size distribution and modelled permeability of some mudstones from the Norwegian margin. *Marine and Petroleum Geology*, *15*(2), 163–175.

Yang, Y., & Aplin, A. C. (2010). A permeability–porosity relationship for mudstones. *Marine and Petroleum Geology*, *27*(8), 1692–1697.

Yeh, W. W.-G. (1986). Review of Parameter Identification Procedures in Groundwater Hydrology: The Inverse Problem. *Water Resources Research*, *22*(2), 95–108.

Young, H. L. & Siegel, D. I. (1992). Hydrogeology of the Cambrian-Ordovician aquifer system in the northern Midwest, United States. *Regional Aquifer System Analysis-Northern Midwest, 1405–B*, 1–99.

Zhao, H., Liao, X., Chen, Y., & Zhao, X. (2010). Sensitivity analysis of CO2 sequestration in saline aquifers. *Petroleum Science*, *7*(3), 372–378.

Zhou, Q., Birkholzer, J. T., Tsang, C. F., & Rutqvist, J. (2008). A method for quick assessment of CO2 storage capacity in closed and semi-closed saline formations. *International Journal of Greenhouse Gas Control*, *2*(4), 626–639.